CTLA4 and *CLEC16A* in Type 1 Diabetes
Looking behind the association

CTLA4 und *CLEC16A* in Typ 1 Diabetes
Ein Blick hinter die Assoziation

Doctoral thesis for a doctoral degree at the
Julius-Maximilians-Universität Würzburg,
Graduate School of Life Sciences, Section Biomedicine,
Rudolf Virchow Center - DFG Research Center for Experimental Biomedicine

submitted by
Kay Gerold

from
Schweinfurt

Würzburg 2011

Submitted on: ……..……..
Office stamp

Members of the *Promotionskomitee*:

Chairperson: **Prof. Dr. rer. nat. Thomas Hünig**

Primary Supervisor: **Dr. rer. nat. Stephan Kissler**

Supervisor (Second): **Prof. Dr. rer. nat. Manfred Lutz**

Supervisor (Third): **Prof. Dr. rer. nat. Ludger Klein**

Date of Public Defence: ……..……

Date of receipt of Certificates: …….

Affidavit

I hereby confirm that my thesis entitled "*CTLA4* and *CLEC16A* in Type 1 Diabetes – Looking behind the association" is the result of my own work. I did not receive any help or support from commercial consultants. All resources and / or materials applied are listed and specified in the thesis.

Furthermore, I confirm that this thesis has not yet been submitted as part of another examination process neither in identical nor in similar form.

Würzburg, 05.09.2011

Eidesstattliche Erklärung

Hiermit erkläre ich an Eides statt, die Dissertation "*CTLA4* und *CLEC16A* in Typ 1 Diabetes – Ein Blick hinter die Assoziation" eigenständig, d.h. insbesondere selbständig und ohne Hilfe eines kommerziellen Promotionsberaters, angefertigt und keine anderen als die von mir angegebenen Quellen und Hilfsmittel verwendet zu haben.

Ich erkläre außerdem, dass die Dissertation weder in gleicher noch in ähnlicher Form bereits in einem anderen Prüfungsverfahren vorgelegen hat.

Würzburg, 05.09.2011

Acknowledgements

Many people took part in helping me completing this thesis and I am very happy to be able to thank them here.

I am heartily thankful to my supervisor Dr. Stephan Kissler, whose guidance, support and elaborate planning made this thesis possible. I especially want to thank him for leaving his door literally open and being always approachable for questions.

I am also very grateful to Prof. Manfred Lutz and Prof. Ludger Klein for their help, support and advise and being part of my supervisory committee.

For agreeing to act as chairperson and especially for inviting me to the seminars at his institute that always resulted in helpful and fruitful discussions I want to thank Prof. Thomas Hünig very much.

I also would like to express my gratitude to Prof. Linda Wicker and Daniel Rainbow who kindly invited me to their laboratory and gave a lot of helpful advise.

I thank PD Dr. Alma Zernecke for her contribution and help especially concerning histology. For teaching me histology techniques I also want to particularly thank Helga Manthey, PhD and Melanie Schott.

For help and support in numerous ways I want to thank Nicole Hain, without who I would not have had any mice for my studies, Katharina Herrmann, Julie Joseph, Fabian Kaiser, Heike Rudolf and Peilin Zheng. I also want to thank Lilli Teresa Probst, for deciding to use her talent to do her medical doctoral thesis in a shared project with me.

Last but not least I want to thank my parents, husband and friends for always being there and supporting me on my way.

Table of contents

1 Summary

Type 1 diabetes is an autoimmune disease that leads to the destruction of insulin-producing pancreatic beta cells and consequently to hyperglycemia. In the last 60 years, the prevalence of type 1 diabetes has been increasing constantly and is predicted to continue rising. About 80% of the disease risk is attributable to the genetic variation. Thanks to genome wide association studies the number of known disease-associated polymorphisms climbed from five to 53 in the last 10 years.

As these studies reveal possible candidate genes but not underlying mechanisms we strove to take the next step and explore the association of two genes suggested by these studies with type 1 diabetes.

As a method of choice we decided to use lentiviral RNAi in non obese diabetic (NOD) mice, a widely-used model for type 1 diabetes, introducing a shRNA directed against the target message into the genome of this mouse strain via a lentivirus. This allowed us to study the partial loss-of-function of the target gene within the context of diabetes, directly seeing its effect on autoimmune mechanisms.

In this thesis we examined two different genes in this manner, *Ctla4* and *Clec16a*.

A type 1 diabetes associated polymorphism in the *CTLA4* gene had been found to alter the splicing ratio of its variants soluble CTLA-4 (sCTLA-4) and full length CTLA-4, the associated allele producing less sCTLA-4 than the protective allele. We mimicked this effect by specifically targeting the *sCtla4* mRNA via lentiviral RNAi in the NOD model. As a result we could confirm the reduction of sCTLA-4 to accelerate type 1 diabetes development. Furthermore we could show a function of sCTLA-4 in regulatory T cells, more specifically at least partly in their ability to modulate costimulation by antigen presenting cells.

The second candidate gene, *Clec16a* was targeted with the shRNA in a way that was designed to knock down most splice variants. As the gene function and the effect of the associated

polymorphism was unknown, we reasoned this method to be feasible to investigate its role in type 1 diabetes. The knockdown of *Clec16a* in NOD mice resulted in an almost complete protection from diabetes development that could be attributed to T cells dysfunction. However, as expression patterns and a study of the Drospophila orthologue suggested a possible role of CLEC16A in antigen presentation we also examined antigen presenting cells in the thymus and periphery. Although we did not detect any effect of the knockdown on peripheral antigen presenting cells, thymic epithelial cells were clearly affected by the loss of CLEC16A, rendering them more activated and shifting the ratio of cortical to medullary epithelial cells in favor of cortical cells. We therefore suggest a role of CLEC16A in the selection of T cells, that needs, however, to be further investigated.

In this thesis we provided a feasible and fast method to study function of genes and even of single splice variants within the NOD mouse model. We demonstrate its usefulness on two candidate genes associated with type 1 diabetes by confirming and unraveling the cause of their connection to the disease.

2 Zusammenfassung

Typ 1 Diabetes ist eine Autoimmunerkrankung, bei der es zur Zerstörung von pankreatischen beta-Zellen und daraus folgend zu einer Hyperglykämie kommt. In den letzten 60 Jahren stieg die Diabetes Prävalenz stetig an und Studien sagen voraus, dass sich dieser Trend in Zukunft noch stärker fortsetzen wird. Man geht davon aus, dass ca. 80% des Erkrankungsrisikos für autoimmunen Diabetes genetischer Natur sind. Dank Genom-weiter Assoziationsstudien wurde dieser Beitrag gerade in den letzten zehn Jahren immer weiter aufgeklärt und bis heute wurden 53 mit Typ 1 Diabetes assozierte Polymorphismen identifiziert.
Da diese Studien es nur leisten können, mögliche Kandidatengene aufzuzeigen, allerdings keine Aussagen über die zugrunde liegenden Krankheitsmechanismen machen können, haben wir es uns zum Ziel gesetzt diesen nächsten Schritt zu gehen und zwei der durch diese Studien vorgeschlagenen Gene auf ihre Rolle in der Typ 1 Diabetes Ätiologie zu untersuchen.

Unsere Methode der Wahl war die lentivirale RNA Interferenz im Mausmodell der *nonobese diabetic mouse* (NOD). Via lentiviralen Vektoren wird die Information für eine shRNA, die an die mRNA des Zielgenes bindet, in das Empfängergenom integriert. Die daraus folgende Herabregulierung der Ziel-mRNA erlaubt es uns den Effekt dieser fehlenden Geninformation auf die Immunregulation zu analysieren.

Auf diese Weise wurden in dieser Thesis zwei Kandidatengene untersucht, *Ctla4* und *Clec16a*.
Der mit Typ 1 Diabetes assoziierte Polymorphismus im *CTLA4* Gen verursacht eine Verschiebung im Splice Verhältnis der beiden Isoformen im Menschen, *soluble* CTLA-4 (sCTLA-4) und *full length* CTLA-4, zu Gunsten der *full length* Variante. Im NOD Mausmodell konnte diese Verschiebung durch eine Einführung einer gegen *sCtla4* gerichteten shRNA nachgeahmt werden. In Folge dessen konnten wir bestätigen, dass eine Reduzierung der sCTLA-4 Variante die Typ 1 Diabetes Entwicklung beschleunigt. Zudem

konnten wir eine Rolle von sCTLA-4 in der Funktion von regulatorischen T Zellen, genauer in deren Fähigkeit die Kostimulation durch Antigen präsentierenden Zellen zu modulieren, zeigen.

Bei dem zweiten Gen, das in dieser Thesis untersucht wurde handelte sich um *Clec16a*. Es wurde von einer shRNA herunterreguliert, die den Großteil der Varianten abdeckt, da die Funktion des Genes, sowie die Auswirkungen des assoziierten Polymorphismus unbekannt waren. Der *Knockdown* von *Clec16a* in der NOD Maus verursachte einen fast vollständigen Schutz vor Diabetes, der im weiteren Verlauf den T Zellen zugerechnet werden konnte. Allerdings hatten das Expressionsmuster, sowie eine Studie am Drosophila Ortholog *ema* eine Rolle von CLEC16A in Antigen präsentierenden Zellen impliziert. Folglich untersuchten wir die Möglichkeit, dass diese Zellgruppe in der Peripherie oder im Thymus durch den CLEC16A Mangel beeinträchtigt sein könnten. Tatsächlich wies die Zellgruppe, die im Thymus für die Selektion von T Zellen zuständig ist einen erhöhten Aktivierungsstatus auf, was auf eine modifizierte T Zell Selektion hindeuten könnte.

Mit dieser Arbeit konnten wir eine praktikable und schnelle Methode, für die funktionelle Analyse von Genen und sogar einzelnen Splice Varianten, aufzeigen. Wir konnten ihren Nutzen weiterhin an zwei mit Typ 1 Diabetes assoziierten Kandidatengenen unter Beweis stellen, indem wir so die Assoziation bestätigen und Licht auf die zugrunde liegenden Mechanismen werfen konnten.

3 Introduction

3.1 Immune Regulation

In order to protect the body from pathogens, the immune system has to recognize a vast variety of chemical structures, like proteins and peptides, lipids and carbohydrates.

There are two branches of the immune system, with different spectra of recognition. The one mainly responsible for the fist line of defense possesses a large but still limited and invariant receptor repertoire. It is called the innate immunity. On the other hand there is the adaptive immunity with cells exhibiting an enormous array of specificities, with every cell having its very own antigen receptor[1].

Two mechanisms are contributing to the huge receptor repertoire of B and T lymphocytes, which are the main cell types of the adaptive immunity.

First they undergo a process called V(D)J- recombination, during which the different segments of the B cell or T cell receptor, V (variable), D (diversity), J (joining) and C (constant) are combined in a unique way for every cell. This somatic recombination happens during B and T cell development in the central lymphoid organs, bone marrow or thymus respectively.

B cells additionally undergo a second round of receptor editing in the periphery, lymph nodes and spleen, called somatic hypermutation.

In case of T cells the theoretical number of different receptors produced by somatic recombination is 10^{18} [2]. Since they are generated in a random process, a considerable number (20-50%[3-6]) of these receptors are not functional or have a potentially harmful affinity for self-antigens. Nevertheless “only” 3-8% of the population suffers from autoimmunity[7], indicating that there are strategies to hold these self-reactive cells in check. These strategies are described in the following sections for T cells.

3.1.1 Central tolerance and T cell development

The first step of control takes place during T cell development in the thymus. Here T cells with inoperative TCR or with high self-affinity die selectively[8]. These processes are called positive and negative selection respectively and contribute to central tolerance.

The progenitors for T cells, like those for B cells, are hematopoetic stem cells (HSCs) and arise in the bone marrow. Whether these are the cells that migrate directly into the thymus or whether the cells entering the thymus are other downstream progenitors is not clear yet. Still it was suggested that many progenitors are able to contribute to the T cell lineage if exposed to Notch signaling in a hematopoetic environment[9,10].

The progenitors enter the thymus in the corticomedullary junction and migrate to the subcapsular zone[11,12] where they proliferate extensively[13]. As earliest progenitors in the thymus several distinct populations were described, of which the double negative (DN1) subsets a and b ($CD3^-$ $CD8^-$ $CD4^-$ $CD44^+$ c-kit^{hi} $CD25^{+ \text{ and } lo}$) showed the most substantial proliferation and best potential as precursor for T cell lineage[14]. They differentiate into DN2 cells (Lin^{lo} $CD44^+$ c-kit^{hi} $CD25^+$) and then DN3 cells (Lin^{lo} $CD44^{lo}$ c-kit^{lo} $CD25^+$), while migrating from entry sites to the inner cortex[11,12]. The latter are already committed to the T cell lineage and undergo somatic recombination of TCRβ or δ and γ loci, depending on whether they are determined to the α/β- or γ/δ-T cell fate[15]. Cells of the α/β-T lineage form a pre-TCR after successful β-chain rearrangement, rescuing them from cell death[16].

After having passed the checkpoint of beta-selection by effective pre-TCR signaling, the cells undergo extensive proliferation and differentiate into double positive (DP; $CD4^+CD8^+$) T cells[17]. Now the α-locus is subject to rearrangement, resulting in α/β-TCR-expression. From that point on all following checkpoints are based on interactions of the α/β-TCR with self peptide/MHC (pMHC) ligands on stromal cells in the thymus[18].

3.1.1.1 Positive Selection

The first of these points of control is called positive selection and takes place in the thymical cortex, with cortical epithelial cells (cTECs) being the major antigen presenting cells. During this process, a survival signal is delivered exclusively for cells having rearranged a functional TCR that is able to recognize self-peptides bound to self MHC with an intermediate affinity[19,20]. Not until then is the α-chain rearrangement terminated, allowing not yet selected DP thymocytes to change their specificities during their 3-4 d lifespan, thereby increasing their chances to receive a positive signal in the end[21]. But despite this, and though the TCR seems to be prone to recognize MHC[6,22], around 90-95% of DP thymocytes die a death of neglect[23,24].

To date only little is known about the selecting peptide-MHC repertoire presented by cTECs *in vivo* (reviewed in ref. 25). However it has been indicated that a complex pMHC repertoire leads to a broad positively selected T cell repertoire[26,27], even if the single peptides are only present with low abundance[28]. Also there have been reports that identified pathways to generate peptide-MHC complexes in cTECs that are not applied in other thymic or peripheral APCs (reviewed in 25).

Cathepsins are lysosomal proteases responsible for the degradation of the invariant chain of MHC class II molecules. Moreover they are able to generate MHC ligands from proteins in the lysosome[28]. In contrast to mTECs and peripheral APCs, cTECs use cathepsin L instead of cathepsin S, suggesting the generation of a different set of peptides due to the usage of a different protease (evaluated in [25]). Indeed a role of cathepsin L in positive selection of CD4 T cells could be shown by silencing the gene coding for this protease, resulting in a 60-80% reduction of the CD4 SP compartment[29].

Further evidence for a distinct pMHC repertoire in cTECs arose from the identification of a cTEC specific gene, *Prss16*, coding for the thymus specific serine protease[30,31]. Its exact role in the pathway of MHC ligand repertoire shaping is as yet unclear, its restriction to

endosomal and lysosomal compartments however points to a role in the proteolytic generation of MHCII peptides. Unlike cathepsin L, knockout of *Prss16* does not have a striking effect on the CD4 SP compartment[32], it does however alter the abundance of single TCR specificities[33]. This may also be the reason why *PRSS16* displays association with type 1 diabetes[34].

TECs highly express MHCII but are unproductive in presenting exogenous antigens via the endocytic pathway[35,36]. Instead they exhibit an exceptionally high constitutional macroautophagy activity, especially in the cortex, that allows them to present self-antigens on MHCII[37,38]. Macroautophagy, in general a mechanism that provides new resources in the case of starvation, is a process in which part of the cytoplasm and /or organelles is enclosed in a double membrane of about 1µm diameter that eventually merges with endosomes and lysosomes, thereby degrading its content and making it available for reuse[39-41]. It thus represents a further pathway by which cTECs are able to present unique pMHC complexes to developing thymocytes.

All aforementioned cTEC mechanisms can largely be attributed to the MHCII pathway, however these cells also feature unique MHCI loading processes. As sole cell subset they employ the subunit β5t in their proteasome, thereby forming a thymoproteasome[42]. It is a variation of the immunoproteasome of APCs and mTECs, that differs from the conventional proteasome by replacement of some β subunits allowing them to produce peptides optimized for MHCI binding[42,43]. It had been suggested that the thymoproteasome lowers the affinity of the peptides for MHCI and makes the binding less stable[25,44]. Knockout of the gene coding for β5t, *Psmb11*, reduces the CD8SP compartment by impaired positive selection of certain TCR specificities and renders them less active[45].

Taken together all these unique ways to produce MHC ligands point to a unique set of peptides presented by cTECs and establishing positive selection. At least part of the necessity for different ligands being presented by cTECs and mTECs/DCs could be attributed to the prevention of a reencounter of the same peptides in the medulla, thereby causing a higher signal and negative selection[25]. However this theory would have to be reconciled with the

postulated vital tonic homeostatic signal provided by T cells facing the same low affinity pMHC complexes on peripheral APCs as previously in the cortex[46,47].

3.1.1.2 Negative Selection

Eventually, positively selected thymocytes migrate to the medullary part of the thymus. Here they are subject to negative selection during their 4-5 day passage[25], a process purging the thymocytes of potentially dangerous auto-reactive cells. During this process about 50-70% of positively selected thymocytes are reckoned to die[48-50]. They do so after high affinity contact to medullary thymic epithelial cells (mTECs) or thymic dendritic cells[18]. This TCR signal results in activation of apoptotic signal transduction pathways, presumably including the MINK/p38/JNK, MINK/Bim/Bcl-2 and ERK5/Nur77 pathways[51].

Among this large number of negatively selected thymocytes, there are however not only thymus-specific T cells but also cells with TCRs recognizing peripheral self-antigens. Already in 1989, it had been assumed that genes from different peripheral tissues are expressed in the thymus, thus allowing the negative selection of those harmful thymocytes[52]. In 2001, the expression of those tissue restricted antigens (TRAs) was seen to be a unique feature of mTECs[53]. Moreover TRAs in the thymus were found to be not only spatially but also temporally restricted[54], and their genes to be highly clustered in the genome, suggesting a contribution of epigenetic mechanisms to regulation of their expression[18]. Furthermore the promiscuous gene expression (pGE) of TRAs by mTECs is at least partly regulated by the autoimmune regulator (Aire)[55], though the mechanism of this regulation remains elusive. TRAs can also be presented by thymic DCs[56], in a process called cross-presentation, after having taken up mTEC derived antigens[57] in a yet undefined manner (reviewed in 58).

In 2008 Aire expression was also detected in stromally derived cells in secondary lymphoid organs, also expressing TRAs and thus likely extending the deletional tolerance to the periphery[59-61].

Also during their passage through the medulla, double positive thymocytes differentiate into single positive (CD4+ or CD8+) T cells. The lineage is dependent on whether the TCR is MHC I (CD8) or MHC II (CD4) restricted and is chosen during positive selection.

3.1.2 Peripheral Tolerance and regulatory T cells

In addition to recessive tolerance, provided by intrinsic processes like apoptosis due to negative selection in the thymus and anergy of T cells chronically stimulated by pMHC without costimulation, there is also a way to dominantly suppress auto-reactive T cells in the periphery. This extrinsic mechanism is to the current knowledge carried out by Foxp3-expressing regulatory T cells (Tregs)[62]. Also Foxp3 negative Tr1[63] and Th3[64-66] cells have been shown to act suppressive especially in the intestine, conveying oral tolerance, however will not be discussed further in this thesis.

First evidence for the existence of Tregs was given after neonatal thymectomy (nTx) studies by Nishizuka and Sakaguchi, revealing a regulatory cell population generated in the neonatal thymus on day three[67-69]. This finding laid the foundation for further characterization of that population. In 1996, it was found that transfer of $CD25^+$ $CD4^+$ T cells can rescue neonatal thymectomized mice from their normally autoimmune phenotype[69]. Later the more specific marker Foxp3 was identified during studies on the genetic contribution to the human autoimmune disorder IPEX (immune dysregulation, polyendocrinopathy, enteropathy, X-linked) and the mouse mutant *scurfy*[70-73]. Loss of function of that X-chromosome encoded forkhead transcription factor leads to fatal lymphoproliferative immune mediated disease. Together with its high and stable expression in regulatory $CD25^+$ $CD4^+$ T cells (Treg cells) and its requirement for their differentiation and function this led to its declaration as marker number one for Treg cells[74-79] .

3.1.2.1 Treg development

There are two types of Foxp3 positive regulatory T cells: thymus derived Treg cells, also called natural Treg cells (nTreg cells) and adaptive Treg cells (iTreg cells), which are induced from naïve CD4 T cells in the periphery. But although they can be clearly differentiated due to their development and TCR specificity, the actual differences in their field of function remain elusive[80].

Natural Treg cells develop along with other T cell subsets in the thymus. The triggers that lead to differentiation into the Treg lineage are still highly controversial. At present three different models are discussed:

The *instructive model* assumes that the strength of the TCR-signal determines Treg differentiation. As already described, low affinity for self causes death by neglect due to lack of positive selection. Too high an affinity causes apoptosis through negative selection. It was proposed that a slightly lower affinity for self would be responsible for Treg formation.
Support for this model came from studies on CD4/ CD8 lineage decision mechanisms[81,82], activation marker expression on Tregs as sign for a strong TCR signal[62] , and Treg TCR repertoire analysis, that showed only partially overlapping[83-85] specificities with conventional T cells that were also more self-affine [85].
These observations were supported experimentally by showing the necessity of endogenous TCR-rearrangement for development of nTreg cells in TCR transgenic mice[86]. Yet later it was found that coexpression of the cognate antigen can rescue Treg development in TCR transgenic mice which lack endogenous TCR rearrangement[87-89].

However negative selection was significantly increased in these studies, supporting a *stochastic-selective model*, in which self-reactive Foxp3 expressing Treg precursors selectively survive in the thymus rather than being “instructed” to express Foxp3[90]. In line

with that finding, molecules that support survival and attenuate TCR signaling, like CTLA-4, display an increased expression in a Foxp3-dependent fashion [62].

An extension of the instructive model is the *two-step model*. This model hypothesizes a second signal additional to TCR signaling, since there is evidence that the TCR signal alone is not sufficient to cause Foxp3 upregulation and thus Treg cell lineage commitment: For instance it is possible that Treg and non-Treg cells express the same TCR with increased reactivity for self[91]. Furthermore only some thymocytes in mice with transgenic TCR and coexpression of cognate antigen become Treg cells, others turn into anergic non-Treg cells[87,89].

One essential second factor for Treg development was found to be IL2[92]. Two other common gamma-chain cytokines IL7 and IL15 can also contribute to the Treg cell fate decision but have a weaker impact[93].

Adaptive regulatory T cells are in contrast to nTregs generated in the periphery from naïve T helper cells under divers circumstances. However the basic requirements for Foxp3 upregulation *in vitro* as well as *in vivo* could be identified to be TCR stimulation plus presence of TGFβ and IL-2[94]. Under these conditions the Foxp3 enhancer element is bound by a cooperation of STAT3 and NFAT[62,80]. IL-2 additionally induces STAT5 that could also drive Foxp3 expression[95]. Also unlike nTregs, iTregs require the upregulation of CTLA-4 for their differentiation from naïve Th cells[96].

As aforementioned, iTregs develop in multiple microenvironments that are to date not fully understood. So, they are found in the GALT (gut-associated lymphoid tissue) to convey oral tolerance[97,98] and as a reaction to microbiota and food antigens[99]. In addition they were seen to arise in chronically allergic inflamed tissues[100] and in reaction to tumor[101] and transplantation[102].

Recently a potential marker to distinguish nTregs and iTregs was suggested to be Helios, a member of the Ikaros transcription factor family only expressed by thymic derived $Foxp3^+$ Tregs[103]. This study also gave first insight into the importance of iTregs, as they amounted to 30% of $Foxp3^+$ cells in the periphery.

3.1.2.2 Mechanisms of Treg function

Natural as well as induced regulatory T cells exhibit multiple processes through which they suppress conventional T cells *in vitro*. Still despite all these candidate molecules and pathways found through different approaches *in vitro*, it is still unclear which or if any of these, are applied *in vivo*[104].

Most of the classic *in vitro* suppression assays include antigen presenting cells (APCs: irradiated spleen cells or non-irradiated dendritic cells) and soluble anti-CD3 to stimulate T cells. Others excluded APCs completely and included bead- or plate-bound CD3 and CD28 antibodies instead. It was shown that although the absence of APCs reduced the suppressive activity of Treg cells, both CD4/CD8 T cells but also in particular APCs can be cellular targets for Treg-mediated suppression[104,105].

As for targeting of conventional T cells, several studies have shown that Treg cells mediate the inhibition of cytokine expression, especially IL2[106,107]. It was also claimed that Treg cells might act on conventional T cells by competing with them for IL2 with their high affinity receptor (CD25, CD122, CD132), thereby causing Bim dependent apoptosis of the effectors[108]. However some studies disagree and explain the IL2 deprivation by consumption through contaminating activated conventional T cells in Treg preparations (both $CD4^+CD25^+$)[104,109].

Though it was demonstrated that Treg cells fail to suppress conventional T cells when separated from them by a semipermeable membrane, cytokine mediated suppression was suggested to be still possible if cell-cell-contact is involved[106,110]. Recently Collison and

colleagues showed that only the induction of suppression and not the Treg function as such is cell contact dependent *in vitro*[111]. They showed that cell contact with conventional T cells induces expression of IL35, a novel inhibitory cytokine[112] and IL10, which then are able to mediate suppression of T cells across a semipermeable membrane. Another candidate for inhibition through secreted molecules is galectin-1 a member of the family of beta-galactoside binding proteins, which could induce cell cycle arrest, apoptosis and inhibition of proinflammatory cytokine production after binding[113].

A further possibility for Treg cells to act on conventional T cells is direct cytolysis. Under certain circumstances they can turn into "cytotoxic suppressor" cells and lyse target cells via granzyme B, perforin or Fas-FasL interaction[104,114,115].

Since it is a crucial task of Treg cells to suppress priming and differentiation of effector T cells *in vivo* and *in vitro*, the APC is an important target.

One of the means to target them is the cytotoxic T-lymphocyte antigen 4 (CTLA-4), which is constitutively expressed on Treg cells and interacts with the costimulators CD80 and CD86 on APCs. This interaction was seen to be able to cause downregulation of the expression of these costimulators in mouse and human DC *in vitro*[116-118]. The function of CTLA-4 in Treg cells was further elucidated by a recent study of Wing and colleagues[119]. They specifically deleted CTLA-4 in Treg cells and could show that the deficiency in this one cell type alone is sufficient to cause fatal lymphoproliferative disease. Their explanation is the impaired suppressive ability of these cells, in particular in their ability to downregulate CD80/86 on DCs. A possible mechanism by which this downregulation could be explained is trans-endocytosis during which Tregs take up surface molecules from APCs in the immunological synapse and that are degraded subsequently[120,121]. Additionally interaction of CTLA-4 with CD80/86 has been claimed to induce indoleamine 2,3-dioxygenase (IDO), a potent regulatory molecule, expression in DCs[122].

Other molecules thought to be involved in APC regulation by Treg cells are LAG-3 (lymphocyte activation gene 3)[123], a CD4 like molecule binding MHCII with high affinity,

CD39[124], an ectoenzyme hydrolyzing ATP thereby inactivating extracellular ATP an indicator of tissue destruction and the fibrinogen-like protein 2 (FLG2)[125], which was also shown to be able to reduce CD80/86 expression on DCs.

All in all the immune system developed, along with its astounding repertoire to recognize foreign antigens, several effective regulatory pathways to prevent this large repertoire from harming the own body. But still as already mentioned, autoimmune disorders are one of the most common diseases with 3-8% incidence and more than 60 different known disorders (Deutsche Gesellschaft für Autoimmunerkrankungen e.V.), meaning that there are also multiple pitfalls where the control can fail.

3.2 Type 1 Diabetes

One of the many different autoimmune disorders is type 1 diabetes, a disease caused by the destruction of insulin producing beta cells in the pancreatic islets of Langerhans[126]. The cells held mainly responsible for the destruction are auto-reactive cytotoxic T cells. They infiltrate the islets together with other leukocytes in the first stage of disease, called insulitis[127]. The second stage, overt diabetes is seen when about 80% of the beta cells have been destroyed. The remaining cells cannot produce enough insulin to provide for a proper regulation of blood glucose level, resulting in hyperglycaemia.[127] In the course of the disease this can lead to severe symptoms like ketoacidosis, kidney failure, heart disease, stroke or blindness[128]. Onset of disease typically happens in the youth, but also adult forms of disease development are possible. Since the 1920s diabetes has been treated by administration of exogenous insulin, so that the ultimate shortening of life expectancy was decreased to about 10 years[128].

There is still controversy about how beta cell antigens are initially exposed to APCs, which can then present them to auto-reactive T cells. One theory is physiological cell death, since a wave of beta cell death can be observed in young rodents at 14-17 days of life and also perinatally in humans[127]. But also the contribution of viruses, especially the coxsackivirus, to onset of diabetes has been widely discussed[129]. However, incidence in animal models of type 1 diabetes is highest under germ-free conditions, arguing against the requirement of an environmental trigger for disease onset[130]. Interestingly, coxsackivirus infection only triggered diabetes in NOD mice with already preexisting insulitis[131-133], suggesting that a similar scenario could be true for humans.

Somehow peptides from beta cells themselves or peptides mimicking them are subsequently presented to CD4 and CD8 T cells in the islets, draining lymph nodes or even at distant sites. There, T cells specific for antigens derived from insulin, glutamic acid decarboxylase, tyrosine phosphatase 1A-2 and 1A-2ß and possibly other proteins are getting activated. Through activation they gain the ability to migrate into the islets, where they reencounter

their antigen and induce beta cell death either under direct T cell/beta cell contact or as a bystander effect after T cell/APC contact[127]. B cells are proposed to act mainly as antigen presenting cells in type 1 diabetes etiology[134], as autoantibodies whose occurrence can be leveraged for early diagnosis are most likely not pathogenic[135].

The correlation between failing regulatory mechanisms and pathogenesis of T1D is summed up in figure 1:

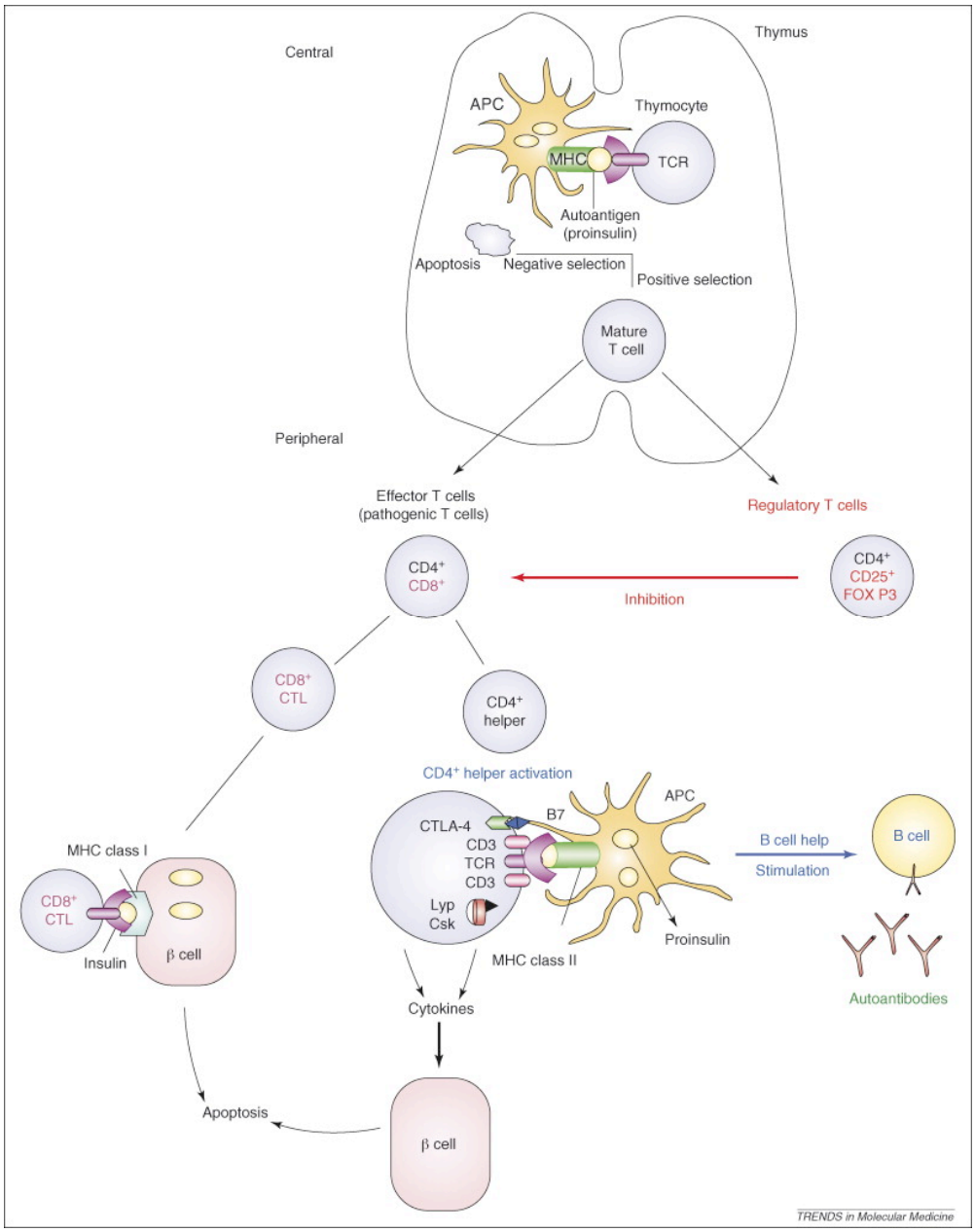

Figure 1: Correlation of control mechanisms of the immune system and T1D; from Ounissi-Benkalha and Polychronakos, 2008[136]

Over the second half of the twentieth century the incidence of type 1 diabetes has been increasing rapidly. Predictions estimate a 40% rise of incidence in children under 15 years of age from 2005 to 2020, with the largest increase of about even 70% in children under the age of 5[137]. Although the phenomenon of increasing incidence is seen worldwide there are vast geographical differences. While there are 40 new cases of type 1 diabetes per 100.000 inhabitants per year in Finland, only 0.1 new onsets per 100.000 occur in Asia and South America, representing the two extremes of a north-south divide[138].

Type 1 Diabetes develops as a result of a combination of environmental and genetic factors. The environment is assessed to contribute approximately 20% of overall disease risk [139]. Over 40 genetic loci have been identified to associate with Type 1 diabetes and many of them also with other autoimmune diseases[140].

The most important susceptibility locus is the HLA region on chromosome 6p21.3. Its variants determine the way peptides are presented to the immune system via MHC and it contributes to about 50% to the genetic susceptibility of T1D[141-145]. To date it is agreed that the major susceptibility markers for T1D are HLA class II DQB1*0302 on the DR4 haplotype and DQB1*0201 on the DR3 haplotype[136].

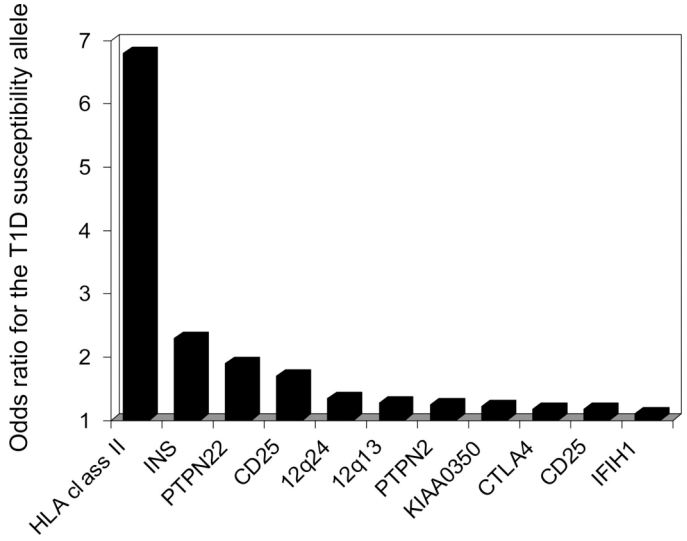

Figure 2: Odd ratios for susceptibility alleles of selected T1D-associated loci; Mehers and Gillespie [146] adapted from Todd et al.[143]

Polymorphisms in the insulin (*INS*), *PTPN22*, *CD25*, *PTPN2*, *CLEC16A* (*KIAA0350*), *CTLA4*, *IFIH1* genes also contribute to T1D susceptibility, albeit to a lesser extent. This thesis focuses on the role of *CTLA4* and *CLEC16A* in T1D, thus only they will be addressed in more detail, as it would go beyond the scope of this report to elaborate on all candidate genes.

3.2.1 CTLA-4 and Type 1 Diabetes

CTLA4 was shown to be associated with several autoimmune disorders, including type 1 diabetes[147]. Here the association was attributed to a single nucleotide polymorphism (SNP) in the 3' UTR (CT60). Depending on which allele of that polymorphism one carries, the susceptibility to T1D becomes higher (G allele) or lower (A allele). This polymorphism affects expression levels of a particular splice isoform of CTLA-4: the soluble CTLA-4 (sCTLA-4). Its mRNA expression is already reduced in the heterozygous state and is least with homozygous susceptibility allele[148].

CTLA-4 is encoded by 4 exons and is expressed in two different isoforms in humans: the full length form, consisting of all 4 exons and the soluble form, lacking the exon coding for the transmembrane domain (exon 3).

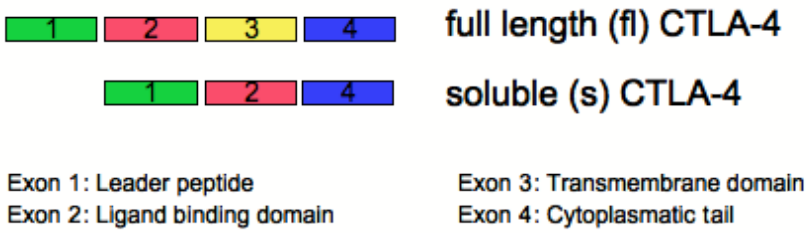

Figure 3: Splice isoforms of CTLA-4 in humans

As already described in section 3.1.2.2 CTLA-4 plays an important regulatory role in the immune system and is expressed in Treg cells and activated conventional T cells. Some of the processes that CTLA-4 is proposed to be involved in are also mentioned in section 3.1.2.2. So far, no information is available as to which extent the two isoforms contribute to the

regulatory function, but the complete knockout of CTLA-4 in mice results in a massive lymphoproliferative disorder.

3.2.2 CLEC16A and Type 1 Diabetes

Association of the genetic locus on chromosome 16 in the region of *CLEC16A* (*KIAA0350*) with type 1 diabetes was found later than *CTLA4* in a genome-wide association study carried out by The Wellcome Trust Case Control Consortium in 2007[149]. This region was further validated by several follow up studies[142,143,150-154] and eventually also claimed to be associated with other autoimmune diseases like primary adrenal insuffiency[155], multiple sclerosis[154,156,157] and crohn´s disease[158].

In humans *CLEC16A*, a gene that spans over 237kb, is alternatively spliced into 14 variants, only half of them coding for proteins between 1053aa to 118 aa of length (www.ensembl.org). SNPs found to be associated with different diseases are all intronic and so far no alteration of regulatory elements by them has been revealed (www.emsembl.org). However transcription ratios of two variants in the thymus have been found to be altered by SNP rs12708716 that was previously shown to be associated to T1D and MS[159].

The function of CLEC16A is still unknown, but its nearly exclusive expression in immune cells indicates a function in immune processes (biogps.org). Computational analysis further identified a putative ITAM[143] (immunoreceptor tyrosine-based activation motif), transmembrane domain (www.ch.embnet.org) and a proposed C-type lectin domain[151] in the human protein that is however disrupted in all other orthologues (prosite.expasy.org).

Recently a study on abnormal synaptic overgrowth and protein trafficking at the neuromuscular junction of *Drosophila melanogaster* revealed a role of the *CLEC16A* orthologue *ema* in endosomal maturation and function[160]. The authors of this study further showed that this effect was partly due to *ema'*s role in abrogating BMP signaling in the endosomes. Notably they were successful in rescuing the phenotype of the *ema* mutant by introducing human CLEC16A, thereby showing that the essential function of *ema* is highly conserved in its orthologues. This is also supported by the presence of highly conserved

CLEC16A orthologues from mouse to Zebrafish, *Xenopus*, *C. elegans* and *Arabidopis* ([160] and www.ensembl.org). Strikingly no orthologue is present in Yeast, suggesting a role for CLEC16A in multicellularity[160].

3.2.3 Non obese diabetic (NOD) mice as model organism

The non obese diabetic (NOD) mouse strain was developed in 1980 emerging from the Jcl:ICR outbred strain[161,162]. NOD mice spontaneously develop autoimmune diabetes between three and six months of age[163]. The disease incidence is gender specific and lies around 60-80% in females and 20-30% in males[162,164], probably due to an estrogen induced Th1 skewing of immune responses[165]. However both time of onset and incidence are intrinsic to each individual animal housing facility[163]. In NODs the course of diabetes is commenced by non-destructive insulitis with infiltrating macrophages and dendritc cells and subsequently also B and T cells[166]. The infiltrating T cells finally destroy beta cells and the disease thus progresses to overt diabetes, finally even forming tertiary lymphoid structures at the site of inflammation[167].

In spite of this more aggressive course of diabetes, NOD mice otherwise develop a disease that shares a lot of characteristics with human type 1 diabetes, like the presence of autoantibodies and auto-reactive CD4 and CD8 T cells. Since the genetic linkage to the disease is also comparable to that in human patients[168], this strain is an extremely suitable model to study T1D and has been used in an extensive number of studies so far.

3.3 Lentiviral RNAi

As aforementioned, genome wide association studies (GWAS) have already revealed 53 loci associated with type 1 diabetes (www.t1dbase.org). The information that can be drawn from these studies does however not point out specific unequivocally responsible genes, it rather results in one or more candidate genes possibly influenced by the associated SNP, especially since these are often found in non-coding regions[169]. Determining these genes and the

underlying pathways responsible for T1D incidence though is crucial to further understand etiology and thus ultimately improve treatment.

As SNPs in most cases have a moderate effect[170] and only seldom completely abrogate gene expression, knockout (KO), albeit being an effective method to assess the basic gene function, is often a too crass an approach to elucidate the effect of the polymorphism in disease. Also, until recently it was hardly feasible to generate a KO on the NOD background, due to the lack of ES cells[171] and the problem of introducing foreign flanking DNA in the process of backcrossing[172].

A more flexible and physiological approach to find the pathway behind an association is RNA interference (RNAi).

3.3.1 RNAi

RNA interference regulates gene expression post-transcriptionally. On the prerequisite of sequence complementarity of short RNAs with target mRNAs, the target gene function is silenced by ablation of translation or degradation of the mRNA. RNAi is a highly conserved mechanism in eukaryotes, that was initially detected in *C.elegans* in 1991[173] and attributed to dsRNA in 1998[174] by Andrew Fire and Craig Mello, who were honored with the nobel prize for medicine / physiology in 2006 for this discovery.

Endogenous microRNAs (miRNAs) of 22 nucleotides length or exogenous small interfering RNAs (siRNAs) are analogically generated from precursors by nuclear (Drosha)[175,176] and cytoplasmic (Dicer)[177] RNases. Mature mi- and siRNAs then associate with the RNA-induced silencing complex (RISC), a protein complex of the argonaute-family[178,179]. Only the guide strand, determined by its thermodynamically more instable 5' end, remains in the complex, the passenger strand being degraded[180-182]. The manner of silencing is subsequently defined by the degree of complementarity of the guide strand with the target mRNA. A perfect match, mostly the case with siRNAs, leads to degradation of the target mRNA by Ago2. Mismatches in the binding, more common with miRNAs, lead instead to inhibition of translation[183].

Even with the experimental application of siRNAs, a complete loss of expression of the target mRNA is unlikely. It rather leads to a diminished amount of expressed protein, a knockdown (KD), thereby providing the possibility to tune the expression in a more physiological manner than with the KO technology.

3.3.2 Lentiviral trangenesis

By establishing DNA-coded shRNAs[184] and the possibility of them being carried by retro- or more specific lentiviruses[185,186], it became practicable to generate animal models with constitutive or also induced RNAi. Plasmids coding for small hairpin RNAs (shRNAs) are introduced in modified, replication-deficient, lentiviral particles that allow the integration of a long terminal repeat (LTR) flanked DNA sequence into the host genome. By infecting single cell embryos of mice with this virus, the integrated DNA and thus the DNA coding for the shRNA is passed along into every cell of the animal, including the germ line. ShRNAs are recognized by Drosha and Dicer in the host cells and thus processed into siRNAs, mediating stable RNAi that is passed on to the progeny.

This very fast and straightforward approach however also involves some difficulties. Although the degradation of mRNA is only possible on the prerequisite of perfect complementarity, unspecific effects could be due to impaired translation of non-targets[187]. Thus controls with a second shRNA are needed if applicable to compass these specific off-target effects and to exclude effects caused by the integration. Also nonspecific off-target effects were described, as long dsRNAs activate the anti-virus response in cells and can also have other toxic effects. However shRNAs have been shown to be less immunogenic than siRNAs, since they are generated by the endogenous processing machinery[188].

As lentiviral transgenesis is not integration site-specific, the so-called position-effect variegation has to be taken into account. Depending on the site of integration, the overall expression and the expression in distinct cell subsets can vary considerably[189].

Still the advantages of this method for our purpose to analyze candidate genes in the NOD mouse model outweigh these pitfalls, that can be addressed by carefully applying controls, and give us the possibility to explore the pathways behind the T1D associated polymorphisms.

4 Aims

4.1 Functional study of sCTLA-4 in type 1 diabetes

One susceptibility gene of human T1D is *CTLA4*. The susceptibility allele reduces the expression of sCTLA-4. Using lentiviral gene transfer, we are targeting the splice isoform sCTLA-4 specifically in NOD mice by RNAi and thereby mimicking the human susceptibility locus in these mice. This will give us the opportunity to explore the outcome of reduced sCTLA-4 on the development of T1D and the role of sCTLA-4 in the immune system in general.

4.2 Functional study of CLEC16A in type 1 diabetes

Not much is known about CLEC16A except that it is associated to several autoimmune diseases and it is expressed in immune cells, including DCs, B cells and natural killer cells. Again by the use of lentiviral RNAi we aim to downregulate the mRNA expression of that gene to be able to study its function in the NOD background.

5 Material

5.1 Antibodies

5.1.1 Cell culture

Antigen	Clone	Concentration	Supplier
CD16/32 (FcgR3/2)	93	1 mg/ml	eBioscience
CD28	37.51	1 mg/ml	eBioscience
CD3ε	145-2C11	0,5 mg/ml	eBioscience
CD40	HM40-3	0,2 mg/ml	eBioscience
IgM	eB121-15F9	0,5 mg/ml	eBioscience

5.1.2 Flow Cytometry

Antigen	Fluorochrome	Clone	Dilution	Supplier
Annexin V	APC		1:100	BD
Annexin V	PE		1:100	BD
B220 (CD45R)	APC	RA3-6B2	1:300	BD
B220 (CD45R)	PE	RA3-6B2	1:300	BD
B220 (CD45R)	APC eFluor 780	RA3-6B2	1:400	eBioscience
CD11b	PE	MI/70		BD
CD11b	PECy7	MI/70	1:800	BD
CD11b	eFluor 450	MI/70	1:1600	eBioscience
CD11c	APC	HL3	1:300	BD
CD11c	PECy7	HL3	1:1600	BD
CD11c	eFluor 450	N418	1:200	eBioscience
CD16/32 (FcgR3/2)	APC	93		eBioscience
CD19	eFluor 450	1D3	1:1600	eBioscience
CD25	Biotin	7D4		BD
CD25	PECy7	PC61		BD
CD25	PerCP-Cy5.5	PC61		BioLegend

CD25	APC	PC61.5		eBioscience
CD25	PerCP-Cy5.5	PC61.5	1:300	eBioscience
CD3ε	FITC	145-2C11		BD
CD3ε	PE	145-2C11	1:300	BD
CD3ε	PerCP	145-2C11	1:200	BD
CD3ε	V500	500A2	1:800	BD
CD3ε	PerCP-Cy5.5	145-2C11		BioLegend
CD3ε	Brilliant Violet 421	145-2C11		BioLegend
CD4	Alexa 647	RM-4-5		BD
CD4	APC-Cy7	GK1.5	1:800	BD
CD4	PerCP-Cy5.5	RM4-5	1:800	BD
CD4	V500	RM4-5	1:1600	BD
CD4	Brilliant Violet 421	GK1.5		BioLegend
CD4	APC	RM4-5	1:800	eBioscience
CD40L (CD154)	PE	MR1		BD
CD44	PECy5	IM7	1:3000	BD
CD45	eFluor 450			
CD45RB	PE	C363.16A	1:1600	eBioscience
CD5	PE	53-7.3	1:300	BD
CD62L	FITC	MEL-14		BD
CD62L	PE	MEL-14	1:200	BD
CD62L	APC-Cy7	MEL-14		BioLegend
CD69	PECy7	H1.2F3	1:300	eBioscience
CD80	Biotin	16-10A1		BD
CD80	APC	16-10A1	1:1600	eBioscience
CD86	Biotin	GL1		BD
CD86	APC	GL1	1:1600	eBioscience
CD86	PE	GL1	1:1600	eBioscience
CD8α	APC	53-6.7	1:800	BD
CD8α	PE	53-6.7	1:800	BD
CD8α	PECy7	53-6.7	1:800	BD
CD8α	eFluor 450	53-6.7	1:1600	eBioscience
CTLA-4 (CD152)	PE	UC10-4F10-11	Intra-cellular:1µg	BD

CTLA-4 (CD152)	PE	UC10-4B9	Intra-cellular:1µg	eBioscience
EpCAM	PE-Cy7	G8.8	1:3200	eBioscience
F4/80	PECy5	BM8	1:400	eBioscience
F4/80	APC	BM8		eBioscience
Foxp3	APC	FJK-16s		eBioscience
Foxp3	PE	FJK-16s		eBioscience
GITR	APC	DTA-1	1:300	eBioscience
GITR-L	Biotin	eBio YGL386		eBioscience
Gr-1 (Ly 6G/C)	PE	RB6-8C5		BD
IgD	PE	11-26c.2a		BD
IgM	PE-Cy7	R6-60.2	1:200	BD
Ly51 (BP-1)	PE	6C3	1:800	eBioscience
PI	Purified/FG		1µl/ $1x10^6$ cells	BD
RT1B (I-Ag7)	PerCP	OX-6	1:800	BD
SA	APC			BD
SA	PE			BD
SA	PerCP-Cy5.5			BD
TCR Vβ 8.3	PE	8C1	1:50	BioLegend
TCR Vβ11	PE	RR3-15	1:100	BioLegend
TCR Vβ12	PE	MR11-1	1:400	BioLegend
TCR Vβ13	PE	MR12-4	1:50	BioLegend
TCR Vβ2	PE	B20.6	1:50	BioLegend
TCR Vβ5.1, 5.2	PE	MR9-4	1:400	BioLegend
TCR Vβ6	PE	RR4-7	1:100	BioLegend
TCR Vβ7	PE	TR310	1:100	BioLegend
TCR Vβ8.1, 8.2	PE	KJ16-133.18	1:100	BioLegend
TCR Vβ9	PE	MR10-2	1:400	BioLegend
TCRβ	APC	H57-597	1:300	BD
TCRβ	Biotin	H57-597		BD
TCRβ	APC eFluor 780	H57-597		eBioscience
TCRβ	PerCP-Cy5.5	H57-597	1:300	eBioscience
Zap70 pY319	Alexa 647	17A/P-ZAP70		BD

5.1.3 Western Blot

Antigen	Conjugated	Dilution	Host	Supplier
CLEC16A	no	1:1000	rabbit	Provided by Lucy Davison, Lab John Todd, Cambridge, UK
Rabbit IgG	HRP	1:2000	goat	Santa Cruz
Biotin	HRP	1:3000		New England Biolabs
Tubulin	no	1:1000	rat	abcam
Rat IgG	HRP	1:3000	donkey	Jackson ImmunoResearch

5.2 Biological Material

5.2.1 Bacteria

Species	Strain	Supplier
E.coli	DH5 alpha MAX	Invitrogen
E.coli	Novablue	Novagen
E.coli	TOP 10	Invitrogen

5.2.2 Cell lines

Cell line	Properties	Supplier	Origin
293 F	fast growing		
293 FT	Fast growing, transformed with SV40 large T antigen, highly transfectable		
293 H	better adherence		

5.2.3 Mouse lines

Line	Genotype	Supplier
C57BL/6	WT	Charles River
NOD	WT	Taconic
NOD	CLEC16A KD #3	were bred in house
NOD	sCTLA-4 KD	
NOD.Idd5	WT	Taconic

NOD.Idd5	sCTLA-4 KD	were bred in house
NOD.SCID	WT	Taconic

5.3 Buffers and Media

5.3.1 Bacteria Culture and DNA preparation

LB Medium:

- 10 g Trypton
- 10 g Yeast Extract
- 5 g Sodium Chloride

ad 1 l dH_2O

adjust to pH 7,0 with NaOH

for selection: add Ampicillin, final concentration 50µg/ml

LB Agar for plates:

- 8 g Agar
- 500 ml LB Medium

for selecting plates: add Ampicillin, final concentration 100 µg/ml

Buffers Mini Preparation:

P1:

- 50 mM Tris-HCL pH 8,0
- 10 mM EDTA
- 100 µg/ml RNase A

in dH_2O

P2:

- 200 mM NaOH
- 1% (w/v) SDS

in dH_2O

P3:

- 3 M Kalium-Acetat

in dH_2O

adjust to pH 5,5 with acetic acid

TAE (50x):

- 242 g Tris
- 57,1 ml Acetic acid
- 100 ml 0,5 M EDTA pH 8,0

ad 1 l dH_2O

DNA Sample Buffer (6x):

- 0,25% Bromine Phenol Blue
- 0,25% Xylene Blue
- 30% Glycerol

in dH_2O

5.3.2 Cell culture

293 HEK cell Medium:

- 10% (v/v) Fetal calf serum (FCS, Invitrogen)
- 2 mM L-Glutamin (Invitrogen)
- 50 U / µg /ml Penicillin / Streptomycin (Invitrogen)

in DMEM (Dulbecco´s modified eagle´s medium, Invitrogen)

Lymphocyte Medium RPMI10:

- 10% (v/v) Fetal calf serum (FCS, Invitrogen)
- 2 mM L-Glutamin (Invitrogen)
- 50 U / µg /ml Penicillin / Streptomycin (Invitrogen)
- 55 µM β-Mercaptoethanol (Invitrogen)
- 10mM HEPES (Invitrogen) 1M

- 1 mM Sodium Pyrovate (Invitrogen)

in RPMI1640 (Roswell Park Memorial Institute medium, Invitrogen)

5.3.3 Cell seperation and flow cytometry

ACK lysis buffer:

- 8,29 g NH_4Cl
- 1 g $KHCO_3$
- 37,3 mg Na_2EDTA
- 1 l dH_2O

pH 7,2 – 7,4

Annexin binding buffer:

- 10 mM HEPES
- 150 mM NaCl
- 5 mM KCl
- 1mM $MgCl_2$
- 1,8 mM $CaCl_2$

ad dH_2O

pH 7,4 (NaOH)

Dynabead separation buffer:

- 0,1% BSA
- 2 mM EDTA

ad PBS pH 7,2

filter sterile

MACS buffer:

- 0,5% FCS
- 2 mM EDTA

ad PBS pH 7,2

filter sterile

PBS.EDTA for blood collection:

- 2 mM EDTA

ad PBS pH 7,2

5.3.4 ELISA

Wash solution for ELISA (PBS.Tween 0,05%)

- 500 ml 10x PBS
- 2,5 ml Tween 20

ad 5 l dH_2O

5.3.5 Western Blot

Reagent	Supplier
Antioxidant	Invitrogen
MOPS Buffer	Invitrogen
NuPAGE LDS Buffer	Invitrogen
RIPA Buffer	Sigma
Protease Inhibitor Cocktail	Sigma
Sample Reducing Agent	Invitrogen

Transfer buffer:

- 2,9 g Glycine
- 5,8 g Tris
- 0,37 g SDS
- 200 ml Methanol

ad 1 l dH_2O

TBS.T:

- 6,05 g Tris
- 8,76 g NaCl
- 800 ml dH_2O

Dissolve and adjust to pH 7,5

- 500 µl Tween 20 (for 0,2% TBST)

ad 1 l dH_2O

Blocking solution:

- 5 g Milk powder (nonfat, dried)
- 100 ml 0,2 % TBS.T

5.4 Chemicals

Chemical	Supplier
Acetic acid glacial	Roth
Agar	Roth
Agarose NEEO Ultra Quality	Roth
Beta mercaptoethanol	Roth
BSA (Albumin Fraction V)	Sigma
$CaCl_2$	Roth
Chloroform	Roth
Cyclophosphamide monohydrate	Sigma
DMSO	AppliChem
dNTPs	Fermentas
Ethanol >99,5% and denatured	Roth
Ethidium bromide	Roth
EDTA	Roth
Glycerol	Roth
Glycine	Roth
HEPES	Applichem
Hydrochloric acid 37%	Roth
H^3-thymidine	Hartmann analytic
Isofluran	cp-pharma
Isopropanol	Roth
Ionomycin	Sigma
KCl	Roth
$KHCO_3$	Roth

Methanol	Roth
Milk powder (nonfat, dried)	Applichem
$MgCl_2$	Roth
NaCl	Roth
Na_2EDTA	Roth
$NaHCO_3$	Sigma
$Na_2HPO_4x2H_2O$	Roth
$NaH_2PO_4xH_2O$	Roth
NaOH	Roth
NH_4Cl	Roth
PFA reagent grade	Sigma
PMA	Sigma
SDS	Roth
Sodium azide	Roth
Tris	Roth
Tris-HCl	Roth
Tween20	Roth

5.5 Consumable supplies

Consumable	**Supplier**
Bis/Tris Polyacrylamide precast gels (NuPAGE®, 4-12%, 1mm x 10/15)	Invitrogen
Cell culture plates 96 well (Flat, U, V bottom)	BD
Cell culture plates 24 well	BD
Cell culture plates 6 well	BD
Cell culture plates 10 cm	BD
Cell culture plates 15 cm	BD
Cover slips	Hartenstein
Cryotubes	Hartenstein
Diastix	Roche
Filter mats	PerkinElmer
Filter sterile 0,45µm	VWR
Glass ware	VWR

Glass slides	Hartenstein
Gloves	VWR
Injection Needles	Hartenstein
Magnets	VWR
Microseals for reaction plates	Applied Biosystem
Nitrocellulose	BioRad
Parafilm	Pechiney
Pipettes (5ml, 10ml, 25 ml)	VWR
Reaction plates 96 well white	VWR
Reaction plates 384 well clear optical	Applied Biosystems
Reaction tube 1, 5 ml	Starlab
Reaction tube 15ml / 50 ml	BD
Reaction tube round bottom	BD
Syringes	VWR
Tips	TipOne, Starlab
Ultracentrifuge tubes	Beckman
Whatman paper	VWR

5.6 Enzymes

5.6.1 DNA Enzymes

All Enzymes were used with accompanying buffers:

Enzyme	**Properties**	**Supplier**
BamHI	Restriction Endonucleases	Fermentas
BsrGI		
CIAP	Phosphatase	Fermentas
DNase I	Deoxyribonuclease I	Invitrogen
EcoRI	Restriction Endonucleases	Fermentas
KpnI		
NheI		
PacI		New England Biolabs
Pfu	DNA Polymerases	Fermentas
Taq (Dreamtaq)		

T4 Ligase	DNA Ligase	
XbaI	Restriction Endonucleases	
XhoI		

5.6.2 Collagenases and Cell culture Reagents

Reagent	Properties	Supplier
Collagenase D	Collagenase	Roche
Dispase I	Collagenase	Roche
eFluor 670	Proliferation dye	eBioscience
FCS	Fetal calf serum	Invitrogen
HEPES	Cell medium supplement	Invitrogen
L-Glutamine	Cell medium supplement	Invitrogen
Liberase Blendzyme II	Collagenase	Roche
LPS	Lipopolysaccharide	Sigma
Penicillin /Streptomycin	Antibiotics	Invitrogen
Snarf	Proliferation dye	Invitrogen
Sodium Pyrovate	Cell medium supplement	Invitrogen
TGFβ	Transforming growth factor	R&D
Trypan Blue Stain	Cell dye	Invitrogen
Trypsin	Serine protease	Invitrogen

5.7 Equipment

Device	Supplier
Agarose Gel chamber	BioRad
Beta counter MicroBeta^2	PerkinElmer
Bio Image Reader Mulitimage III	Alpha Innotech
Blotting Chamber	BioRad
Centrifuge MiniStar	VWR
Centrifuge 5810R	Eppendorf

Centrifuge 5424	Eppendorf
ELISA Reader	
FACS Aria II	BD
Flow Cytometer FACS Canto	BD
Freezer / Fridge	Liebherr
Freezer -80°C Hera Freeze	Thermo
Gel Imager	Herolab
Harvester	PerkinElmer
Heating plate	Heidolph
Hemacytometer	Hartenstein
Homogenizer Polytron	Kinematica
Incubator Bacteria	Thermo Electron Corporation
Incubator Cell culture	Thermo Electron Corporation
Laminar Flow	Luft & Reinraumtechnik GmbH
Luminometer	bMG Labtech
Microscope Axiovert 40CFC	Zeiss
Microwave	Bomann
pH Meter	Mettler Toledo
Photometer	Implen
Pipettes (P2, 10, 200, 1000)	Gilson
Pipetus	Hirschmann Laborgeräte
Power Supply Unit	BioRad
Protein Gel Chamber Mini	Invitrogen
Rocker Switch	Heidolph
Scale	Kern & Sohn GmbH
Scale (special accuracy)	Mettler Toledo
Thermoblock	Eppendorf
Thermocycler PXE 0.2	Thermo Electron Corporation
Thrmocycler (real time)	Applied Biosystems
Ultracentrifuge	Beckman Coulter
Vaccuum pump	VWR
Vortex Genie 2	Scientific industries
Waterbath	Julabo

5.8 Kits

Kit	Supplier
Cytometric Bead Array Flex Sets	BD
DNeasy blood and tissue kit	Qiagen
Dual luciferase system	Promega
Dynal CD8 isolation Kit	Invitrogen
Dynal	Invitrogen
ECL	Perkin Elmer
FoxP3 staining kit	eBioscience
Gel purification kit	Qiagen
MACS Separation Kit CD4	Miltenyi
MACS Separation Kit CD4+ CD25+	
MACS Separation Kit CD4+ CD62L+	
MACS Separation Kit CD43	
MACS Separation Kit Pan T cells	
Maxiprep kit	Qiagen
PCR Purificatio Kit	Qiagen
RNeasy Kit	Qiagen
Transcriptor first strand DNA synthesis kit	Roche
Trizol	Invitrogen
Universal probe library (UPL) probes	Roche
Universal probe master mix (ROX)	Roche

5.9 Primer and shRNAs

5.9.1 qPCR Primer

Clec16a / UPL 7

fwd: 5’-TGTCCACCTTGTACGTCATTTC-3’

rev: 5’-TGTACTCATCTTCAAACATGTCCA-3’

Clec16a / UPL 9

fwd: 5’-AACAGATGATGTCTTGGATCTGAA-3’

rev: 5'-AACCGCTGGACCATACCAC-3'

GAPDH / UPL 9

fwd: 5'-AGCTTGTCATCAACGGGAAG-3'

rev: 5'-TTTGATGTTAGTGGGGTCTCG-3'

5.9.2 shRNAs

Target sequences :

sCTLA-4:

GCAGATTTATGTCATTGCTAAA

Clec16a #1:

CGTGGAGTATCTCATGATGGAT

Clec16a#2:

ATCTGGCTGTGTCATCAAGGAT

Clec16a#3:

AACCTTGTACGTCATTTCTATA

Ordered shRNA oligo sequences:

TGCTGTTGACAGTGAGCG–target sense –TAGTGAAGCCACAGATGTA –target antisense –TGCCTACTGCCTCGGA

5.10 Software

Software / Website	Supplier / Web address
Adobe Photoshop CS2	Adobe Systems Inc.
ApE – A plasmid editor	M.Wayne Davis
Bio Gene Portal System	Biogps.org
Ensembl Genome Browser	www.ensembl.org
Expasy Prosite	prosite.expasy.org
FACS Diva	BD
FlowJo 9.2	Treestar Inc.

Mac OS X 10.5.8	Apple Inc.
Microsoft Office 2004 for Mac	Microsoft Corporation
National Center for Biotechnology Information	www.ncbi.nlm.nih.gov
Prism	Graph Pad
TM pred – Prediction of Transmembrane Regions	www.ch.embnet.org

5.11 Standards

Standard	**Supplier**
DNA ladder 1Kb plus	Fermentas
DNA ladder low range	Fermentas
See Blue Plus 2 Pre Stained Standard	Invitrogen
Biotinlyated Protein Ladder Detection Pack	Cell Signaling

6 Methods

6.1 Microbiological methods

6.1.1 Liquid overnight culture

For mini-preparations bacteria were grown overnight in 3ml LB-medium in a sterile Falcon Polypropylen tube. The LB-medium was supplemented with 50µg/ml Ampicillin. The medium was inoculated with a single bacteria colony picked from an LB/Amp-Agar-plate and grown in an incubator over night at 37°C and 220rpm.

An overnight culture for maxi-preparations had a volume of 100ml LB/Amp-medium and was inoculated with 100-200µl of a 3ml starter-culture. The maxi-culture was also grown over night at 37°C with 220rpm.

6.1.2 LB-Agar-Plates

To select bacteria, which had been transformed with Ampicillin-resistance containing plasmids, 150µl bacteria-suspension were plated out on Ampicillin containing LB-Agar-plates. The final-concentration of Ampicillin in the plates was 100µg/ml.

6.1.3 Transformation

Approximately 5-10 ng of ligated vector or plasmid stock for retransformation were added to competent cells. NovaBlue cells were used for cloning and DH5 or TOP10 for retransformation. After 20 minutes incubation on ice, the cells were subjected to a heat shock at 42°C for 90 seconds. They were plated out on LB/Amp Agarplates immediately after cooling down and adding 150µl LB-medium.

6.2 Molecular biological methods

6.2.1 DNA precipitation

In order to precipitate DNA, cations are added binding to the negatively charged pospho-backbone. The cations are added as a salt to the solution. By exchanging the Water for Ethanol as a solvent the DNA precipitates as insoluble salt.

Protocol:

½ volume 6M NaCl was added to the DNA solution, shaken vigorously and incubated on ice for 10 minutes. Insoluble components were then spun down for 10 minutes at 5000g. The supernatant, containing the DNA was then transferred to a new tube, where 1,3 volumes isopropanol were added. The tube was inverted and then incubated for 15 minutes at room temperature. The DNA could then be spun down at maximum speed for 10 minutes. Supernatant was removed and the pellet left for air drying for about five minutes. Finally the pellet was reconstituted in sterile H_2O.

6.2.2 Agarose gel electrophoresis of DNA

Ususally 1% Agarose (for separation of smaller fragments: 1,5 -2%) were dissolved in TAE buffer by boiling. 3 µl of ethidium bromide were added after the solution had cooled down for 2 minutes. Before loading the DNA into the wells, it was mixed with a 6x loading dye containing bromphenol blue. The separation was usually conducted at 100 V. The DNA was observed on UV-light box.

6.2.3 PCR (Polymerase chain reaction)

6.2.3.1 Standard PCR

By polymerase chain reaction specific DNA fragments can be amplified. Both DNA strands are firstly denatured to allow specific oligonucleotides (primer) to anneal to their corresponding sequence. Emanating from these begins the 5'-3' strand-elongation through thermoresistant polymerases upon usage of dNTPs and magnesium.

For analytical purposes the Taq polymerase (from thermophilus aquaticus) was used. It amplifies 1000 nucleotides per minute and creates an adenosine- 3'-overhang. Moreover it does not possess a proof reading ability.

However to amplify with a high accuracy, for preparative purposes, Pfu-polymerase was used. It possesses a proof reading ability and amplifies 500 nucleotides per minute.

Pipetting instruction:

100ng Template

1µl Primer forward (10µM)

1µl Primer reverse (10µM)

5µl Polymerase buffer (10x)

1µl dNTPs (10mM)

0,5µl Polymerase (Pfu Polymerase or DreamTaq™, both Fermentas)

ad 50µl H_2O

The thermocycler-protocol was adapted each time to the individual PCR-reaction, adjusting the annealing-temperature, elongation time and cycle number.

1 Cycle	initial denaturation	2 min	95°C
25-35 Cycles	denaturation	30 s	95°C
	primer annealing	30 s	temperature primer-dependent
	elongation	1 min per 1000 bp (Taq) 2 min per 1000 bp (Pfu)	72°C
1 Cycle	final elongation	10 min	72°C
1 Cycle	cooling	∞	4°C

6.2.3.2 Colony – PCR

Colony-PCR is a fast and easy method to check if a plasmid with insert is present in selected transformed bacteria-clones. The principle is equal to a standard PCR, except that bacteria clones are directly used as template, instead of purified DNA. Clones are picked with a sterile tip from a plate and the tip is first swiveled in sterile dH_2O and then put into 3ml of LB-Amp Medium to be able to grow positive clones subsequent to testing for inserts. The H_2O-bacteria suspension is then used in a PCR reaction with primers specific for the inserted DNA-sequence.

6.2.3.3 Reverse transcription PCR (RT-PCR)

Reverse transcription PCR is used to transcribe mRNA into cDNA using the enzyme reverse transcriptase.

RT-PCR was conducted using the RETROscript® Kit (Ambion) according to manufacturers instructions.

6.2.3.4 Sequencing of DNA

Sequencing of DNA, based on a chain termination-reaction[190] was conducted by the company *eurofins mwg operon*.

6.2.4 Purification of plasmid DNA

The methods of purification of plasmid DNA out of bacteria clones are based on the principle of alkaline lysis. Proteins, chromosomal and plasmid DNA are thereby precipitated. Spinning down clears the solution of proteins and chromosomal DNA, whereas RNA is degraded by the use of RNases.

For Maxi-preparations the QIAfilter Plasmid Maxi Kit© was applied. It is also based on alkaline lysis, the spinning step however is replaced by application of an anion-exchange-resin. DNA binds to that resin at low salt and low pH condition and can after washing with a medium salt buffer be eluated by a high salt solution.

6.2.5 DNA extraction from tissue samples

To obtain DNA from tissue samples like ear or tail pieces they were first digested with an appropriate amount of digestion buffer (ALT buffer, Blood and Tisssue Kit, Qiagen; 90µl for ear samples) and proteinase K (10µl for ear samples). Digestion was carried out at 56°C for about 5 hours, with regular vortexing inbetween. Following the DNA was precipitated.

6.2.6 Gel extraction of DNA

To extract DNA out of an agarose gel, the QIAquick Gel Extraction Kit© was used, according to manufacturers instructions.

6.2.7 Purification of digested vectors and PCR-products

To clear DNA from buffers used in restriction digest or PCR QIAquick PCR Purification Kit© was used, according to manufacturers instructions.

6.2.8 Photometric concentration-measurement of DNA

DNA concentration was measured per photometer by absorption at a wavelength of 260 nm. This is the maximal absorption for nucleic acids. The purity of DNA can be detected by taking the ratios of $OD_{260/280}$ and $OD_{260/230}$. Absorption at 280 nm shows contamination through proteins, at 230 nm through peptides, aromatic compounds and carbohydrates. The ratios for pure nucleic acids should be: $OD_{260/280} = 1,8$ and $OD_{260/230} = 2,0$.

6.2.9 Restriction digest of DNA

Restriction endonucleases of type II cut DNA specifically at a defined, mostly palindromic sequence motive of 4-6 nucleotides length. The double strand cleavage is hydrolytic and gives rise to either a blunt, 5' or 3' sticky end.

Pipetting instruction:

2µg DNA

2µl Buffer (10x)

0,3µl Restriction enzyme

(optional 0,3µl second restriction enzyme)

ad 20µl H_2O

The mixture was incubated at 37°C for 2-3h.

6.2.10 Dephosphorylation

In order to avoid religation of a digested vector, the generated 5' ends were dephosphorylated by calf intestine phosphatase (CIAP).

1µl of CIAP was added 1h before the end of the restriction digest. After the incubation period, the enzyme was inactivated at 85°C for 10 minutes.

6.2.11 Ligation of DNA fragments

Ligation connects DNA-fragments with complementary DNA-overhangs. The enzyme working in this process is the T4-Ligase. It creates a new phosphodiester bond in the DNA-backbone under usage of one ATP molecule. For a successful ligation, vector and insert have to be available in stoichiometric amounts. A 1:4 ratio has proved to be suitable.

Pipetting instruction:

100ng Vector

4 x Insert

1µl T4 Ligase (Fermentas)

1µl T4 Ligase buffer

ad 10µl H_2O

The incubation was carried out for 4 hours at room temperature.

6.2.12 RNA isolation from organs

Mice were sacrificied by isofluran inhalation. After disinfection of the fur the internal cavity was exposed and organs of interest taken out. They were directly put into 1ml of Trizol, immediately homogenized and processed according to manufacturer's instructions.

6.2.13 DNAse I treatment of RNA

In order to prevent false positive signals in the quantitative PCR a DNase I digest was performed. For this the DNase I from Fermentas was used according to manufacturer's instructions.

6.2.14 cDNA production

The DNase I digested RNA was used to produce cDNA via the Roche Transcriptor First Strand cDNA Synthesis Kit. OligodT Primer as well as Random Hexamers bind to RNA and form the starting point for the Reverse Transcriptase to synthesize cDNA.

6.2.15 Quantitative real time PCR

Measuring the amount of mRNA in cells or tissues is possible via quantitative real time PCR. In addition to the conventional PCR method, it includes the binding of fluorescent probes to the template cDNA. The probes used in this report were obtained from the Universal Probe Library (UPL) from Roche. These are labeled at the 5' end with a FAM reporter and are quenched by a dark quencher at the 3' end. As the probe anneals together with the primers to the cDNA template, it is degraded by the 5'-3' exonuclease activity of the Taq polymerase. By this, the FAM reporter is set free and gives a fluorescent signal that is detectable via Laser excitation and increases together with the product during the PCR. To enable a relative quantification, a reference gene, here GAPDH, was measured along with the gene of interest.

Procedure:

Pipetting instruction:

5µl 2x Fast Start Universal Probe Master (Rox) (Roche)

0,4µl Primer fwd (10µM)

0,4µl Primer rev (10µM)

2,1µl H_2O

0,1µl UPL Probe (10µM)

2µl cDNA (diluted 1:2)

The reaction was conducted in a 384 well plate that was closed with adhesive seals and shortly spun down prior to the reaction. Usually Triplets were measured.

PCR protocol:

1 Cycle	initial denaturation and hot start of Taq Polymerase	10 min	95°C
40 Cycles	denaturation	15 s	95°C
	primer /probe annealing and elongation	1 min	60°C

In the result analysis the threshold cycles (Ct), the cycles in which the fluorescent signal of a sample rises above the background signal, of reference samples and target samples were put in relation to obtain a relative quantification.

$$\Delta Ct = Ct_{target} - Ct_{reference}$$

6.3 Protein biochemistry

6.3.1 Preparation of protein lysates from cells

Suspension cells could be spun down and resuspended in RIPA buffer, supplemented with Protease Inhibitor Cocktail (x10; Sigma) and DNase I (x1000; Invitrogen). For up to 5 million cells 60µl of this homogenization buffer was added. All samples were kept on ice for 15 minutes and vortexed intermittently. Subsequently the samples were spun down again and the supernatants transferred to a new tube. The lysates were stored at -80°C.

6.3.2 Preparation of protein lysates from tissues

Tissues, e.g spleen, were homogenized on ice with a rotor-stator homogenizer in 500µl RIPA buffer, supplemented with Protease Inhibitor Cocktail. Following procedures were conducted as described in the previous section.

6.3.3 Quantification with bicinchoninic acid (BCA) assay

A small protein lysate aliquot was reserved for protein quantification by using the BCA assay, since the RIPA buffer does not interfere with it. The Novagen® BCA Protein Assay Kit (Merck) was used according to manufacturer's instructions.

6.3.4 Protein Gel Electrophoresis

Proteins can be separated by size via gel electrophoresis. In this report the NuPAGE® Bis/Tris Precast Gel System (Invitrogen) was used, which is based on the traditional SDS-PAGE system according to Laemmli[191]. However the lower pH of the NuPAGE® system ensures higher protein stability, which was crucial for the detection of CLEC16A. To further provide stability, all samples were defrosted and kept on ice only shortly before starting the procedure. Reducing agent (10x) and NuPAGE® 4x LDS Buffer (both Invitrogen) were added prior to denaturing the samples at 70°C for five minutes. Following the samples were cooled down for five minutes on ice and then spun down. The supernatants were loaded onto a NuPAGE® 10 well 1.0mm 4-12% Bis Tris gel that was set up with MOPS buffer and antioxidant (both Invitrogen) in the running unit. The separation was then conducted at 200V for about one hour.

6.3.5 Western Blot

Transfer of proteins from an acrylamide gel to a membrane, here nitrocellulose, is possible by using the method of western blotting. Here the proteins migrate again along an electrical field towards the anode. The migration takes place in a tank blot chamber, which is filled with transfer buffer. In order to ensure an even transfer, all components of the assembly had to be

pre soaked in transfer buffer and be built up without air bubbles. The transfer was carried out at 100V for one hour in the cold room.

6.3.6 Detection of proteins on membranes

Detection of specific proteins on nitrocellulose membranes is possible by staining with specific antibodies. To prevent unspecific binding the membrane first had to be blocked in 5% milk powder in TBS-T 0,05% (blocking buffer) over night at 4°C.

The membrane could then be incubated for one hour at room temperature with the primary antibody, which had been diluted in 6ml blocking buffer. Subsequently the membrane was rinsed in dH_2O and washed three times for ten minutes with TBS-T 0,2% (wash buffer). After that the incubation with the matching horse radish peroxidase (HRP)-coupled secondary antibody was carried out again in 6ml blocking buffer for one hour at room temperature. Excess Antibody was washed from the membrane again by rinsing with dH_2O and washing three times with wash buffer.

To detect the signal of the HRP, the membrane was dried with tissue and then incubated for one minute with enhanced chemiluminescence reagent. It contains luminol that is catalyzed by the peroxidase under emission of light. For luminescence detection the… was used.

6.3.7 Luciferase Assay

The *in vitro* validation of the knockdown efficiency of a specific shRNA was tested by performing a luciferase assay. 293F cells were plated out on a 24-well plate at a density of 2,5 x 10^5. The next day they were cotransfected with 300ng of the shRNA construct as well as with 100ng of the reporter plasmid psiCHECK2 carrying the target cDNA.

The psiCHECK2 vector contains sequences for two luciferases, Renilla and Firefly. The Firefly sequence is expressed constitutively and serves for normalization purposes. The Renilla luciferase is however expressed together with the target cDNA in a bicistronic mRNA and gets degraded alongside the target sequence if the an appropriate shRNA is added.

After two days incubation the cells were washed once with PBS and are then lysed with passive lysis buffer (Promega). The luciferase activity was measured in an opaque 96 well plate, using 5µl of the cell suspension and the Dual-Luciferase® system (Promega). The measurement was carried out in a Fluostar Optima luminometer.

6.3.8 Enzyme-linked immunosorbent assay (ELISA)

ELISAs were performed for measuring IFNγ and IL-2 levels. Matching Ready-Set-Go!® Kits from eBioscience were used according to manufacturers instruction.

6.3.9 Cytometric Bead Array (CBA)

Multiple cytokines could be measured simultaneously by using the Cytometric Bead Array® System from BD. IL1, IL-2, IL-4, IL-6, IL10, IL-12, IL17A, TNF and IFNγ were detected by using this method. Briefly, antibodies, bound to uniquely labeled beads, bind to soluble proteins and thus make it possible to detect them via flow cytometry. A second antibody, labeled with another fluorophore binds to the bead-bound protein and shows the abundance of it via its mean fluorescent intensity. The Kit was used according to manufactures instructions, however amounts of buffers and samples were reduced to one fifth of the suggested volumes. Results were analyzed with the FCAP Array® software (BD).

6.4 Cell biological methods

All eukaryotic cell lines as well as primary cells mentioned in this report were cultured in the appropriate media at 37°C and 5% CO_2. Spinning, if not explicitly described otherwise, was always carried out at 453g for 7 minutes at 4°C. All media were preheated to 37°C before use and were sterile.

6.4.1 293F Cell line

The 293F cell line is derived from human embryonic kidney cells and is a fast growing variant of the standard 293 cell line. It was maintained on advanced DMEM supplemented

with 10% FCS, penicillin / streptomycin and glutamine. Cells were passaged every 3 days in a 1:10 ratio. Ideally the cell density did not exceed 80%.

6.4.2 Evaluation of cell density

Cell density was quantified via a Neubauer hemocytometer. The cells were resuspended and mixed (mostly in a 1:10 ratio) with trypan blue. The staining allows to distinguish between living and dead cells, since the dye only enters dead cells. Per definition one quadrant of the hemocytometer has a volume of 0,1 µl.

From the number of cells in one quadrant the cell concentration in the cell suspension can be calculated. To minimize the statistical error, four quadrants were counted.

$$D = N/Q \times V \times 10^4$$

with: D = cell concentration per ml

N = number of counted cells

Q = number of counted quadrants

V = dilution factor of cells (mostly 10)

6.4.3 Transfection of eukaryotic cells

Introduction of foreign DNA, in this case plasmid DNA, into eukaryotic cells is called transfection. The transfection agent used here was Fugene 6© (Roche), a cationic lipid. After mixing this reagent with plasmids, it coats and condenses them by electrostatic association. The overall positively charged complexes associate with negatively charged cell surfaces and are internalized via endocytosis. Eventually the lipids provided in the transfection agent work in destabilizing the endosomal membrane by inducing non-bilayer lipid structures. By this cytoplasmatic delivery of the introduced plasmids is facilitated [192].

Protocol:

On day 0 confluent 293F cells were split in a 1: 2,5 ratio onto a new cell culture plate. They reached 80% confluence on the next day on which they could be transfected with the

plasmids of interest. These were premixed with serum free medium and Fugene 6. After 30 minutes of incubation at room temperature the mixture was added drop wise to the cells. Depending on the size of the culture plate, different amounts of DNA and transfection reagent were used:

- 20 cm plate: 35 µg DNA with 70 µl Fugene 6 in 1ml serum free medium
- 10 cm plate: 10 µg DNA with 30 µl Fugene 6 in 500 µl serum free medium
- 6 well plate: 2µg DNA with 8 µl Fugene 6 in 150 µl serum free medium

6.4.4 Virus production

6.4.4.1 shRNA-pLBM construct

Design of the shRNAs was done by using the algorithm which is available online at http://katahdin.cshl.org:9331/homepage/siRNA/RNAi.cgi?type=shRNA. Synthetic oligos were ordered from Sigma-Aldrich. To generate a double strand, sequences were amplified per PCR and then cloned into the pLBM vector between the XhoI and EcoRI recognition sites.

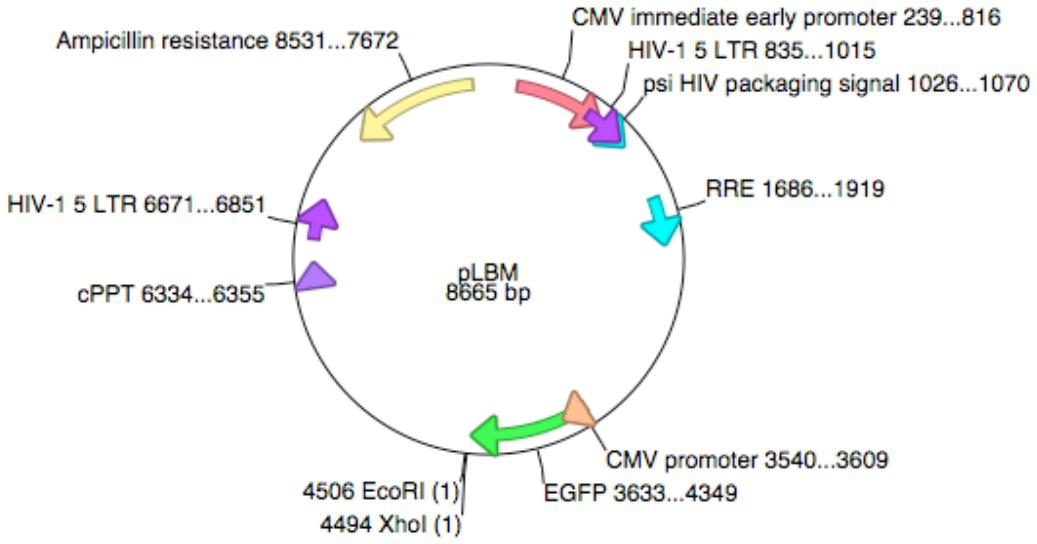

Figure 4: Map of pLBM vector

6.4.4.2 Production of lentivirus

Lentiviruses were used to introduce genes or shRNAs into the genome of cells. To produce them, 293F cells were cotransfected with the lentiviral vector, carrying the DNA sequence of interest flanked by LTRs (pLBM) and helper vectors. For production of larger amounts of virus, 20 cm plates were transfected with

- 3 µg pCMV VSVg
- 3 µg RSV-rev
- 4 µg pMDL-gag/pol rre
- 5 µg pAdvantage
- 20 µg pLBM

The cell supernatant containing the produced virus was collected 48 h and 72 h after transfection. To remove 293 cells and cell debris the supernatants were first spun down for 7 minutes at 1065g and then filtered through a 0,45µm filter. Following the supernatants were ultra centrifuged for 90 minutes at 25000 rpm (ultracentrifuge, Beckmann), thereby concentrating the virus into the pellet. After aspirating the supernatant thoroughly and carefully, the pellet was resuspended in 100 µl sterile PBS by overnight incubation at 4°C. If not used immediately, the viral suspension was split into 25µl aliquots, frozen in liquid nitrogen and stored at -80 °C.

6.4.5 Lentivirus titration

To assess the concentration of virus particles in the concentrated virus suspension 293 F cells were infected. On day 0 they were plated out at a density of 4 x 10^5 cells / well in a 6 well plate. On the next day the cell supernatants were removed and reconstituted by a virus dilution of 1 µl virus in 1 ml fresh medium. To be able to calculate also very high virus concentrations, the cells were also infected with a 1:10 and 1:100 dilution of the initial virus suspension. On day 3 or 4 the percentage of infected cells could be assessed from GFP expression, which was quantified from FACS analysis.

6.4.6 Flow cytometry

Cell suspensions can be analyzed very specifically by means of flow cytometry. The method allows an examination of cell number, size, granularity and presence of specific antigens. These have to be stained by fluorescently labeled antibodies. Also the expression of fluorescent proteins like GFP can be analyzed.

Inside the flow cytometer a cell suspension is aspirated in a capillary in which the cells individually pass a laser beam. This causes the light to be scattered and in case of fluorescence a shift in the maximal emission to higher wavelengths. There are several detectors picking up the scattering, one in line with the laser (forward scatter, FSC) and some perpendicular to it (side scatter, SSC and fluorescence detectors). The FSC picks up the diffraction, which gives information about the particle size. The SSC however is determined by the scattering of light, defining the granularity of cells.

All measurements were done at the BD FACSCantoII™ or on the BD FACSAriaIII™. Analyzes were carried out using the FlowJo 9.2© (Tree Star) software.

6.4.6.1 Extracellular staining of cells for flow cytometry

Staining was always performed on cells in suspension. 100 µl of a cell suspension containing about 3-5 x 10^5 cells in PBS supplemented with 1% FCS (PBS 1% FCS) were if necessary first blocked with Fc-receptor block for 10 minutes at 4°C. After that the directly labeled or biotinylated antibodies could be added. The antibody dilution was titrated previously individually for every antibody. After 20 minutes incubation at 4°C in the dark, the cells were washed once with PBS 1% FCS. If needed, secondary antibodies or fluorescent labeled streptavidin was added to the cells and incubated another 30 minutes at 4°C. After the final washing step, the cells could be resuspended in 300-400 µl PBS 1 % FCS before FACS analysis.

6.4.6.2 Intranuclear staining of Foxp3

Staining of the transcription factor Foxp3 in primary murine T cells was performed using the Foxp3 staining Kit of eBioscience according to manufacturer's instructions.

6.4.6.3 Intracellular staining of *CTLA-4*

Intracellular staining was carried out on 1 x 10^6 cells per tube. The Fc-receptors were first blocked with Fc-Block for 10 minutes at 4°C. After that the surface staining was performed as described above. To fix the cells they were subsequently treated with 2% paraformaldehyde (PFA) for 10 minutes at room temperature in the dark. For a gentle permeabilisation the cells were first washed with 0,03% saponin in PBS. The staining with anti-CTLA-4 however was then conducted in 0,3% saponin, supplemented with 2% FCS. Per 1 x 10^6 cells 1µg of antibody was required. To ensure an even permeabilisation and staining the suspension was vortexed before incubation at 4°C in the dark for 30 minutes. Before FACS analysis the cells were washed twice with 0,03% saponin and once with pure PBS.

6.4.6.4 Fluorescence-activated cell sorting

Sorting of cells was conducted at the BD FACSAriaIII™ using BD FACSDiva™ Software. The nozzle size was chosen according to the type of cells being sorted. Lymphocytes were sorted with the 70µm nozzle, Macrophages by using the 85µm nozzle. Before starting to sort, the stream had to be adjusted for drop delay and spillover. Samples were acquired with a proper compensation and without a threshold value. Gates were set stringently to avoid contamination in the sorted subsets. In general, sorting precision was set to "purity".

6.5 Histology

6.5.1 Sample preparation for colon histology

For histology, mice were sacrificed by isofluran inhalation, the fur was disinfected and the internal cavity was opened. The colon was taken out in one piece from the rectum to the

caecum, mesenteric connections being removed in the process. Subsequently the colon was placed immediately in 4% PFA fixative and incubated at 4°C over night to ensure a thorough fixation.

The fixed colon could then be further processed by excising four approximately 4mm long tubes from different sections. Then the tubes were very carefully cleaned from feces without injuring the tissue.

6.5.2 Paraffin processing and embedding of tissues

Fixed and prepared colon tubes were placed in embedding cassettes and put in the processing machine over night. Here an increasing Ethanol series was operated before exchanging the medium for Xylene and then paraffin wax.

On the next day the tissues could be embedded in paraffin wax.

6.5.3 Paraffin sections

Paraffin blocks were trimmed and cut at the microtome into 3-4µm sections. Sections were then stretched on a large drop of dH_2O placed on a SuperFrost® plus glass slide (Menzel-Gläser), by putting the slides on a 37°C heating plate. After the section had stretched completely, the water was removed by applying pressure with an ethanol soaked filter paper.

6.5.4 Deparaffinization of tissue sections

Dried tissue sections were deparrafinized by incubating the slides twice for five minutes in Xylene. Following the slides were put through a descending ethanol series from 100% to 70%, incubating two minutes in each concentration. Finally the slides were put into dH_2O for 2 minutes.

6.5.5 Hematoxylin / Eosin staining (H/E staining)

The rehydrated tissue slides were immediately incubated in Hämalaun Mayer for 3 ½ minutes and then put under running tap water for ten minutes to ensure bluing of the Hematoxylin.

The slides were then dipped in dH_2O and stained in Eosin for 45 seconds. Careful not to wash away the water soluble Eosin, the slides were only dipped very shortly in dH_2O to remove excess dye and then put into an ascending ethanol series starting right away with 96% ethanol. Finally the slides were incubated twice in Xylene for five minutes and then mounted in the xylene-based medium Eukitt.

6.5.6 Colitis scoring

Scoring of colon sections for colitis was performed in a blind fashion by Dr. Alma Zernecke. The sections were scored into four stages 0-4[193]: grade 0 = no changes; grade 1 = minimal scattered mucosal inflammatory cell infiltrates, with or without minimal epithelial hyperplasia; grade 2 = mild scattered to diffuse inflammatory cell infiltrates, sometimes extending into the submucosa and associated with erosions, with minimal to mild epithelial hyperplasia and minimal to mild mucin depletion from goblet cells; grade 3 = mild to moderate inflammatory cell infiltrates that are sometimes transmural, often associated with ulceration, with moderate epithelial hyperplasia and mucin depletion; grade 4 = marked inflammatory cell infiltrates that are often transmural and associated with ulceration, with marked epithelial hyperplasia and mucin depletion[194].

6.6 Mice

6.6.1 Generation of transgenic mice

Depending on the project, B6 or NOD (non obese diabetic) single cell embryos (B6 and NOD for KIAA0350 knockdown and NOD for sCTLA-4 knockdown) were injected with the relevant virus sample containing a shRNA-bearing vector (pLBM). Living embryos were then transferred into pseudopregnant foster mice (CD1). The procedure was carried out by Nicole Hain. Successful incorporation of the shRNA could be verified by taking blood of the offspring, because of the presence of a GFP reporter in all constructs. GFP positive mice were further bred to obtain homozygous mice.

6.6.2 Diabetes monitoring

NOD mice are genetically prone to develop diabetes at 12-16 weeks of age. The onset of diabetes was determined by weekly testing of glucosuria with Diastix® (Bayer). A mouse was considered diabetic at the first of two consecutive positive results.

6.6.3 Adoptive transfer of lymphocytes into NOD.SCID mice

NOD.SCID mice are homozygous for a autosomal recessive mutation in the *Prkdc* gene. It results in a severe combined immunodeficiency, caused by a lack of functional T- and B-lymphocytes. Natural killer cells and the circulating complement system are also affected.

Lymphocytes for adoptive transfer were washed and resuspended in sterile PBS. 200µl of the cell suspension were injected into the tail vein.

6.6.4 Cyclophosphamide mediated diabetes induction

Upon administration of low dose cyclophosphamide (CY), an alkylating chemotherapeutic drug, NOD mice simultaneously develop diabetes[195-197]. The onset occurs around two to three weeks after administration and correlates with the loss of natural regulatory T cells[195,197,198]. NOD mice were injected on day 0 and day 14 with 200mg/kg cyclophosphamide. Adoptively transferred NOD.SCID mice were injected only once on day 21 after transfer.

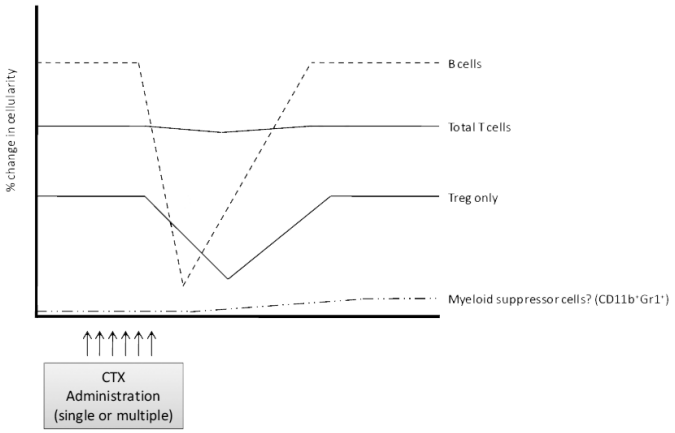

Figure 5: Impact of low dose CY treatment on lymphocyte numbers, modified from Brode and Cooke, 2008[198]

6.6.5 Colitis induction

NOD.SCID mice develop colitis upon adoptive transfer of $CD4^+CD45RB^{hi}$ lymphocytes[199]. We transferred 4 x 10^5 WT $CD4^+CD45RB^{hi}$ cells alone or with 10^5 $CD4^+CD25^+$ Tregs from WT NOD or sCTLA-4 KD NOD mice into NOD.SCID recipients. After 8-9 weeks, mice were sacrificed and histology of the colon was performed.

6.7 Immunological Assays

6.7.1 Cell-sorting using magnetic beads

Mice were euthanized by isofluran inhalation. Then, the fur was disinfected and the internal cavity exposed. Lymph nodes and spleen were dissected and ground between two rough microscope slides in 5 ml of PBS 1% FCS. For dendritic cells the spleen had to be incubated in Collagenase (Liberase Blendzyme, Roche) for 20 minutes before grinding. Erythrocytes were lysed, remaining cells washed and filtered with a 40µm filter, ensuring a single-cell suspension. This was subsequently used in different magnetic cell sorting kits (MACS®, Miltenyi or Dynabeads®, Invitrogen).

6.7.2 Proliferation assays

All proliferation assays were carried out in RPMI-10 (RPMI1640, supplemented with 10% FCS, antibiotics, glutamine, 2-Mercaptoethanol and sodium pyruvate) medium in a 96-well (U-bottom) plate.

Magnetically sorted CD4 T cells or lymphocytes were activated with different concentrations of anti-CD3, PMA/Ionomycin or beads coupled with anti-CD3 and anti-CD28.

B cells were activated with different concentrations of Lipopolysaccharide (LPS) or anti-CD40.

To assess the proliferation, 0,5µCi thymidine^{3H} (in RPMI-10) were added per well after 72h incubation at 37°C and 5% CO_2. 16h hours later the plate was harvested and incorporated radioactivity analyzed with help of a beta-counter (Perkin-Elmer).

Alernatively the cells were stained initially with Cell Proliferation Dye eFluor® 670 (eBioscience) according to manufacturers instructions. Proliferation could then be measured via flow cytometry and dilution of the dye.

6.7.3 Suppression assay

To carry out a suppression assay to assess the suppressive activity of regulatory T cells *in vitro*, effector T cells ($CD4^+CD25^-$) and Treg cells ($CD4^+CD25^+$) from young (6-8 weeks) male NOD mice were purified using MACS®. After cell purification, 25.000 effector T cells were mixed in different ratios with Treg cells (1:1 up to 1:32) in RPMI-10 supplemented with 1µg/ml anti-CD3 in a 96-Well (U-bottom) plate. Costimulation was provided by 400.000 APCs (irradiated spleen cells) per well. After 72h incubation, proliferation was assessed by incorporation of radioactively labeled thymidine.

6.7.4 Coculture of dendritic cells with Treg cells

Effector T cells (Teff, $CD4^+CD25^-$), Treg cells ($CD4^+CD25^+$) as well as dendritic cells ($CD11c^+$) were purified using MACS®. Teff asl well as Treg cells were then stained with 0,5µM CFSE. In RPMI-10 with 1µg/ml anti-CD3, cells (usually 40.000 DCs and 150.000 Tregs or Teffs or both) were mixed together in a 96-well U-bottom plate and incubated for 42h at 37°C and 5%CO_2. Before staining for flow cytometric analysis, cells and wells were treated with 3mM EDTA 1% FCS in PBS to prevent the dendritic cells from sticking to the wells and to separate dendritic cells from T cells, since they are claimed to form clusters[118].

6.7.5 Staining of phosphorylated ZAP70

Before staining of phosphorylated ZAP70 the T cells had to be activated. First a single cell suspension was created from lymph nodes. 1 x 10^6 cells were added to a FACS tube in 50µl

RPMI10 and then activated with 10µg/ml anti-CD3 (hamster anti mouse, in 50µl RPMI10). After 30 minutes incubation on ice, cells were washed with RPMI10. Next the anti-CD3 antibody was cross-linked by incubation with 10µg/ml anti-hamster (100µl in RPMI) for 15 minutes on ice. T cells were then activated in a water bath at 37°C for different periods of time. Immediately after activation the cells were fixed with 2% PFA for 5 minutes at room temperature. After a washing step cells were permeabilized by adding 0,5ml 2%PFA and 4ml Methanol and incubating 30 minutes on ice in the dark. Washing was now performed with PBS 0,5% BSA, which was then also used to block the cells for 15 minutes before adding the antibody. The antibody for ZAP-70 (20µl/ 1 x 10^6 cells) was then incubated for one hour at room temperature in the dark. Flow cytometric analysis could be carried out after a washing step with PBS 0,5% BSA.

6.7.6 *In vitro* differentiation of regulatory T cells

In order to produce induced Treg cells, naïve T cells ($CD4^+CD62L^+$) were isolated from murine lymph nodes cell suspensions via magnetic cell separation. The naïve T cells were then incubated in a 24-well plate at a concentration of 0,5 x 10^6 cells/ml with 2µg plate bound anti-CD3, 2µg soluble anti-CD28 and 2ng TGFβ in RPMI10 for 4 days at 37°C and 5% CO_2.

6.7.7 Mixed lymphocyte reaction

T cells are MHC restricted, however about 1-10% of them respond to allogeneic MHC molecules and recognize them as foreign. To test this ability to proliferate upon stimulation with foreign MHC, 2 x 10^5 splenocytes from NOD or NOD CLEC16A KD mice were mixed together with 2 x 10^5 irradiated (20 Gy) NOD, NOD CLEC16A KD or C57BL/6 splenocytes. The cells were cultured together in RPMI10 for 72h, before 0,5 µCi thymidine^{3H} was added for the last 16h of culture. The proliferation could then be measured by harvesting the incorporated radioactive thymidine.

6.7.8 Enrichment of thymic epithelial cells (TECs)

The protocol for the thymic epithelial cell (TEC) isolation was kindly provided by Prof. Dr. Ludger Klein (LMU, Munich).

Thymi were put in a 60 mm culture dish on ice and connective tissues were removed carefully with forceps, before the thymi were minced with scissors. 500 µl of RPMI with 0,2 mg/ml collagenase and dispase I (both Roche) as well as DNase (Invitrogen) were then added and pipetted up and down with a cut-tip P1000. The suspension was then incubated for 30 minutes at 37°C, during witch it was frequently pipetted up and down with a Pasteur pipet, that had been heated briefly in a burner flame, to minimize the opening size. Once a single cell suspension had been produced, EDTA (0,36 M) was added to a final concentration of 10 mM and incubated for another five minutes to break up rosettes. The suspension was then filtered through a 40 µm Falcon filtered and washed with PBS 1%FCS. After that a Percoll gradient was layered in a 15 ml Falcon tube. For that, the tube was first coated with 2 ml and then drained upside down. Then the spinned cells were resuspended in 4 ml Percoll (density 1.115) and transferred into the 15 ml tube. Above the cell layer, a less dense Percoll layer (density 1.06) of 2 ml was carefully and slowly pipetted with a Pasteuer pipet, while tilting the tube 45°. On top a 1ml layer of PBS was carefully stacked. The gradient was then centrifuged at 1350g for 30 minutes at 4°C without a brake. The layer between the less dense Percoll and PBS then contains the TECs, they were carefully aspirated with a Pasteur pipet. Between the dense and the less dense Percoll layer the thymocytes are positioned. The cells are then washed once more with PBS 1%FCS.

7 Results

7.1 Functional study of sCTLA-4 in T1D

The *CTLA4* susceptibility polymorphism CT60 correlates with a reduction of the sCTLA-4 splice variant expression. To elucidate if this reduction is causal for conveying susceptibility and shedding light on the mechanism behind it is the objective of this thesis.

For this purpose transgenic NOD mice bearing a knockdown for sCTLA-4 were generated by Stephan Kissler. To introduce this project and facilitate comprehension, the generation and first phenotyping of the transgenic mice will be described although they were not part of this thesis.

7.1.1 ShRNA design and *in vitro* validation

Mice in contrast to humans have 3 different splice isoforms of CTLA-4. In addition to full length CTLA-4 and sCTLA-4 there is a transcript called ligand independent CTLA-4, lacking the second exon. Since the splice isoform sCTLA-4 should be targeted specifically without influencing other splice products, the shRNA was designed to bind the junction between exon 2 and 4, which is unique for sCTLA-4 (Figure 6).

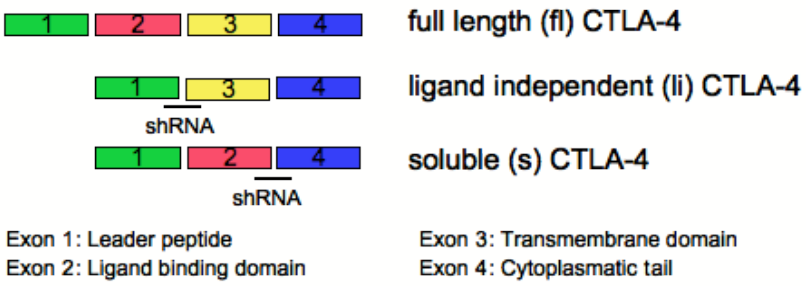

Figure 6: Design of splice isoform specific shRNAs

The shRNA was cloned into a pLBM vector behind the reporter gene GFP, so that a bicistronic mRNA is transcribed. Both sequences are under control of a CMV promoter and

lie between two long terminal repeats (LTRs, Figure 7) which contain the signals of integration for the viral integrase.

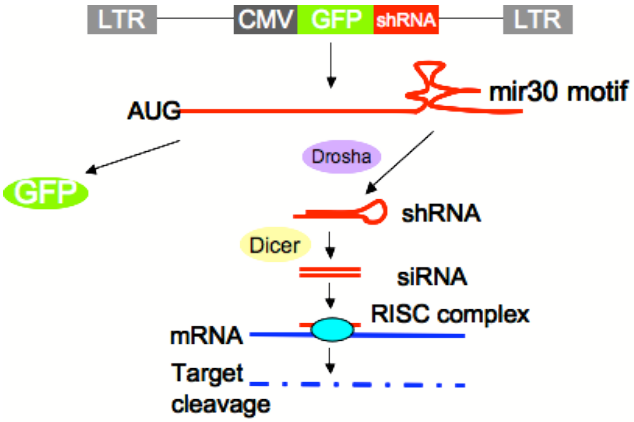

Figure 7: Integration cassette of the pLBM vector, bicistronic RNA transcript and RNAi pathway

Subsequently for validation of the knockdown efficiency and specificity of the shRNA directed against sCTLA-4, the cDNAs of the different murine CTLA-4 isoforms were cloned into the psiCHECK-2 vector and a luciferase assay was performed. This *in vitro* reporter assay is based on the bicistronic expression of the target-cDNA and renilla luciferase. Both vectors, the pLBM-sCTLA-4-shRNA and one of the three psiCHECK (full length (fl), soluble or ligand independent (li)-CTLA-4) were then transfected into 293F cells and the knockdown was measured for all three sequences (Figure 8).

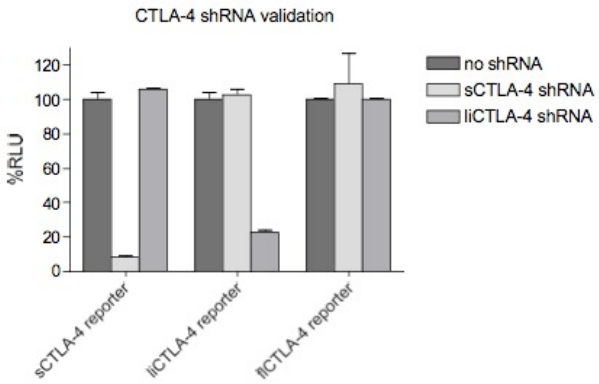

Figure 8: Luciferase assay validating specific and efficient knockdown through sCTLA-4-shRNA, data provided by Stephan Kissler

The knockdown was thus demonstrated to be efficient (around 90%) and specific for sCTLA-4 alone.

7.1.2 Generation of transgenic mice and *in vivo* knockdown validation

Since the shRNA proved to be reactive and specific *in vitro* the construct was used to produce lentivirus. This was then injected into NOD embryos and resulting transgenic pups were bred to be homozygous to reduce variegation. Integration of the shRNA-EGFP construct was assessed on DNA level by southern blot with a probe against EGFP (Figure 9 A) and also on protein level by flow cytometric analysis of splenocytes (Figure 9 B).

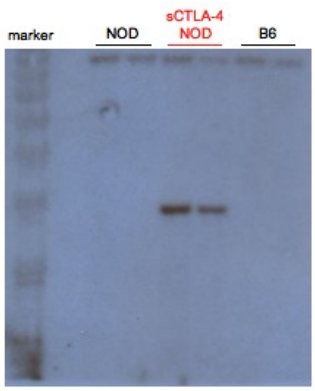

(A)

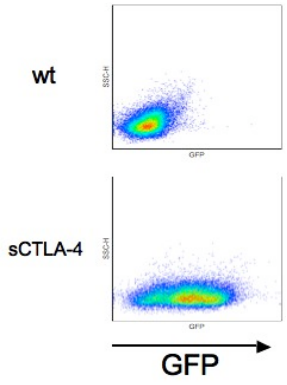

(B)

Figure 9: (A) Southern Blot for EGFP with DNA from wildtype NOD and B6 and transgenic NOD containing the shRNA(sCTLA-4)-GFP construct (data: Florian Beck); (B) FACS for GFP expression in wildtype (WT) and sCTLA-4 knockdown cells (data: Stephan Kissler)

Both demonstrate the expression of GFP in the transgenic animals. The FACS data additionally quantifies the GFP expressing splenocytes to about 60-70% of the total cell number.

Still the insertion and expression of the reporter does not give proof that the shRNA is functional also *in vivo*. Since there is no antibody for sCTLA-4 available, the knockdown verification was accomplished by quantitative real time PCR on splenocytes. Along with the expression of sCTLA-4 in WT and transgenic animals, the mRNA level of flCTLA-4 and

liCTLA-4 was defined, showing that the mRNA level for sCTLA-4 alone is specifically reduced in transgenic animals (Figure 10 A). The degree of reduction can be calculated from the difference in cycles and amounts to about 70% (Figure 10 B).

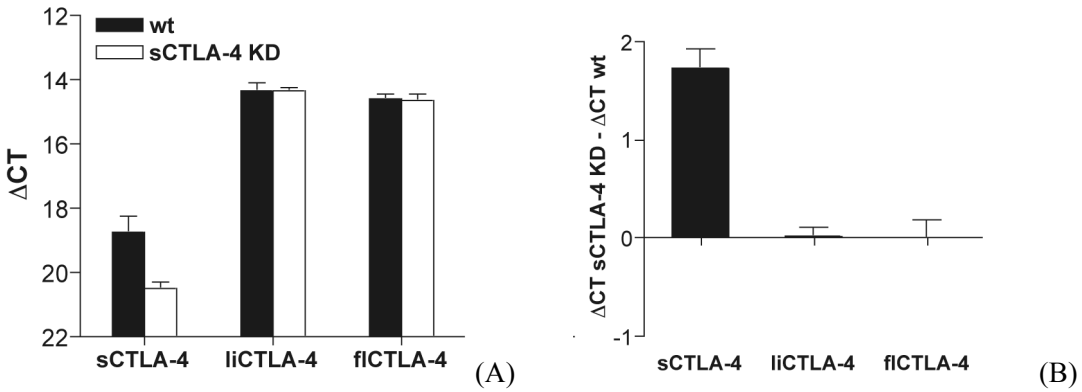

Figure 10: (A) Quantitative real time PCR for flCTLA-4, sCTLA-4 and liCTLA-4 in WT and transgenic NOD splenocytes; (B) differences of cycles (data: Dan Rainbow, Cambridge)

7.1.3 Characterization of cell ratios

The quantitative real time PCR had revealed that there indeed is a specific sCTLA-4 knockdown in the transgenic mice. With that knowledge phenotyping of the sCTLA-4 knockdown (sCTLA-4 KD) could be started.

Given that CTLA-4 is expressed by T cells, and CTLA-4 -/- mice show a skewing of the CD4/CD8 cell ratio towards the CD4 lineage[200], ratios of different T cell subsets were analyzed first. Developing T cells in the thymus can be characterized in their stage of development for instance by expression of the both surface markers CD4 and CD8. When staining thymi of WT and sCTLA-4 KD mice for those two markers no differences in DN, DP or single positive cell ratios were observed (Figure 11).

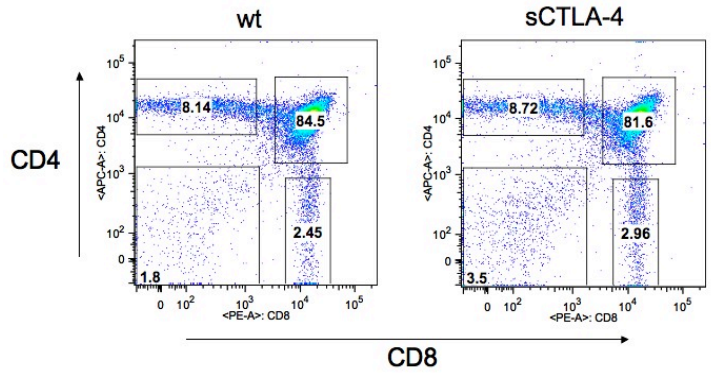

Figure 11: FACS staining of WT and sCTLA-4 KD thymi for CD4 and CD8 (data: Stephan Kissler)

Also in the spleen, where mature T cells are present, $CD4^+$ vs $CD8^+$ T cell percentages were the same in WT and sCTLA-4 KD mice (Figure 12).

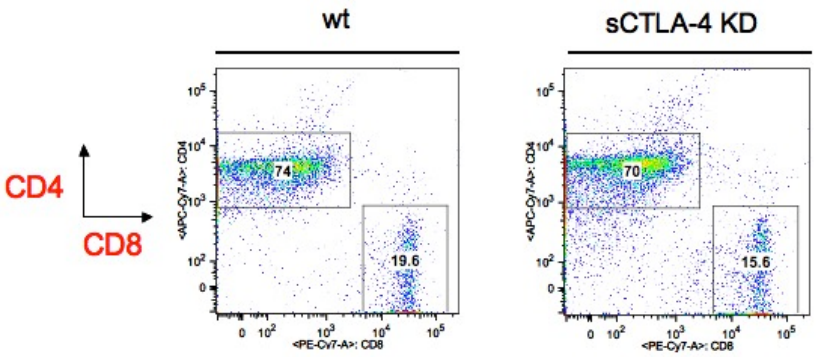

Figure 12: FACS staining of WT and sCTLA-4 KD spleens for CD4 and CD8 (data: Stephan Kissler

CTLA-4 is an activation marker for conventional T cells. As a consequence looking for other activation markers seemed reasonable. Thus spleen cells were stained for CD5 and CD25, showing a similar activation status in WT and sCTLA-4 KD spleens (Figure 13).

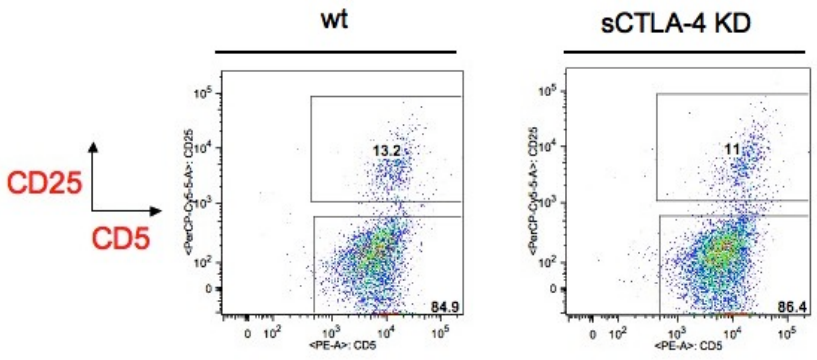

Figure 13: FACS staining of WT and sCTLA-4 KD spleens for CD5 and CD25 (data: Stephan Kissler)

Subsequently CD4/CD8 T cell ratios as well as TCR levels were also determined for lymph node cells. In addition to that the number of regulatory T cells ($Foxp3^{+}CD25^{+}$) was interesting, since they express CTLA-4 constitutively and also need it for their function. However all cell ratios were comparable between WT and sCTLA-4-KD lymph nodes (Figure 14).

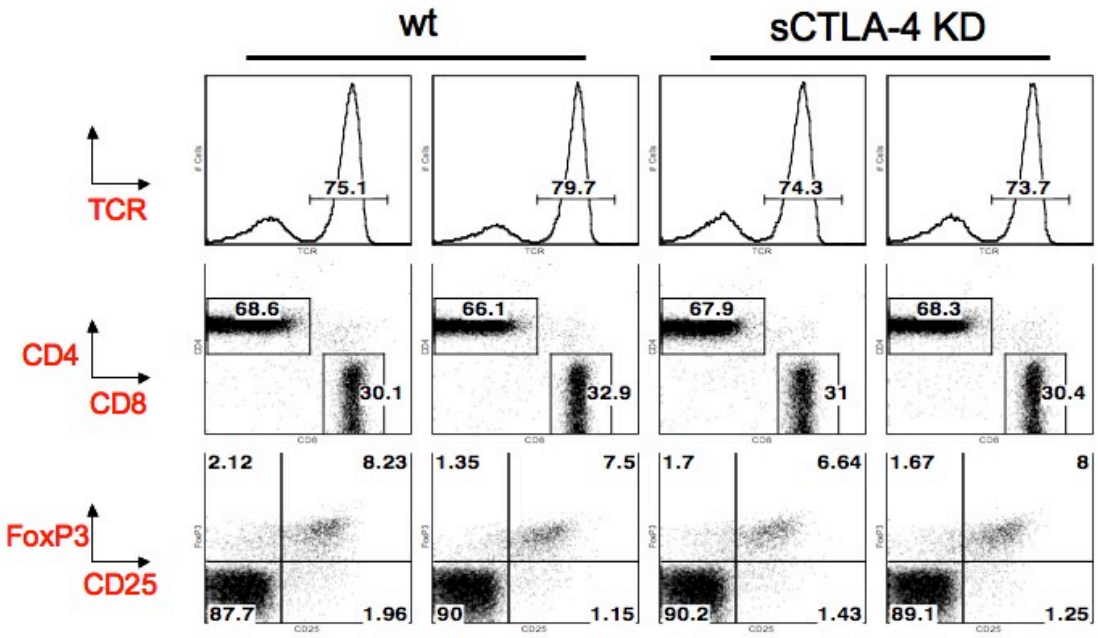

Figure 14: FACS staining of WT and sCTLA-4 KD lymph nodes for TCR CD4, CD8, Foxp3 and CD25 (data: Stephan Kissler)

7.1.4 T cell activation *in vitro*

There were no abnormalities detected in the ratios of the different T cell subsets, suggesting that there are probably no differences in signaling favoring one subset in sCTLA-4 KD mice. This phenotypic characterization did not, however, reveal whether the TCR signaling in general is affected.

To clarify this, lymph node cells were firstly activated with different concentrations of anti-CD3 *in vitro*, demonstrating that WT and sCTLA-4 KD T cells proliferated to exactly the same extent (Figure 15).

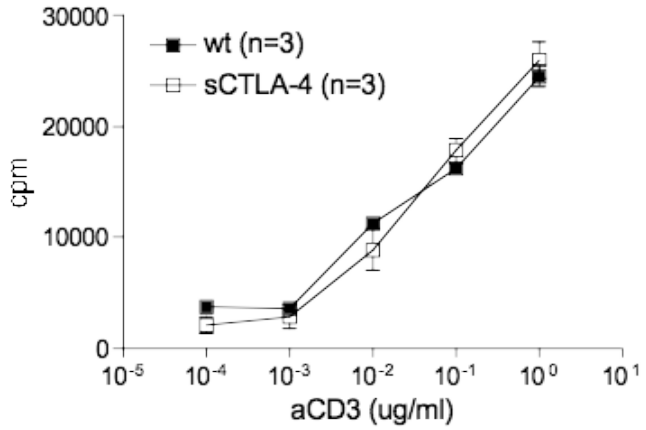

Figure 15: Proliferationassay, Thymidine incorporation measured after activation of lymph node cells with increasing anti-CD3 concentrations (data: Stephan Kissler)

Subsequently I started my own work by analyzing T cell activation in more detail, by looking at the phosphorylation state of the proximal signal transduction protein ZAP-70. First of all the timecourse of ZAP70 phosphorylation following TCR activation and crosslinking was assessed. The concentration of anti-CD3 used was in this case 10µg/ml, which was then crosslinked by an anti-hamster antibody (also 10µg/ml). As already described by Houtman and colleagues[201], the phosphorylation of ZAP-70 peaked very early (here 30 seconds) after activation-start. In our approach however the phosphorylation state turned out to be instable,

since its signal decreased already at 2 minutes of activation time and was almost gone at the 5 minutes timepoint (Figure 16).

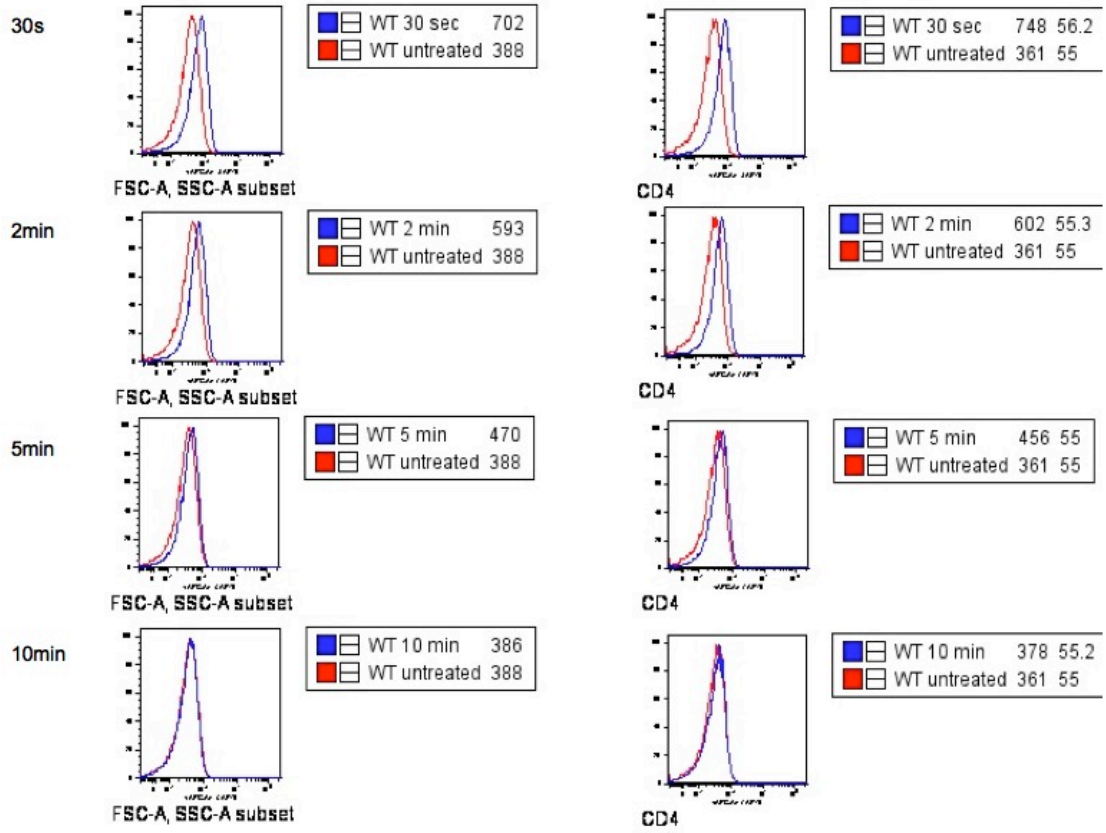

Figure 16: Flow cytometric analysis of phospho-ZAP-70 in lymph node cells activated with crosslinked anti-CD3 at different periods of time in 37°C

Now WT and sCTLA-4 KD lymph node cells were compared with respect to their activation state reflected by phospho-ZAP70 amount. Since the largest signal was seen for WT cells at 30 seconds to 2 minutes of activation, these time points were also chosen in this experiment. After experiments with 5 mice for WT and sCTLA-4 KD respectively it became clear that no significant difference exits in this two strains concerning proximal TCR signal after anti-CD3 activation *in vitro* (Figure 17).

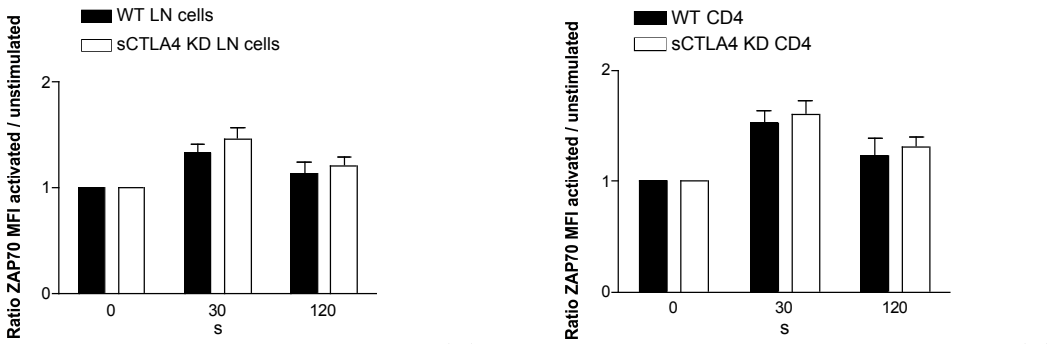

Figure 17: Flow cytometric analysis of phospho-ZAP-70 in WT (n=5) and sCTLA-4 KD (Tg, n=5) lymph node cells activated with crosslinked anti-CD3 at different periods of time in 37°C (A) whole lymph nodes (B) gated on $CD4^+$

7.1.5 Function of regulatory T cells

In vitro proliferation of stimulated T cells was not affected by a reduced sCTLA-4 expression. Still CTLA-4 is not only a potent negative regulator of conventional T cells[202] but also one of the most important effector molecules for regulatory T cells[119]. The next step consequently was to have a closer look at the function of these cells, first *in vitro*.

7.1.5.1 Conventional *in vitro* suppression assay

For this, a conventional suppression assay was performed, in which effector T cells (Teff) are cocultured with Tregs at different ratios under anti-CD3 stimulation. Figure 18 shows a representative result from 4 independent experiments. Especially at higher Teff / Treg ratios these show a reduced suppressive activity of sCTLA-4 KD regulatory T cells. This effect is independent of the origin of the effector T cells (WT or transgenic).

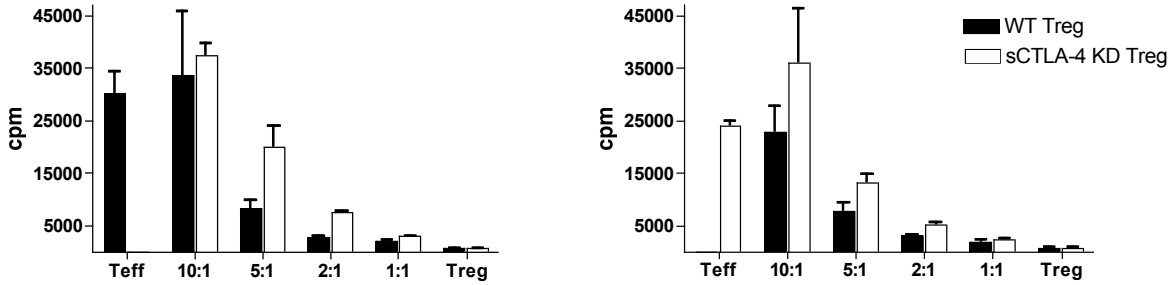

(A) (B)

Figure 18: Proliferation of Teff, (A: WT, B: sCTLA-4 KD) assessed via thymidine^{3H} incorporation, after 72h culture together with different amounts of WT or sCTLA-4 KD Tregs.

7.1.5.2 Cytokine production

Regulatory T cells inhibit or abrogate the activation of naïve T cells. Apart from proliferation, this can also be seen in the levels of cytokines secreted by these Teffs.

Directly in correlation with proliferation stands the secretion of IL-2 as well as the heightened response to it. Along with activation of naïve T cells CD25, the IL-2 receptor alpha chain, gets upregulated, thereby providing a high-affinity IL-2 receptor, allowing an autocrine action of this cytokine. Tregs constitutively express CD25 thus acting as an IL-2 sink.

In the *in vitro* setting of the suppression assay, a large proportion of Teffs differentiates into T_{H1} cells, secreting IFNγ. A reduction of this cytokine in the presence of Tregs also is an indication for the abrogated activation of Teffs.

To test the ability of sCTLA-4 KD Tregs to inhibit Teff activation on the cytokine level, the supernatants of a classic suppression assay were tested for IL-2 and IFNγ by ELISA (Figure 19) and CBA (data not shown, confirm ELISA results).

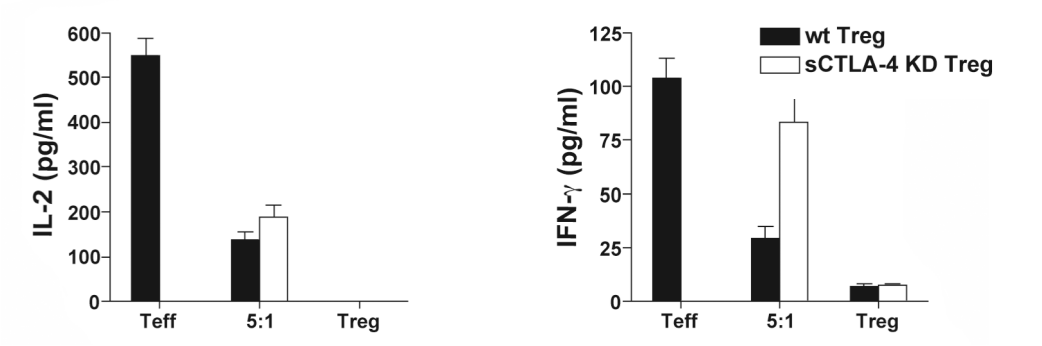

(A) (B)

Figure 19: Cytokine levels, assessed by ELISA, in the supernatant of a representative suppression assay, (A) IL-2 levels, (B) IFNγ levels

Consistent with the finding, concerning the suppression of proliferation, Treg cells lacking sCTLA-4 were defective in dampening the IFNγ production of Teff in the culture. IL-2 inhibition however was not affected by the knockdown of sCTLA-4.

7.1.5.3 Treg phenotype

Since the regulatory T cells of sCTLA-4 KD mice are defective *in vitro* in inhibiting activation of conventional T cells, the question arose if the overall Treg phenotype is somehow altered in the transgenic animals.

During the characterization of different cell ratios (section 7.1.3), $CD25^{+}Foxp3^{+}$ cells of WT and transgenic mice were seen to be the same in number and in the expression levels of these two markers. However there are other markers for Treg cells, like CTLA-4 and the glucocorticoid-induced tumor necrosis factor receptor (GITR), which are constitutively expressed in Tregs and upon activation also in conventional T cells, similar to CD25.

Since CTLA-4 is predominantly present in intracellular compartements[203], like the trans golgi network[204], lysosomal vesicles[205], endosomes and secretory granules[206], intracellular expression of CTLA-4 was assessed.

GITR and CTLA-4 expression were observed in lymph node cells, activated with 0,5 µg/ml anti-CD3 for five days. Figure 20 shows the expression level of intracellular CTLA-4 (A, B)

and GITR (C, D) in $CD4^+CD25^-$ cells (A, C) and $CD4^+CD25^+$ cells (B, D) from day 0 to day 3.

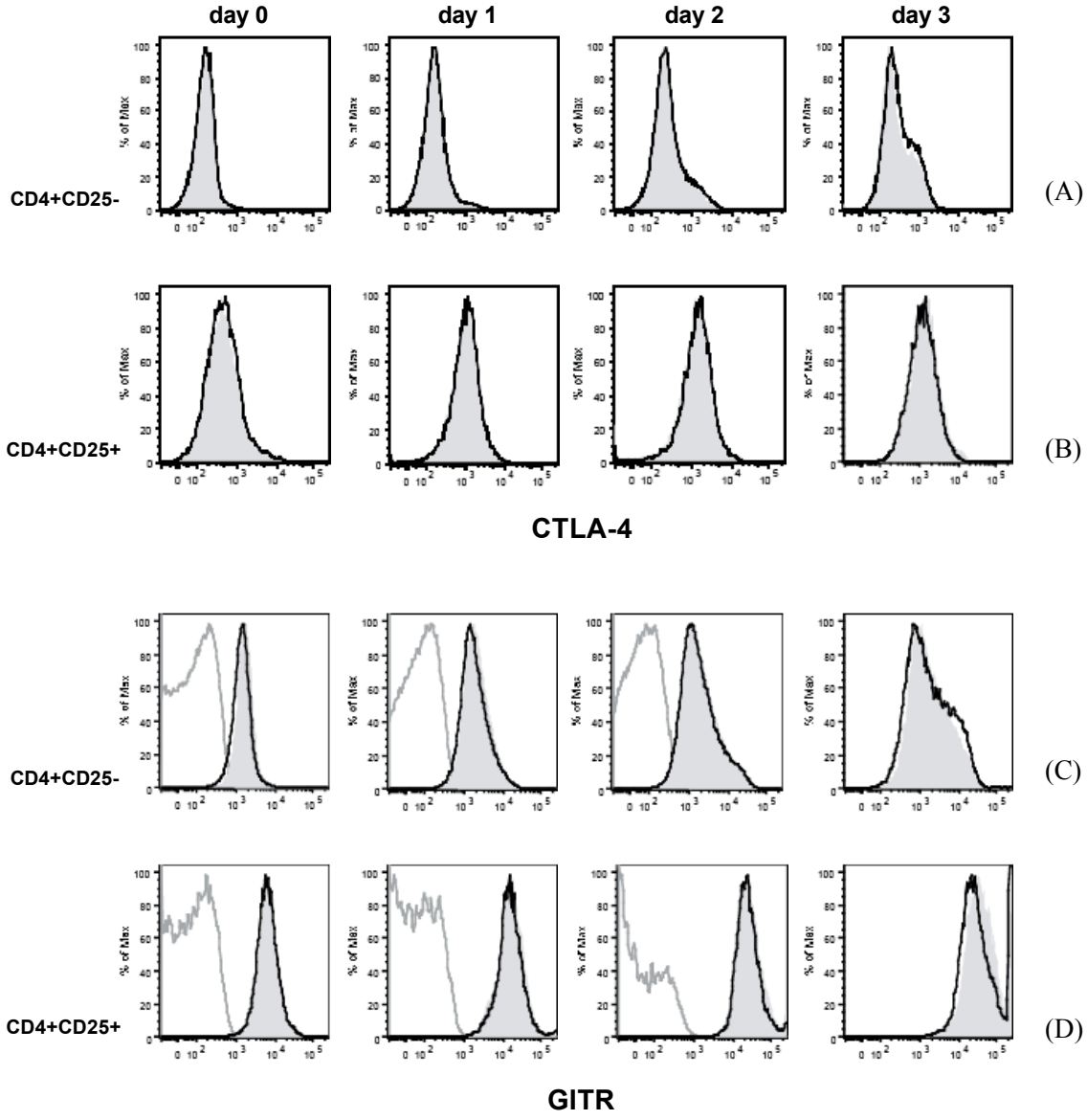

Figure 20: Flow cytometric analysis of intracellular CTLA-4 (A, B) and surface GITR (C, D) expression over four days activation in $CD4^+CD25^+$ (B, D) and $CD4^+CD25^-$ cells (A, C); cells from WT mice (black line) or sCTLA-4 KD mice (filled grey histogram); for GITR staining isotype control is shown (grey line)

WT and sCTLA-4 KD lymph node cells behaved the same in respect to flCTLA-4 as well as GITR expression and upregulation. Expression levels on day 4 and 5 are not shown, but were also the same in WT and sCTLA-4 KD cells. The staining showed that the knockdown of sCTLA-4 apparently does not influence the expression of the full length form.

7.1.5.4 Coculture of Treg cells with dendritic cells

After having found out that there seems to be some defect in the function of regulatory T cells from mice with reduced sCTLA-4 expression, in the absence of an obvious phenotype, the next step was to narrow down the cause of this defect. The interaction with APCs is claimed to be one of the most important modes of action for Treg cells at least *in vitro* and recently it could be shown that loss of CTLA-4 in Treg cells alone affects the downregulation of CD80/86 on DCs[119].

With that background, a coculture experiment with splenic dendritic cells and regulatory T cells was carried out to gain information about the ability of sCTLA-4 KD Treg cells to downregulate CD80/86 on DCs. For this 40.000 DCs were mixed either with 150.000 Teff and Treg cells or Treg cells alone. The T cells were activated with 1µg/ml anti-CD3 and incubated with the DCs for 42 hours. Following coculture, cells were stained for CD80/86, CD11c and propidium iodide. Living dendritic cells, characterized by being propidium iodide negative and CD11c positive were then analyzed for their CD80/86 expression. Despite problems concerning viability of the splenic dendritic cells a downregulation of CD86 by WT Treg cells could be observed. Treg cells from sCTLA-4 KD mice were clearly defective in that ability (Figure 21 A and B). This phenomenon was even stronger when no Teff cells were coincubated (Figure 21 A). CD80 expression however was not seen to be differentially downregulated (Figure 21 C and D). The signal for CD80 on day 2 as well as the extent of downregulation by Treg cells was also generally lower then that of CD86. The histograms are representative for two independent experiments.

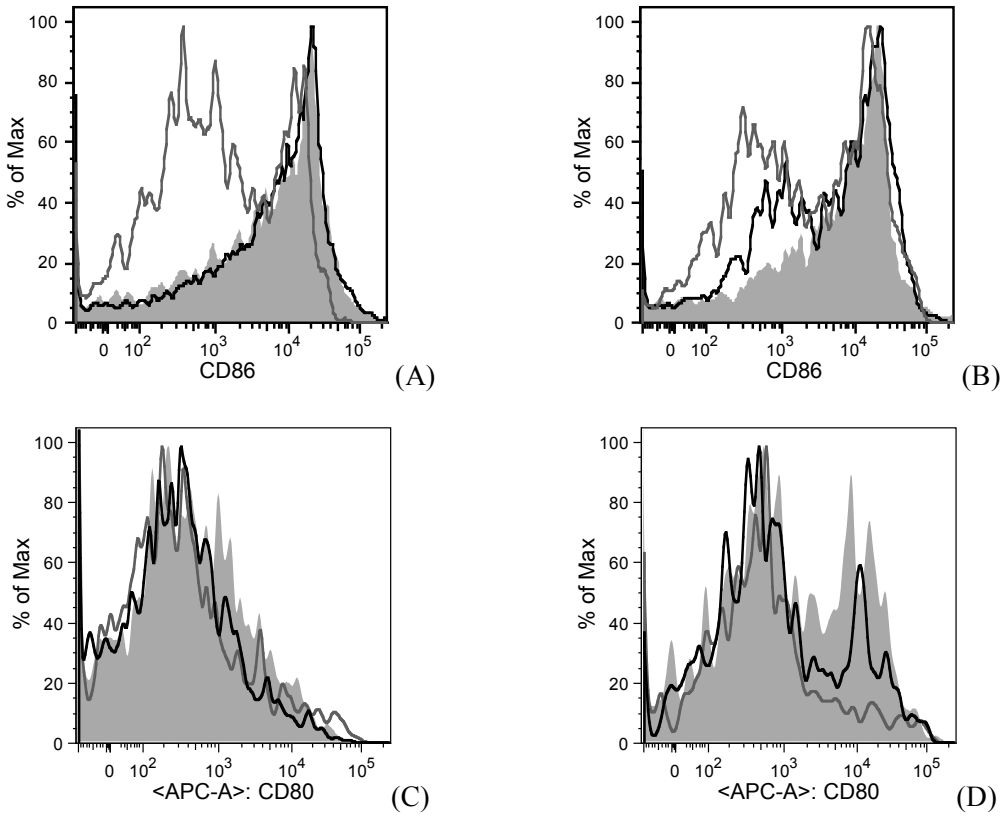

Figure 21: Expression level of CD86 (A,B) or CD80 (C,D) on DCs after coculture with WT Treg (grey line) or sCTLA-4 KD Treg (black line) or alone (filled grey histogram), without (A,C) or with (B,D) Teffs

7.1.5.5 Suppressive activity of induced regulatory T cells

There are two main subsets of Foxp3$^+$ regulatory T cells, natural and induced Treg (iTreg) cells, which differ in their development. Natural Treg (nTreg) cells emerge from the thymus and induced Treg cells develop from conventional naïve CD4$^+$ T cells in the periphery upon stimulation with TGFβ. The question that came up after having found a defect in Treg function and one of the possible mechanisms behind it was, if this effect is intrinsic to natural Treg cells and thus somehow linked to development of these cells.

In order to address this question, induced Treg cells were tested for their suppressive ability. For this they first had to be differentiated from naïve CD4$^+$CD62L$^+$ T cells *in vitro*. The

optimization process revealed that 2µg of plate bound anti-CD3 (24 well plate, 0,5 x 10^6 cells per well) with 2µg soluble anti-CD28 and 2ng TGFβ gave the best yield of $Foxp3^+$ cells after 4 days (Figure 22).

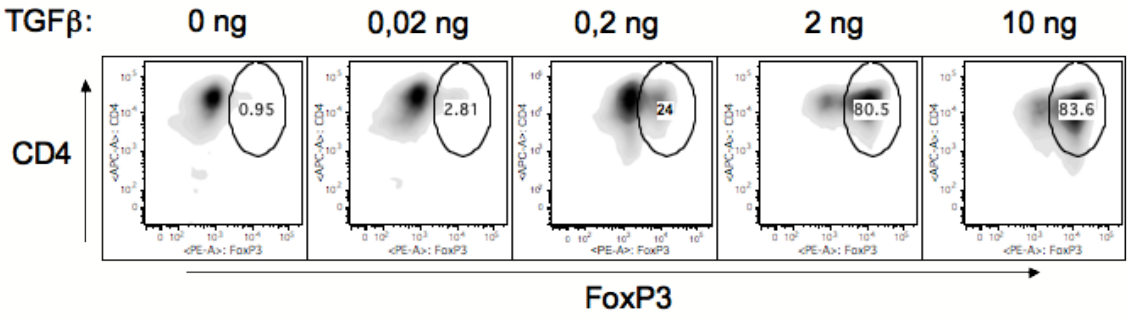

Figure 22: Optimization of TGFβ amount for iTreg production *in vitro*, 2µg anti-CD3 plate bound, 2µg anti-CD28

With these conditions Treg induction was effective and consistent so that iTregs could be produced (Figure 23 A) and used for a conventional suppression assay analogous to that already performed with natural Treg cells (section 7.1.5.1). The data concerning the Treg/Teff ratios was adjusted to the yield of iTreg cells in the preparation.

Similar to the suppression assay with nTregs the induced Treg cells from sCTLA-4 KD mice are defective in inhibition of Teff proliferation (Figure 23 C and D). The results shown are representatives of three independent experiments.

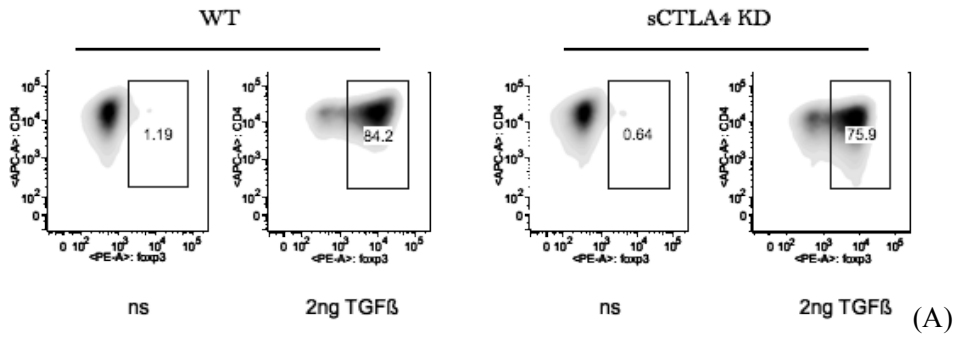

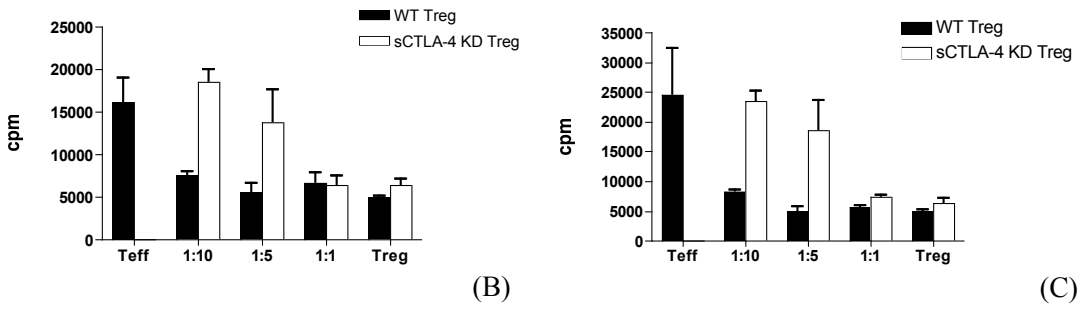

Figure 23: (A) CD4 and Foxp3 staining of *in vitro* induced Treg cells, these were used for (B) and (C) Suppression assay iTregs, corrected to amount of $Foxp3^{+}$Treg cells in the assay; (B) WT Teff; (C) sCTLA-4 KD Teff

By this experiment it could be shown that Tregs with diminished sCTLA-4 expression are defective in their ability to suppress Teff activation, independent of their development and origin.

7.1.6 *In vivo*: influence of sCTLA-4 knockdown on autoimmunity

In vitro experiments so far indicated a defect in regulatory T cells in sCTLA-4 KD animals. The goal of the study however was to evaluate whether the reduction of sCTLA-4 expression, would have an effect on autoimmunity *in vivo*.

7.1.6.1 Suppressive Treg activity *in vivo*: Colitis model

An *in vivo* model that had been shown to be sensitive to CTLA-4 blockade and to be reversible by administration of Tregs is the $CD4^{+}CD45RB^{hi}$ cell induced colitis [207,208]. The underlying studies have not been performed on the NOD background, however another report showed that the adoptive transfer of $CD4^{+}CD45RB^{hi}$ cells into NOD.SCID mice results predominantly in high colitis incidence[209]. Given the known CTLA-4-dependent Treg action in this model we concluded that this would be a reasonable setting to test the *in vivo* functionality of Tregs with disrupted sCTLA-4 expression.

We therefore transferred NOD.SCID mice with 4 x 10^5 $CD4^+CD45RB^{hi}$ cells alone or together with 10^5 WT or sCTLA-4 KD Tregs. After 8-9 weeks colitis severity was assessed via histology. Figure 24 shows the combined results of two consecutive experiments.

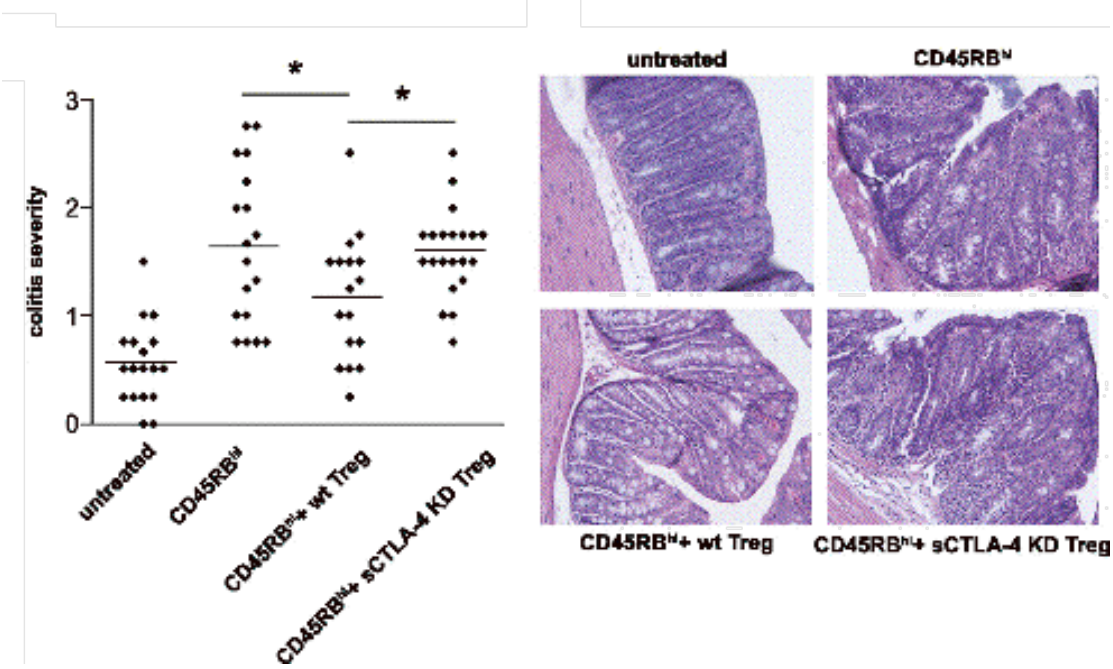

Figure 24: Colitis reversal by WT and sCTLA-4 KD Tregs;
left: Individual colitis scores of two independent experiments each group with n= 17-21; CD45RBhi vs. CD45RBhi+ WT Treg P = 0.045; CD45RBhi+ WT Treg vs. CD45RBhi+ sCTLA-4 KD Treg: P = 0.0116; CD45RBhi vs. CD45RBhi+ sCTLA-4 KD Treg: P = 0.83; right: representative colon histology sections

The adoptive transfer of $CD4^+CD45RB^{hi}$ cells resulted in a mild but significant colon inflammation. This pathology could be significantly reduced by the administration of WT regulatory T cells. In line with our *in vitro* findings we observed an abrogated sCTLA-4 KD Treg function that failed to inhibit the inflammation caused by $CD4^+CD45RB^{hi}$ cells.
Together with the *in vitro* data, this experiment provides further evidence for a role of sCTLA-4 in the function of regulatory T cells.

7.1.6.2 Spontaneous diabetes

To decipher whether the correlation of sCTLA-4 splice frequency reduction with a susceptibility polymorphism in humans is a causal relationship, the impact of sCTLA-4 KD on diabetes development in NOD mice was observed. Since NOD females already have a high incidence of developing diabetes, we decided to also follow disease onset in the protected congenic strain *Idd5.1* NOD, and thus also bred the sCTLA-4 shRNA onto this background. The rationale for choosing this congenic line was that *Idd5.1* provides a protective CTLA-4 allele from the C57BL/10 line, with heightened liCTLA-4 expression but an unchanged sCTLA-4 splice variant. This allowed us to see the effect of sCTLA-4 loss in the environment of an otherwise unaltered, protective CTLA-4 locus.

Over a period of approximately 200 days cohorts of NOD WT, sCTLA-4 KD, Idd5.1 WT and Idd5.1 sCTLA-4 KD were followed up on diabetes onset. They were tested weekly for glycosuria (Figure 25).

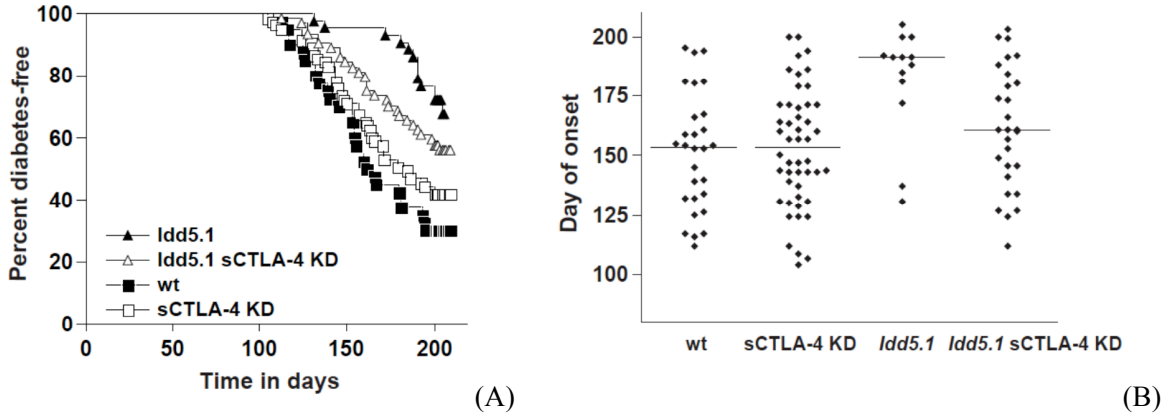

Figure 25: Diabetes development in female cohorts of different genotype: NOD WT (n = 40), sCTLA-4 KD (n = 83), Idd5.1 (n = 43), and Idd5.1 sCTLA-4 KD (n = 64);

(A) diabetes incidence survival curve,

Log-rank test: WT vs. sCTLA-4 KD P = 0.16; WT vs. Idd5.1 P < 0.0001; WT vs. Idd5.1 sCTLA-4 KD P = 0.0026; sCTLA-4 KD vs. Idd5.1 P = 0.0009; sCTLA-4 KD vs. Idd5.1 sCTLA-4 KD P = 0.0547; Idd5.1 vs. Idd5.1 sCTLA-4 KD P = 0.0893.

(B) day of onset of all diabetic mice, lines indicate median;

WT n = 28; sCTLA-4 KD n = 48; Idd5.1 n = 13, Idd5.1 sCTLA-4 KD n = 28. t test: WT vs. sCTLA-4 KD P = 0.77; WT vs. Idd5.1 P = 0.0006; WT vs. Idd5.1 sCTLA-4 KD P = 0.14; sCTLA-4 KD vs. Idd5.1 P = 0.0004; sCTLA-4 KD vs. Idd5.1 sCTLA-4 KD P = 0.16; Idd5.1 vs. Idd5.1 sCTLA-4 KD P = 0.0186.

As expected no influence of the sCTLA-4 KD could be seen on the fully susceptible NOD background. Moreover loss of sCTLA-4 on the protected Idd5.1 background did not result in a significant increase of incidence (Figure 25 A). However protection conveyed by the Idd5.1 congenic allele was completely reversed by the knockdown as to the day of onset (Figure 25 B). This is also reflected and supported by the statistical analysis that shows a significant difference between the onset of diabetes in Idd5.1 and Idd5.1 sCTLA-4 KD strains, but not between Idd5.1 sCTLA-4 KD mice and WT or sCTLA-4 KD backgrounds.
Loss of the sCTLA-4 splice variant was thus shown to accelerate susceptibility to diabetes.

The aim of this thesis was to understand if the reduced sCTLA-4 splice variant expression associated with the susceptibility allele CT60 is causative for an increased risk of T1D.
We decided to study the impact of sCTLA-4 loss in the NOD mouse model and introduced an shRNA directed specifically against this isoform via lentiviral transgenesis. The newly generated mouse line proved to be defective in sCTLA-4 expression however had no alterations in immune cell composition or ability of effector T cells to be activated.
When examining the function of regulatory T cells *in vitro* and *in vivo*, we found their function to be clearly impaired due to the loss of sCTLA-4. The underlying mechanism could at least partly be attributed to the failure of sCTLA-4 KD Treg cells to modulate costimulation by antigen presenting cells. Furthermore we could show that loss of sCTLA-4 renders NOD mice with an otherwise protective CTLA-4 allele more prone to diabetes.

7.2 Functional study of CLEC16A in T1D

CLEC16A was identified as a susceptibility locus for several autoimmune disorders, including T1D. To clarify its function in the immune system and its connection with type 1 diabetes, the transcript was knocked down on the NOD and the C57BL/6 background.

7.2.1 *In vitro* verification of *Clec16a* shRNA

Thus three different shRNA sequences complementary to the murine *Clec16a* cDNA were chosen by using the described algorithm and cloned into the pLBM vector. Subsequently they were tested for their activity to promote RNAi in a luciferase reporter assay. Sequence #3 had the highest knockdown efficiency with about 85% reduction of expression and was chosen for the generation of transgenic animals (Figure 26).

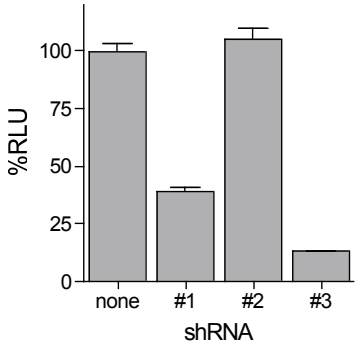

Figure 26: Luciferase assay for three different shRNAs specific for *Clec16a*

All vectors (pLBM-shRNA-Clec16a#1; #2 and #3) were previously cloned and validated by Daniela Blassfeld during her bachelor thesis in the laboratory.

7.2.2 Generation of transgenic mice

After sequence #3 was chosen, it was used to produce lentivirus in 293F cells. Virus preparations with high titers (above 10^8 particles/µl) were subsequently injected into NOD and C57B/L6 embryos. Injections resulted in founder mice with about 50% GFP expressing

NOD lymphocytes and 40% in C57B/L6. Expression was even higher in granulocytes. They were then further bred to see if the expression is stable and to obtain homozygosity. Homozygous NOD CLEC16A KD mice manifested 70% EGFP positive cells among lymphocytes and even > 85% in B cells and granulocytes in subsequent generations. The EGFP expression was somewhat lower in C57BL/6 CLEC16A KD mice with 62% in lymphocytes and 77% in granulocytes (Figure 27).

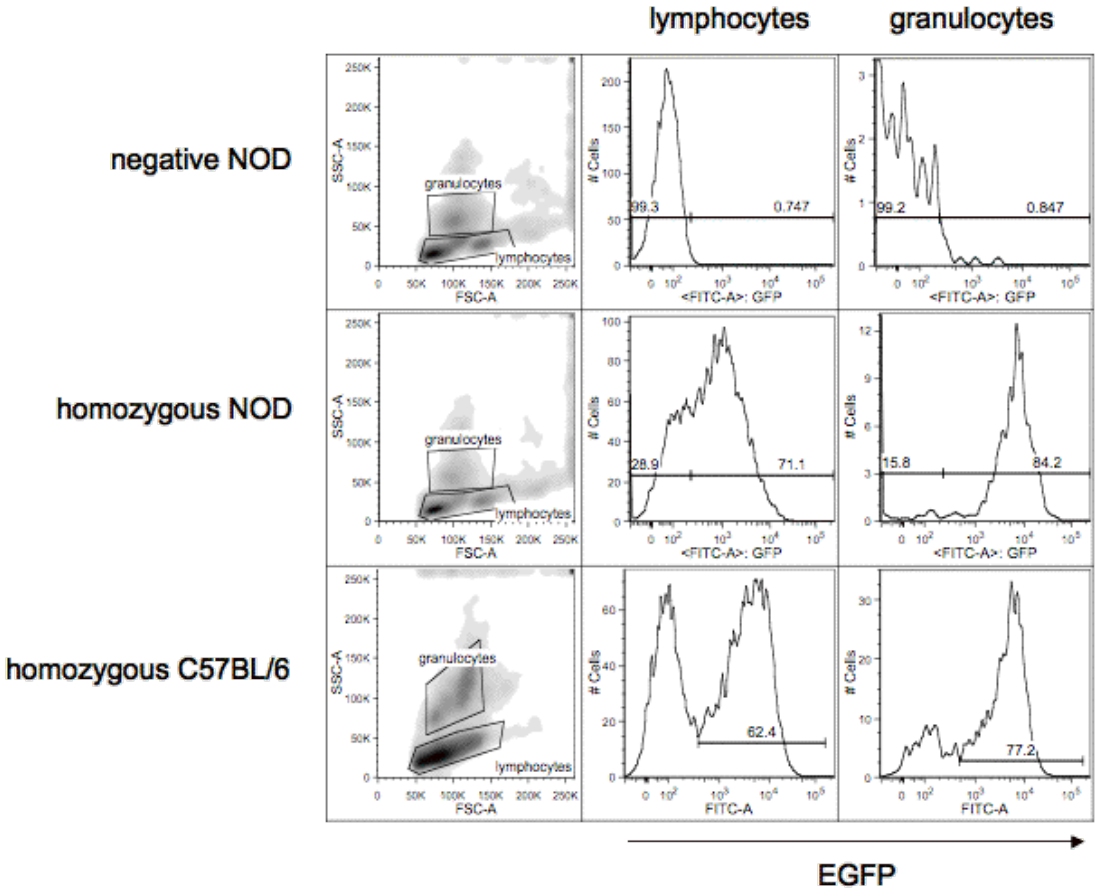

Figure 27: Flow cytometric analysis of blood samples taken from offspring of two F2 NOD and one C57BL/6 mouse derived from a breeding of CLEC16A KD heterozygous mice. Upper row shows negative mouse, middle row gives GFP expression of granulocytes and lymphocytes in a homozygous NOD CLEC16A KD mouse,

7.2.3 Knockdown examination

The GFP expression alone does not prove the reduction of CLEC16A expression, thus the knockdown was to be validated.

7.2.3.1 CLEC16A mRNA expression in transgenic mice

Since the shRNA targets the *Clec16a* mRNA, we first conducted a quantitative PCR to assess the mRNA reduction. As the expression of CLEC16A was shown to be largely restricted to antigen presenting cells we reasoned to first validate the knockdown in lymphoid organs. We therefore extracted RNA from lymph nodes and spleens of WT and CLEC16A KD NOD mice and performed a qPCR based on the UPL system by Roche for *Clec16a* and *Gapdh* with the cDNA obtained from it.

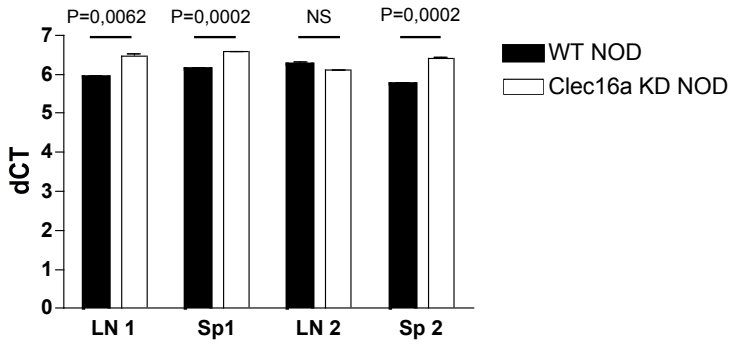

Figure 28: ΔCT of *Clec16a* mRNA expression against *Gapdh* in WT and CLEC16A KD LN and spleen of two mice of each genotype; UPL7 for *Clec16a* and UPL9 for *Gapdh* were used with the appropriate primer sets

A slight but significant reduction of *Clec16a* mRNA expression in CLEC16A KD NOD could be observed (Figure 28). The experiment was repeated also with a different UPL/Primer set, however the reduction of *Clec16a* expression in the transgenic organs did not always reach significance, probably due to the small difference.

Additionally we also tested the knockdown in sorted B and T cells. Both cell types are available in sufficient cell numbers in lymph nodes and spleen to perform a qPCR and

expression in B cells had been shown before. They were sorted at the FACS-AriaIII after staining for CD19 and TCRβ chain. The cDNA obtained after RNA extraction was then used for qPCR.

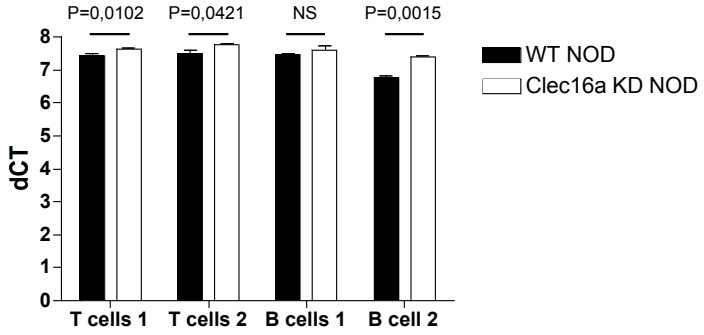

Figure 29: ΔCT of *Clec16a* mRNA expression against *Gapdh* in WT and Clec16a KD (GFP^+) T and B cells of two mice of each genotype; UPL9 for *Clec16a* and *Gapdh* were used with the appropriate primer sets

The knockdown could not be confirmed with UPL7, but by employing UPL9 with the suggested *Clec16a* Primer set (Figure 29).

However also in the sorted B and T cells the extent of the expression difference, as already seen in the whole organs, is small and ranges about ½ cycle, which can be calculated to an mRNA expression reduction of approximately 25%. Both experiments have been performed on male and female mice without revealing a gender difference.

7.2.3.2 CLEC16A protein expression in CLEC16A KD mice

In addition to the mRNA reduction induced by the introduced shRNA, the assumed consequential loss of CLEC16A protein was to be tested by Western blot. The polyclonal antibody directed against the human form of CLEC16A, but also reactive for the murine form, was kindly provided by Lucy Davison from the Lab of John Todd, Cambridge, UK. Also the protocol to detect this very unstable protein was developed by her.

Since the knockdown had earlier by qPCR been indicated to be rather modest, we decided to perform the western blot on cells that had been sorted for GFP expression since we anticipated the effect to be visible there.

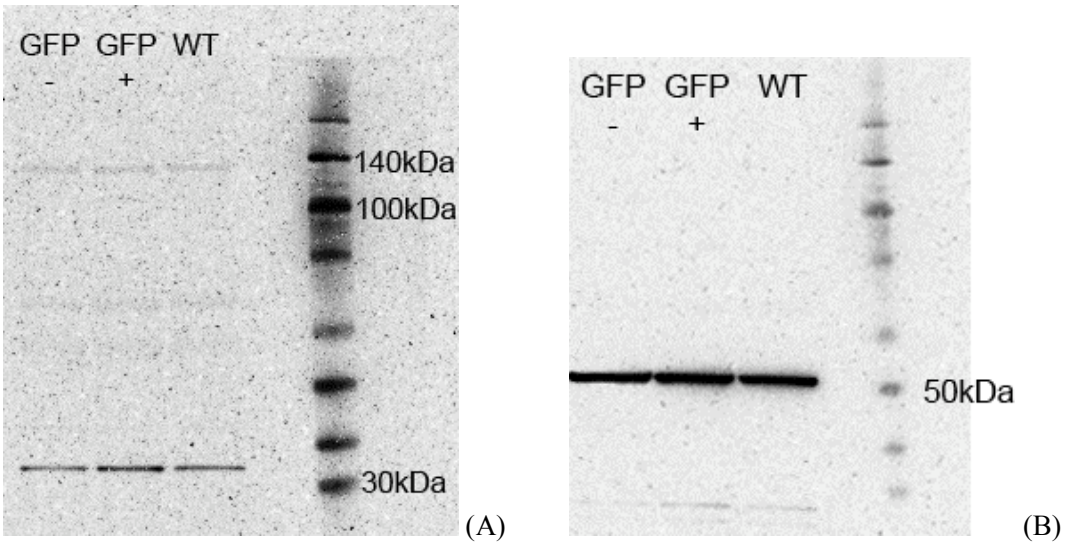

Figure 30: Protein detection after SDS-PAGE and Immunoblot of FACS sorted spleen cells, (A) detection with CLEC16A antibody, (B) Tubulin antibody

However detection of the full length isoform of CLEC16A (117kDa) proved to be difficult because of the small half-life and the instability of the protein. The instability index, calculated with the ProtParam tool at ExPASy Proteomics Server (http://expasy.org/cgi-bin/protparam) accounts for 54.41 for the full length isoform. A protein with a value above 40 is considered unstable. The half-life in human cells is estimated to 1.1h.

Nevertheless a weak signal at around 117kDa was visible in the western blot, though no altered expression in the GFP^+ cells from CLEC16A KD NOD mice could be detected (Figure 30). Additionally the antibody bound to a protein with the size of 35kDa, not corresponding to any of the known mCLEC16A protein isoforms.

Taken together, a small reduction of mRNA expression was detected, however this could not be confirmed by the western blot results, probably due to instability and small half-life of the protein. Thus validation of the *Clec16a* knockdown remained inconclusive.

7.2.4 Diabetes protection of CLEC16A KD mice

Since the locus of *CLEC16A* is associated with human diabetes we wanted to determine its role in disease development in the NOD mouse and in doing so learn more about its function in the immune system.

7.2.4.1 Spontaneous diabetes

For this WT and CLEC16A KD NOD mice were monitored weekly over 200 days for diabetes development, by testing for glucosuria.

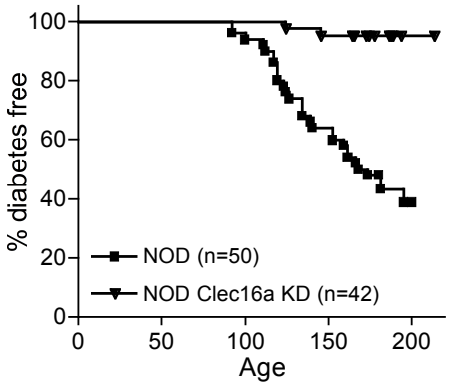

Figure 31: Diabetes development in female cohorts of different genotype; Logrank Test: P<0.0001

Surprisingly NOD CLEC16A KD mice were almost completely protected from diabetes development; only two out of 42 mice became diabetic during the testing period (Figure 31).

7.2.4.2 Cyclophosphamide induced diabetes

To further examine the protection from diabetes development of NOD CLEC16A KD mice, we accelerated disease onset by administration of cyclophosphamide. The chemotherapeutic drug preferentially targets proliferating lymphocytes and thus reduces the pool of regulatory T cells. It also interferes with the function of these cells and skews the T helper cell population towards the T_{H1} type due to a cytokine storm. By these mechanisms it causes a simultaneous onset of diabetes in NOD mice [195-198].

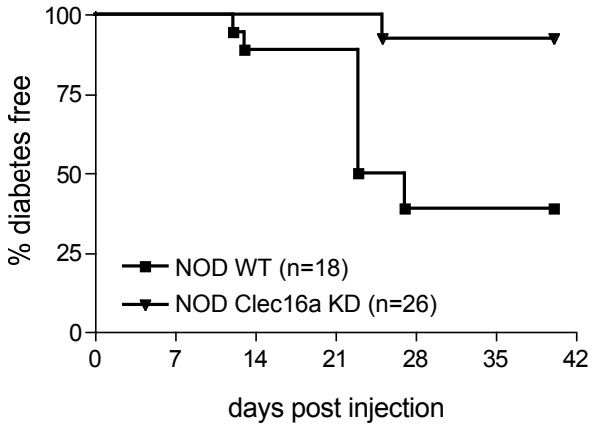

Figure 32: Diabetes development in female groups of different genotype (8-9 weeks old) after cyclophosphamide treatment; two independent experiments are depicted in one graph; Logrank Test: $P<0.0001$

Independent of the loss of regulatory T cell function, NOD CLEC16A KD mice are still strongly protected from developing diabetes (Figure 32). Where NOD WT mice had a comparable diabetes incidence to the spontaneous form, NOD CLEC16A KD mice hardly got sick, also in line with spontaneous diabetes assessment.

7.2.4.3 CY induced diabetes in splenocyte transferred NOD.SCID mice

The experiments so far did not give any information if the cause for the protection from diabetes in NOD CLEC16A KD mice lies in the immune system or in the beta cells themselves. To address this question, we adoptively transferred NOD.SCID mice with splenocytes from WT or CLEC16A KD NODs and induced diabetes with cyclophosphamide after the transferred cells had time to populate the peripheral lymphoid organs. The rationale behind this experiment was to test the ability of CLEC16A KD immune cells to protect WT beta cells from being destroyed.

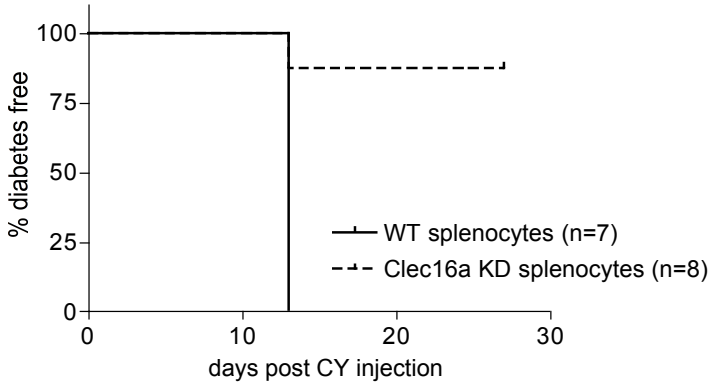

Figure 33: Diabetes development in female NOD.SCID mice (10-14 weeks old) transferred with 10^7 splenocytes from either NOD WT or NOD CLEC16A KD females, injection of CY on day 21; Logrank test P= 0,0057

The protection seen in spontaneous and CY induced diabetes could be replicated in the adoptive transfer setting (Figure 33). In NOD.SCIDs transferred with WT splenocytes the diabetes incidence even reached 100%, CLEC16A KD splenocytes conveyed the disease however only in one out of eight tested mice. This suggests that the protection is at least partly derived from an altered immune function, as CLEC16A KD splenocytes fail to destroy WT beta cells. Whether beta cells in CLEC16A KD mice are also altered will be more

conclusively investigated by the generation and testing of NOD.SCID CLEC16A KD mice that are currently being bred.

7.2.4.4 CY induced diabetes in B and T cell transferred NOD.SCID mice

We have shown that the protection from diabetes is due to the altered immune function in CLEC16A KD mice. To further narrow down the exact population that is responsible for the lack of diabetes development in these mice, we focused on the two most abundant cell subsets in the spleen, B and T cells.

		T Cells	
		WT	CLEC16A KD
B Cells	WT	1	2
	CLEC16A KD	3	4

Table 1: Genotype combinations of B/T cell transfer into NOD.SCID mice

Since we wanted to determine which one of the two subsets alone is responsible for disease protection, we transferred these cells in different genotype combinations (Table 1) into NOD.SCID mice and challenged them with CY after three weeks. Two million cells of each subset were transferred, after they had been negatively selected by MACS preparation.

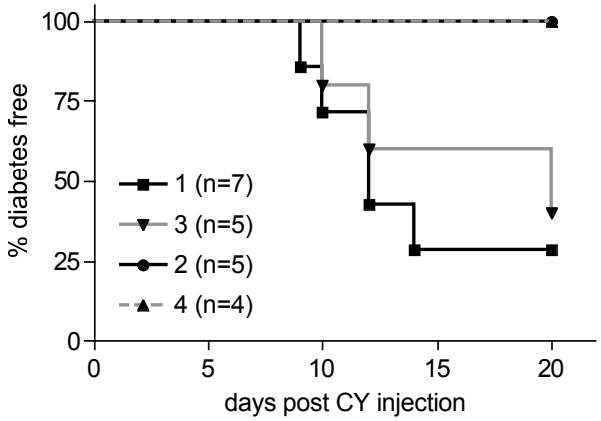

Figure 34: Diabetes development in female NOD.SCID mice (8 weeks old) transferred with T and B cells (2 x10^6 each) of different genotypes, combinations see Table 1; Logrank test of combined 1/2 vs. 3/4 : P=0.0027

Transfer of B and T cells alone resulted in a similar incidence of diabetes after CY treatment, when comparing the purely WT and purely transgenic subset combinations (Figure 34, 1 and 4). Notably the protection of NOD.SCID mice from developing diabetes was still apparent when WT B cells were cotransferred with CLEC16A KD T cells (group 2). However the protective effect was not seen when WT T cells were cotransferred with Clec16a KD B cells (group 3). Thus a significant difference in diabetes development is observable, depending on the origin of the transferred T cells (groups 1 and 2 versus 3 and 4).

7.2.5 T cell characterization

In vivo adoptive transfer experiments had revealed that the diabetes protection we could observe in Clec16a KD mice could be T cell inherent. Consequently we examined T cell function *in vitro* to detect possible alterations that could be causative to this observation. Most of the following *in vitro* experiments were performed by or together with Lilli Teresa Probst in the course of her doctoral thesis.

7.2.5.1 T cell proliferation

For initial evaluation of the proliferative ability, $CD4^+CD25^-$ T effector cells derived from WT NOD or Clec16a KD NOD lymph nodes and spleen, were activated with anti-CD3 and antigen presenting cells, also from different genotypes.

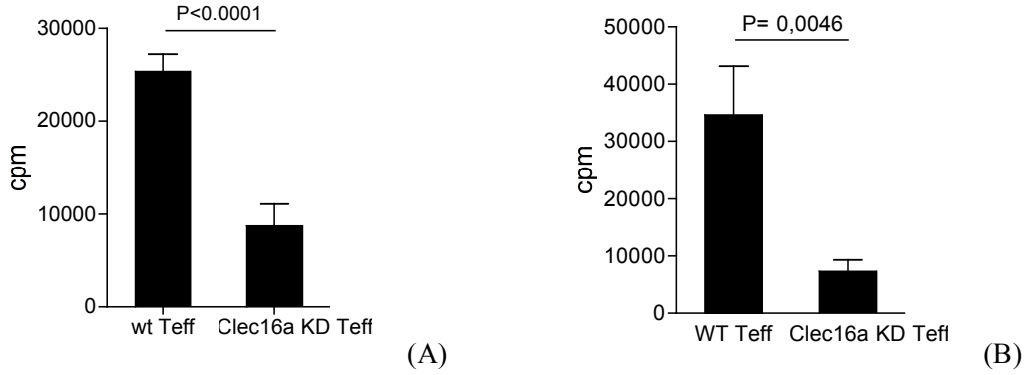

Figure 35: H^3-Thymidin uptake of 25.000 $CD4^+CD25^-$ T cells activated for 3 days with 1µg/ml anti-CD3 on 3 x 10^5 WT APCs (A) or Clec16a APCs (B); both figures show combined results from four independent experiments; data provided by Lilli Teresa Probst

Both WT and Clec16a KD T cells proliferated upon stimulation with anti-CD3 and APCs. However Clec16a KD T cells were clearly hampered in their proliferative activity on both APCs (Figure 35). This also held true for other anti-CD3 concentrations, as seen in dose response experiments conducted by Lilli Teresa Probst (data not shown).

A second way to assess the proliferative capacity of Clec16a KD T cells was the mixed lymphocyte reaction. In this assay T cells that recognize allogeneic MHC are activated and proliferate. This happens without addition of anti-CD3, thus displaying the capability of an allo-reactive subset, accounting for 5-10% of total T cell repertoire, to get activated by TCR-MHC contact.

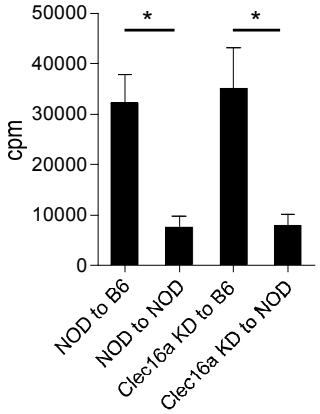

Figure 36: H^3-Thymidin uptake of splenocytes after 3 days incubation with respective APCs (irradiated splenocytes), graph is a summary of three independent experiments, data provided by Lilli Teresa Probst

Surprisingly, unlike in the anti-CD3 / APC induced proliferation, the mixed lymphocyte reaction showed a strong proliferation of CLEC16A KD allo-reactive T cells (Figure 36), although only a small fraction of T cells would be activated in this setting. However no separation of CD4 and CD8 T cells had preceded this assay, so the subset of the proliferating T cells could not be distinguished. This suggests that in principle CLEC16A KD Tcells have the ability to respond to certain stimuli similarly to WT cells.

To further elucidate the disadvantage of CLEC16A KD T cells on stimulation with anti-CD3 and WT APCs, we chose two alternative means of activating the T cells without the use of APCs. On the one hand we employed anti-CD3 and anti-CD28 coupled beads (Invitrogen) as a strong stimulator, both giving first and second signal. On the other hand we overrode the necessity to stimulate via the TCR, by adding PMA/Ionomycin to the cells, which directly activates the PKCθ /Ca^{2+} dependent signal transduction.

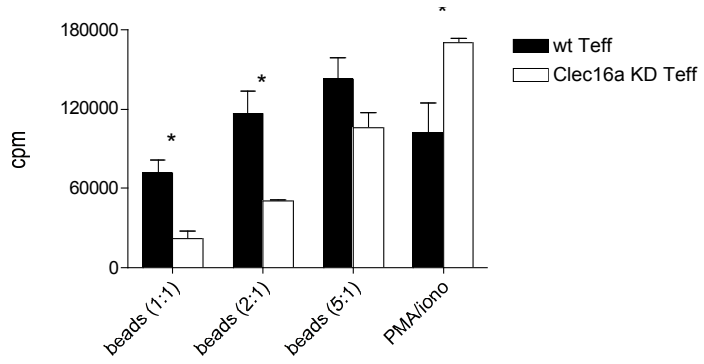

Figure 37: H^3-Thymidin uptake of 25.000 CD4 T cells activated for 3 days with anti-CD3/anti-CD28 covered beads or PMA/Ionomycin, data provided by Lilli Teresa Probst

In line with the previous anti-CD3 mediated CD4 T cell proliferation assay, CLEC16A KD T cells proliferated significantly less, when activated with antibody-coated beads, compared to WT T cells. However this effect was completely lost in the setting of targeting the signal transduction pathway further downstream, as by PMA/Ionomycin (Figure 37).

7.2.6 Characterization of Antigen Presenting Cells

Adoptive transfer experiments (7.2.4.4) as well as *in vitro* T cell proliferation assays (7.2.5) clearly showed a defective T cell function in CLEC16A KD mice that leads to protection from diabetes. However since CLEC16A has been shown to be expressed in antigen presenting cells[151] and the Drosophila orthologue being crucial for the maturation of endosomes[160] we hypothesized a defect in APCs due to the knockdown could be altering T cell function.

7.2.6.1 Activation of peripheral APCs

In order to test this hypothesis we proceeded with assessing the *in vitro* functionality of antigen presenting cells. Most experiments were conducted by Lilli Teresa Probst and are in greater detail described in her doctoral thesis. We commenced this assessment by activating NOD WT and CLEC16A KD B cells and dendritic cells (DCs) with lipopolysaccharide (LPS)

or anti-CD40 and looked for upregulation of T cell stimulatory molecules, that if altered could be causal for the lack of responsiveness of CLEC16A KD T cells.

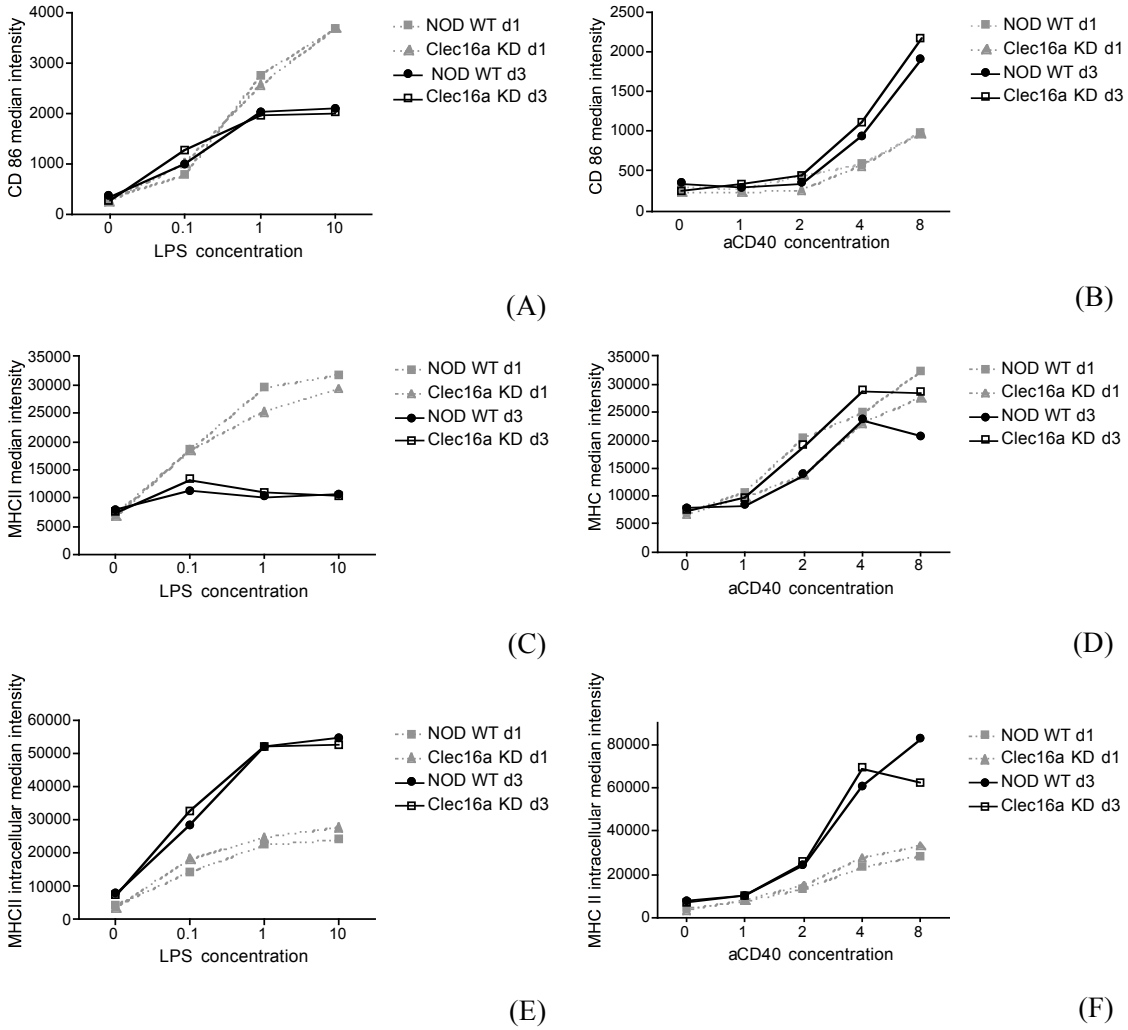

Figure 38: Upregulation of CD86 and MHC in LPS or anti-CD40 stimulated B cells; cells were activated for one or three days with different concentrations of LPS or anti-CD40, concentrations are given in µg/ml, CD86 and MHC were measured by FACS staining, median fluorescent intensities are shown; (A), (C) and (E) show measurements after LPS stimulation; (B), (D) and (F) measurements after anti-CD40 stimulations; (A) and (B): CD86 level; (C) and (D): extracellular MHCII level; (E) and (F) intracellular MHCII level

Activation in both NOD WT and CLEC16A KD B cells with respect to upregulation of CD86 and MHCII was comparable (Figure 38). Data obtained with dendritic cells is not shown in

this thesis, however it did not display any altered function in CLEC16A KD cells either. This information as well as data about proliferation, upregulation of PDL-1 /2, CD54, GITR-L and CD40 can be found in Lilli Teresa Probst´s doctoral thesis. These additional data again did not reveal any difference between NOD WT and CLEC16A KD antigen presenting cells.

As already mentioned above, the very conserved Drosophila orthologue *ema* had been shown to be important for endosomal maturation[160], therefore we decided to test endosomal uptake and processing in CLEC16A KD macrophages. These were obtained by peritoneal lavage and after activation by culturing on tissue plates, fed with fluorescently labeled E.coli (pHrodo™, Invitrogen). The pHrodo™ SE dye does not give a fluorescent signal at pH 7 or higher, equating the extracellular pH value, thus rendering quenching unnecessary. Only upon acidification, as it takes place in maturing endosomes, can a fluorescent signal in the PE channel be detected, this signal growing stronger the lower the pH gets. This dye allowed us to examine the time course of antigen uptake and processing in NOD WT and CLEC16A KD macrophages.

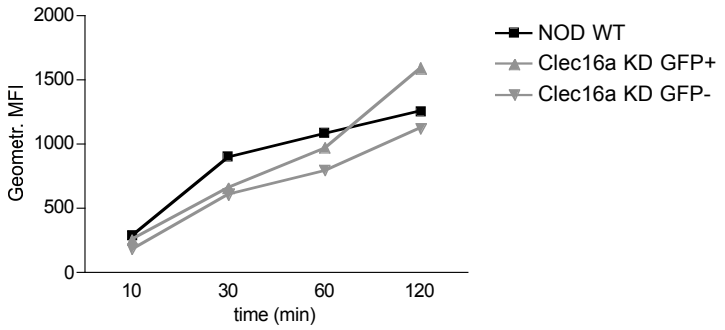

Figure 39: pHrodo™ labeled E.coli uptake and processing time course; CLEC16A KD macrophages were sorted by GFP expression prior to the experiment; shown is the geometric mean fluorescent intensity of pHrodo, representative of three comparable experiments

Again in this experiment that was designed to shed light on endosomal processes in antigen presenting cells, no defect in CLEC16A KD cells could be detected. Both WT and CLEC16A KD macrophages took up the labeled E.coli particles and processed them in a comparable way that could be observed by increase of fluorescent intensity over time indicating an acidification of endosomes (Figure 39).

7.2.6.2 Characterization of thymic epithelial cells

Since no obvious defect in CLEC16A KD peripheral APCs was detected, we next turned to essential antigen presenting cells in the thymus, the thymic epithelial cells (TECs). There are two types of thymic epithelial cells important for T cell development, the cortical and medullary cells. Cortical TECs (cTECs) are considered mainly responsible for positive selection[210], medullary TECs (mTECs) for negative selection. Defects in one of these or both could alter selection of T cells and thus render them less reactive as we have observed in CLEC16A KD mice.

To determine number and activation status of TECs in NOD WT and CLEC16A KD thymi, these first had to be digested by collagenases. Then epithelial cells were separated from thymocytes by running a Percoll gradient. cTECs and mTECs are identified in the epithelial cell fraction by an antibody staining for $CD45^-$ $EPCAM^+MHCII^+Ly51^+$ or $Ly51^-$ respectively (Figure 40).

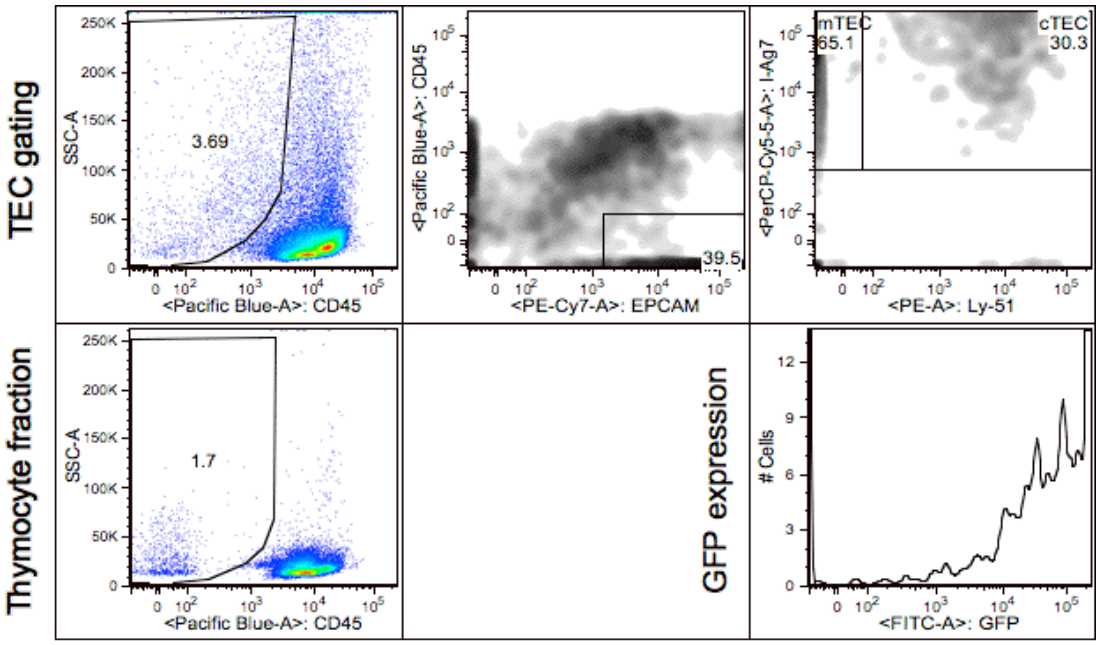

Figure 40: Gating strategy for cTEC/mTEC staining; TEC fraction after Percoll gradient, was first gated on CD45$^-$, then on EPCAM$^+$, cTEC/mTEC subsets were distinguished by Ly51 expression; lower row shows CD45 expression of thymocyte fraction after Percoll gradient and GFP expression of CD45$^-$ EPCAM$^+$ cells

To also assess activation status and ability to provide costimulation to developing T cells, expression levels of CD86 and CD80 were measured along with the flow cytometry analysis.

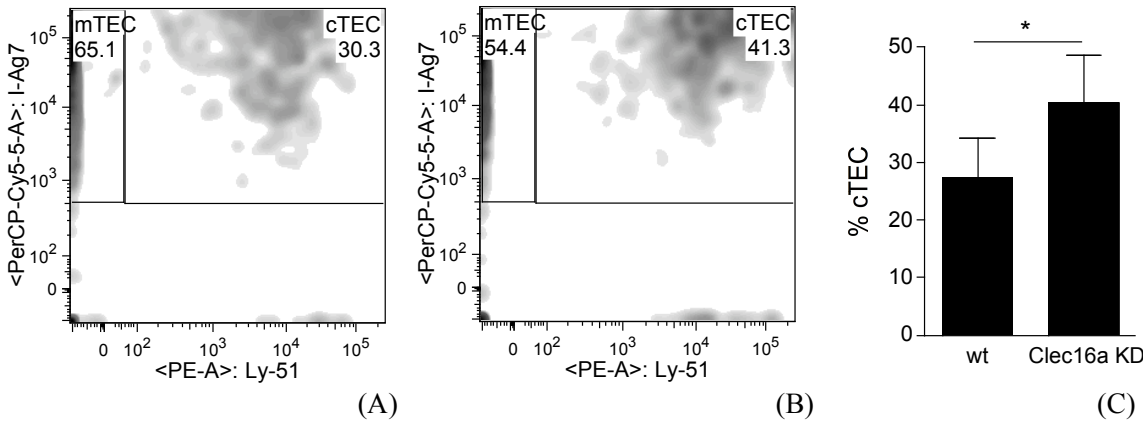

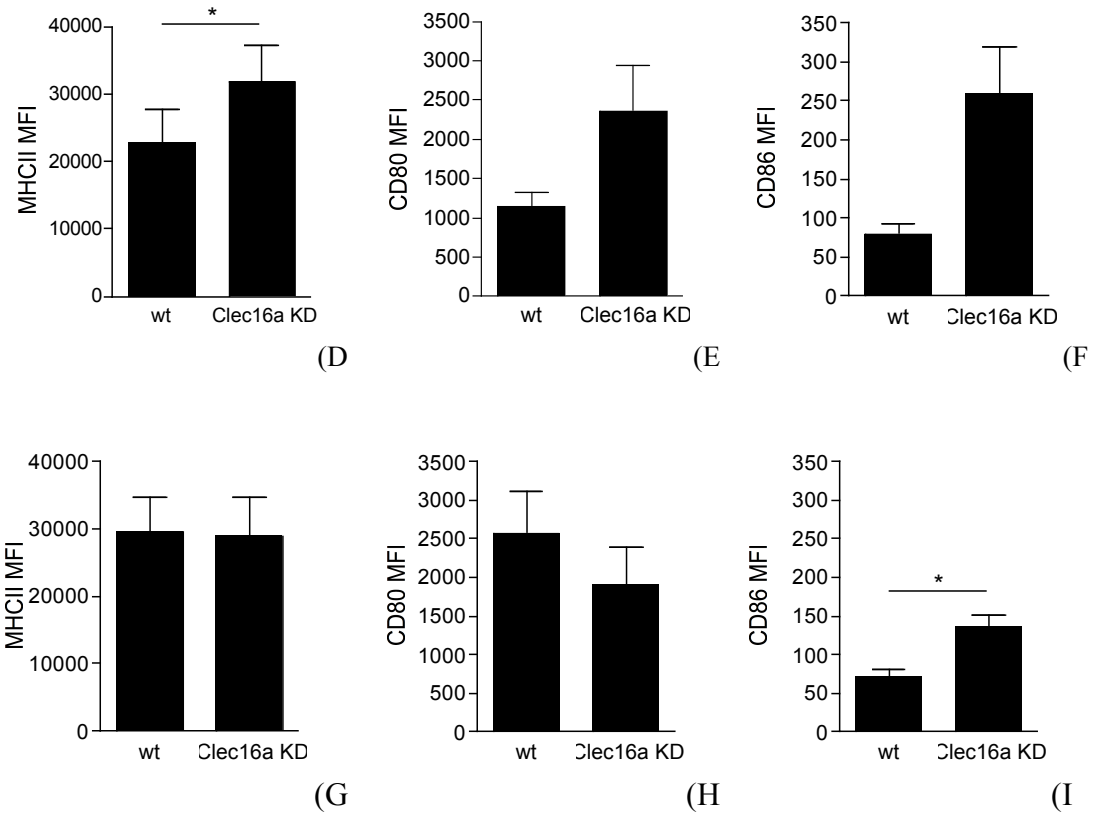

Figure 41: cTEC and mTEC proportions in (A) NOD WT and (B) NOD CLEC16A KD thymi, (C) summarizes six independent experiments P=0,0391; (D) to (I) summarize five independent experiments, geometric mean fluorescent intensities are given; (D) MHCII level of cTECs, P=0,0207; (E) CD80 level of cTECs, not significant (ns); (F) CD86 level of cTECs, ns; (G) MHCII level of mTECs; (H) CD80 level of mTECs; (I) CD86 level of mTECs, P=0,0247

The staining for TECs revealed that in CLEC16A KD thymi the cTEC compartment was clearly and significantly enlarged. Additionally a significant higher expression of MHCII and tendency to higher CD80/86 expression were featured by this CLEC16A KD cTEC subset (Figure 41). Costimulatory molecule and MHCII expression in mTECs did not differ to that extent between NOD WT and CLEC16A KD thymi, however a significantly higher CD86 expression could be seen.

7.2.6.3 Analysis of the TCR repertoire

As cTECs are crucial for positive selection and alterations in antigen processing in these cells can have effects on single TCR specifities[33] we decided to analyze the TCR repertoire of CLEC16A KD NOD mice. For this we compared abundance of ten different Vβ chains in splenocytes and thymocytes of NOD WT and NOD CLEC16A KD mice by flow cytometry.

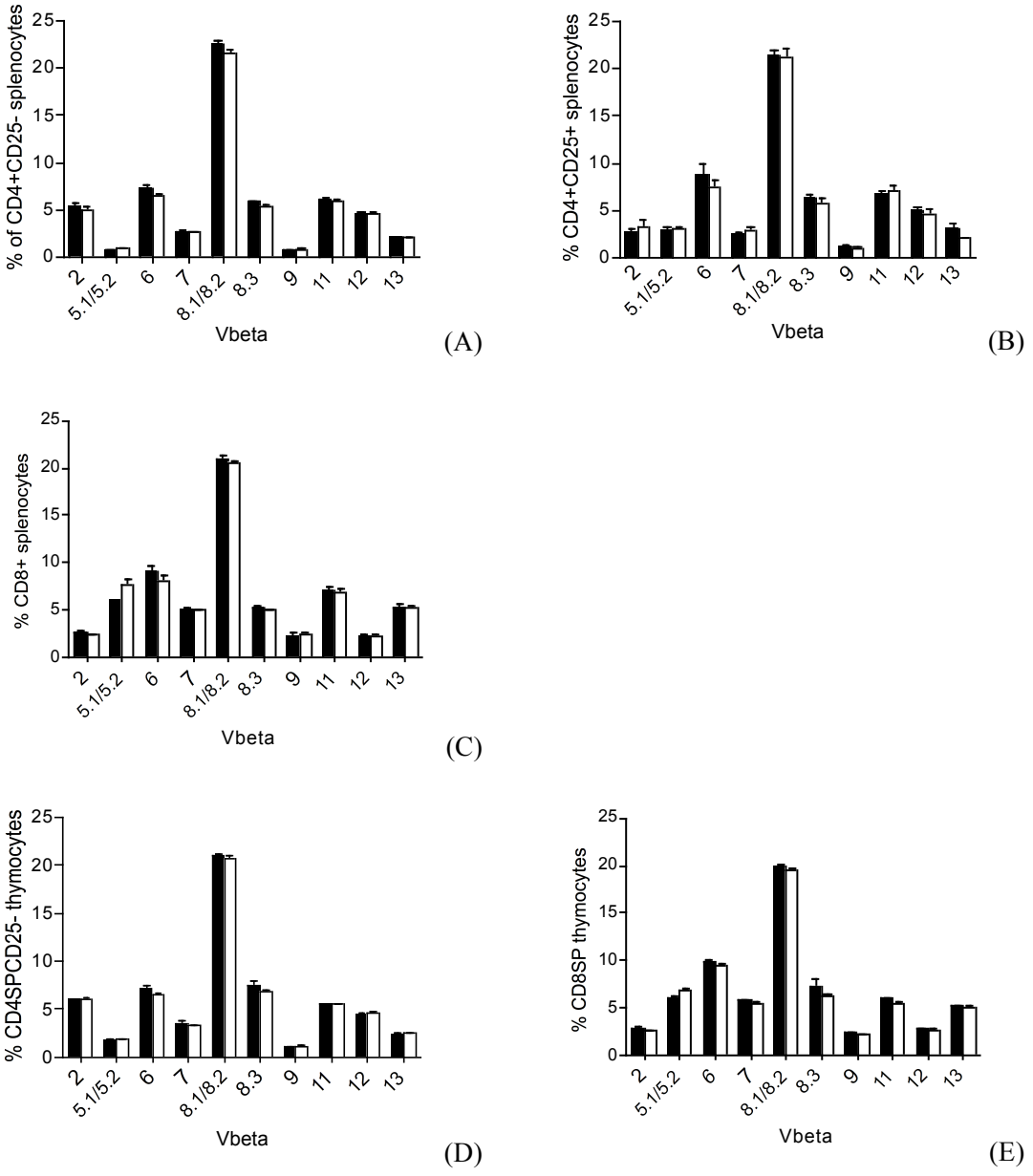

Figure 42: Flow cytometric analysis of distribution of ten Vβ chains in NOD WT (black) and NOD CLEC16A KD (white) $CD4^+$ $CD25^-$ (A), $CD4^+$ $CD25^+$ (B),

$CD8^+$ splenocytes (C) and CD4 SP (D) or CD8 SP thymocytes (E); combined results of six different mice for splenocytes and five for thymocytes

Analysis of these ten specific Vβ chains however did not reveal any difference in thymic selection of these specifities (Figure 42).

In this report it was shown that NOD CLEC16A KD mice are clearly protected from diabetes development. The origin of this protection could be narrowed to the T cell compartment, which was found to be hyporeactive *in vitro*. Analysis of antigen presenting cells revealed an enlarged and activated cTEC compartment, suggesting a possible alteration in the thymic selection of T cells in CLEC16A KD mice.

8 Discussion and Outlook

8.1 Functional study of sCTLA-4

Genome association studies showed that a polymorphism in the *CTLA4* gene conveys susceptibility to T1D.[147] The susceptibility SNP was correlated with reduced expression of the splice isoform sCTLA-4[148].

To date there is no information about the differential functions of CTLA-4 isoforms. A lot of the knowledge that is now available about CTLA-4 function is based on studies on CTLA-4 knockout mice. However these mice lack exon 2 and part of exon 3[202], affecting all three isoforms present in mice. With these mice a differentiated examination of the isoforms is thus impossible.

With our approach we intended to target sCTLA-4 alone by RNAi, mimicking its human T1D susceptibility expression pattern and therewith studying its function in the immune system and T1D. To provide a genetic background generally vulnerable to T1D development, the knockdown was done on the NOD background.

At the begin of my studies, sCTLA-4 knockdown mice with 70% knockdown efficiency (Figure 10) had already been generated by Stephan Kissler. Expression of the transgene (shRNA plus EGFP) could be detected in approximately 65-75% of lymphocytes (Figure 9). This effect is due to the variability of transgene expression. Since the site of integration is largely random with the use of lentiviral vectors, the possibility of epigenetic modification and silencing cannot be excluded[211]. This is also an explanation for the different percentages of EGFP in different cell subsets[212].

Though CTLA-4 knockout animals show a massive lymphoproliferation, which goes along with skewing cell ratios towards $CD4^+$ subsets[200], this is not the case if sCTLA-4 is selectively reduced (Figure 11,12). There is also no increase in activated T cells (Figure 13)

or alteration in responsiveness to TCR signaling (Figure 15, 16, 17), although CTLA-4 is considered to be a potent negative regulator of conventional T cells[202]. Especially during the activation of lymph node cells with anti-CD3, CTLA-4 is thought to be able to inhibit the costimulation by competition with CD28 for CD80/86 binding[213], disruption of CD28 and/or TCR localization in the immunological synapse[214,215], negative effects on the cell cycle[216,217] or also downregulation of CD80/86[119,120]. Still the reduction of sCTLA-4 does not seem to affect these mechanisms in such extend that it would influence the outcome of this strong activation by anti-CD3 (Figure 15). In line with that finding is the consistency of GITR and overall surface and intracellular CTLA-4 expression of Treg and Teff cells. These results suggest that the general phenotype of these cells is largely unaffected by the reduction of sCTLA-4 expression (Figure 20).

CTLA-4 is also supposed to be mainly active in Treg cells, since it may be one of their most important modes of action[119,207,208,218-221]. In conventional Treg assays (unlike *in vivo*), as performed here, cell-cell-contact is essential for mediating inhibition, though it may be sufficient to provide it at the initial phase of the culture[111].

At high ratios of Treg/Teff, Treg cells with less sCTLA-4 were working as well as WT Treg cells. However when Treg cells were further diluted, to a degree where inhibition becomes weaker, they failed to mediate suppression (Figure 18).

This finding was further supported by the fact that sCTLA-4 KD Treg cells were unable to suppress IFN-γ production at these ratios. As anticipated, the level of IL-2 was not dependent on the Treg genotype, since it is mostly reduced by the presence of the high affinity receptor CD25, that was not altered by the knockdown (Figure 19).

These results gained further impact after repeating them with *in vitro* differentiated Treg cells, showing that the outcome of sCTLA-4 reduction is independent of Treg development (Figure 23).

Whether this is due to a reduced expression of cell-contact mediating surface-molecules or to a shortage in soluble mediators of inhibition, potentially sCTLA-4 itself, remains elusive. Yet

from the impairment at low ratios it can be inferred that there is either a mechanism affected, which comes into action when direct inhibition through cell contact has become impossible, or that the threshold of the common mechanism is marked up by reduction of sCTLA-4.

To further clarify the cause for the Treg impairment, we examined one of the modes of action found to be dependent on CTLA-4 expression in more detail. As already mentioned, Treg cells were found to be able to downregulate CD80/86 on APCs, by an as yet incompletely clarified mechanism[116-118]. Recently Qureshi et al.[120] showed that flCTLA-4 depletes CD80/86 from the surface of APCs by transendocytosis. However the contribution of other CTLA-4 isoforms were not addressed in this study.

Coculture experiments with DCs and Treg cells revealed the necessity for sCTLA-4 in this mechanism, since transgenic Treg cells were heavily impaired in their inhibitory function (Figure 21).

It was only possible to show this for CD86 but not CD80, because in the majority of experiments there was no sufficient upregulation of this costimulator in splenic DCs after 42h. This is consistent with findings concerning the temporal expression pattern of CD80/86, with CD86 being constitutively expressed on T cells and APCs and CD80 being induced after T-cell/APC contact, with its peak after 48h of activation[222].

Thus we could show that sCTLA-4 is involved in the modulation of costimulation by splenic dendritic cells, thereby suggesting a possible pathway in Treg cells in which sCTLA-4 is at least partly effectual. These results also closely resemble the defects demonstrated by Wing et al.[119] when conditionally knocking out CTLA-4 in Foxp3 expressing cells. Whether this is also the mechanism responsible for our findings in the conventional Treg assay remains to be clarified.

Mechanisms of inhibition by Treg cells are claimed to be different *in vitro* and *in vivo*[104]. However it is not yet clear if the mechanism we revealed to be defective in sCTLA-4 KD Treg cells is also important in *vivo*. The aim of this study being to clarify the role of sCTLA-4

in vivo, we strived to evaluate the *in vitro* finding of impaired sCTLA-4 KD Treg cells in an *in vivo* model.

Since CTLA-4 on Treg cells had been shown by Read et al.[207,208] to be crucial in the $CD4^{+}CD45RB^{hi}$ induced Colitis model, we set out to test the ability of sCTLA-4 KD Treg cells to protect in this setting. Due to the use of the NOD strain instead of the more commonly used BALB/c strain for colitis induction, overall disease severity was less pronounced than seen by Read et al.[207,208]. Nevertheless Treg cells with silenced sCTLA-4 failed to protect from colitis development, consistent with our *in vitro* data (Figure 24). A reduction of sCTLA-4 thus shows a comparable outcome to antibody mediated CTLA-4 blockade by Read et al.[208]. These results demonstrate a notable role of sCTLA-4 in Treg cell function also *in vivo*.

The T1D susceptibility allele of CTLA-4 causes a shift in splicing ratios towards the full length CTLA-4 variant, thereby reducing the relative amount of sCTLA-4. Whether this reduction is causative to conveying susceptibility was to be ascertained in this thesis.

Cohorts of WT NOD, sCTLA-4 KD NOD as well as Idd5.1 WT and Idd5.1 sCTLA-4 KD mice were therefore monitored for diabetes onset and incidence. Following diabetes development also on the Idd5.1 congenic background facilitated examining the effect of the sCTLA-4 KD on an otherwise protective CTLA-4 locus[223,224]. Indeed, sCTLA-4 silencing only transferred additional susceptibility to diabetes on the Idd5.1 background (Figure 25). This approach avoided a potentially confounding effect of the reduced expression levels of the liCTLA-4 splice variant in the fully susceptible NOD strain that was likely to render memory/effector T cells more receptive to initial activation by weaker stimuli[224].

Of note, the liCTLA-4 splice variant is not produced from the human *CTLA-4* gene[148], indicating that the role of sCTLA-4 may even be more prominent in humans, being the only other splice variant apart from flCTLA-4.

CTLA-4 had been shown to be essential to Treg cells in preventing autoimmune diseases in multiple studies[207,208,219-221], however no discrimination between splice variants had been addressed. We have now shown that sCTLA-4 plays a role in Treg cell function *in vitro* and *in vivo*, and that it also conveys protection in the setting of autoimmune diabetes in the NOD model. Thus the reduction of sCTLA-4 correlated with the susceptibility allele of the locus CT60 is likely to be responsible for conveying higher odds to developing T1D. The underlying mechanism may partly be cell extrinsic in acting on antigen presenting cells, however the relative contribution of flCTLA-4 and sCTLA-4 in this mode of action still remains to be clarified.

8.2 Functional study of CLEC16A in T1D

CLEC16A was found to be associated with several autoimmune diseases, with T1D[143,151,153,225,226] and multiple sclerosis[227,228] in particular. To date its function remains absolutely elusive. From expression analysis (BioGPS.org) the putative function could be linked to the immune system, (DC, B cells, NK cells) in concordance with its association with autoimmune diseases. Its predicted ITAM motif also contributes to that notion[151]. Furthermore a study on the Drosophila orthologue *ema* indicated a possible role of CLEC16A in endosomal maturation[160].

The aim of this study was the functional analysis of CLEC16A, especially in the setting of type 1 diabetes. To achieve this goal, we introduced an shRNA targeting *Clec16a*, previously validated *in vitro* (Figure 26), into NOD embryos. This was accomplished by injecting the embryos with lentivirus carrying the shRNA. To allow for the flexibility of including studies with transgenic TCR mouse lines, many of which are on the C57BL/6 background, we later also integrated the same shRNA into the C57BL/6 mouse line. However only few experiments have been conducted with this second mouse line so far.

Both virus injections were successful as they yielded founder mice with substantial EGFP expression. Since the transferred shRNA was coupled to the EGFP sequence, this was an indirect proof of shRNA transfer to these mice. Further breeding subsequently led to homozygous mouse lines with improved and consistent EGFP expression levels, also indicating that a single copy of the construct had integrated into each mouse line. Otherwise a larger variety of EGFP expression would be expected, due to segregation. The EGFP expression of 70% in NOD and 62% in C57BL/6 lymphocytes can be attributed to the site of integration, as has been addressed in 8.1. Notably the expression of EGFP was higher in granulocytes, 85% in NOD and 77% in C57BL/6, which was beneficial as CLEC16A had been hypothesized to be active in antigen presenting cells especially (Figure 27).

As previously mentioned, EGFP expression can only provide indirect evidence for the presence and effectiveness of the shRNA. A direct read-out of RNAi induced by the shRNA is possible by mRNA quantitation by qPCR or protein quantitation via western blotting. Both methods were applied in this thesis to gain insight to knockdown efficiency in the NOD-CLEC16A KD mouse line.

ShRNA #3 that was used to generate NOD CLEC16A KD mice aligns with a sequence in exon 19 of murine *Clec16a*. This exon is included in nine of eleven splice variants, two of which are non coding and one other that is predicted to undergo nonsense mediated decay (Ensembl). Only one putative coding mRNA, a truncated splice variant of 356bp, is not targeted by this shRNA, CLEC16A-006. To obtain information about the effect of the shRNA, firstly a qPCR based on the Universal Probe Library (Roche) was conducted, applying various probe and primer sets. One of these primer sets (UPL7) directly amplified the region that was complementary to the shRNA. However all these efforts did only reveal a minor knockdown of about 25% (Figure 28, 29). A high basal expression of non-coding mRNAs not seen in the expression analysis (BioGPS) could give an explanation. On the one hand the shRNA could be captured by these overexpressed mRNAs. On the other hand this would also explain the very high expression level of *Clec16a* in T cells that was very comparable to B cells but was not implied in the BioGPS analysis. However through personal communication with Lucy Davidson from the Lab of John Todd, Cambridge (UK), we learned that the knockout of *Clec16a* could also not be confirmed adequately by qPCR. This would rather imply the presence of a pseudogene that was not targeted by the knockout and thus still gives a qPCR signal after the knockout had been accomplished. This alternative would also explain the lack of knockdown efficiency detected by qPCR and not exclude the possibility that the knockdown is higher in reality.

To rule out the possibilities of pseudogenes or non-coding variants interfering with qPCR, we carried out western blot experiments for CLEC16A on organs and EGFP sorted splenocytes. The polyclonal antibody used here was directed against the human protein of CLEC16A. As

mentioned in the results section the protein is very unstable and has a relatively short half-life. Consequently only mild signals could be obtained from western blotting for the full length isoform (117kDa, Figure 30). However these mild signals did not reveal a reduction of CLEC16A in knockdown cells. Curiously the bands appearing in western blot do not match the predicted protein weights of the different isoforms of CLEC16A, they are rather due to nonspecific binding. Hence the knockdown could also not be proved by western blot, however also this technique failed to convincingly prove the contrary. We therefore decided to create an additional NOD-CLEC16A KD mouse line with another shRNA, to be able to confirm results obtained from the first mouse line and thus circumvent the need of showing the knockdown on the molecular level. An effective shRNA has now been cloned into an improved vector (pUGM) and the first NOD embryos have been microinjected with lentivirus generated from this new vector.

We then evaluated the effect of the presumed loss of CLEC16A in NOD mice and its influence on disease incidence. On this matter we followed cohorts of NOD WT and NOD CLEC16AKD females for 200 days as to glycosuria occurrence. Surprisingly, almost no NOD CLEC16A KD mice became diabetic, indicating a strong protection due to CLEC16A KD (Figure 31).

Comparable protection could also be seen when inducing diabetes by cyclophosphamide administration (Figure 32). As part of its action CY causes the death of fast proliferating lymphocytes, thereby significantly diminishing the pool of peripheral B and Treg cells[198]. Since this depletion takes part between d2 and d7 after administration[198] and diabetes onset takes place soon after, an acute role for peripheral B cells and Treg cells in the protection conveyed by knockdown of CLEC16A seems improbable.

Expression pattern and the putative ITAM motif pointed to a role of CLEC16A in the immune system. We used adoptive transfer experiments to assess whether the protective effect of CLEC16A KD was intrinsic to the immune system, as expected. Splenocytes were transferred into NOD.SCID mice and diabetes was then induced by cyclophosphamide

administration. As foreseen, splenocytes of NOD CLEC16A KD mice were unable to transfer diabetes susceptibility to NOD.SCID animals, thereby excluding a beta-cell intrinsic effect (Figure 33). However to obviate a role of CLEC16A in beta-cells, the experiment would have to be repeated with transfer of NOD WT splenocytes into NOD.SCID CLEC16A KD mice. These mice are currently being bred and the first mice homozygous for both the transgene and the SCID mutation are were born and are being mated to establish the new mouse line.

To further determine which cell subset could be responsible for diabetes protection we repeated the previous experiment with purified B and T cells in different genotype combinations. We thereby established that diabetes susceptibility was dependent on the genotype of T cells alone, independently of whether WT or CLEC16A KD B cells were used (Figure 34). Even though we initially hypothesized a role for CLEC16A in antigen presenting cells this finding was not entirely surprising, since T cells are the crucial cell type responsible for beta cell destruction and they are considerably influenced by peripheral and/or central APCs in their reactivity.

All *in vivo* data led us to draw the conclusion that CLEC16A KD rendered T cells less autoreactive. We subsequently tested this implication in several *in vitro* assays.

Indeed all efforts that were designed to activate CLEC16A KD CD4 T effector cells via antibody stimulation of CD3 and CD28 revealed the diminished reactivity of these cells. This held true regardless of the origin of APCs they were stimulated with (Figure 35), also contributing to the notion that APC genotype may not be crucial in the acute phase of activation, as already mentioned in conjunction with the CY experiments with regards to B cells.

CD4 T effector cells are however in principle able to react to activation by proliferation, as seen after PMA/Ionomycin treatment. This indicates a defect or down tuning of signal transduction upstream of PKCθ activation and Ca^{2+} release, as these are the steps of the signaling chain whereupon PMA/Ionomycin acts (Figure 37). Notably CD4 T effector cells did not show a typical anergic phenotype (data not shown) as to CTLA-4 expression[229].

Also, mixed lymphocyte reactions that only activate 5-10% of allo-reactive T cells did not show a reduced responsiveness of CLEC16A KD T cells (Figure 36). However in this assay full splenocytes were used as responder cells, so discrimination of CD4 and CD8 T cell response was not possible. Thus CD8 T cell response might mask the lack of proliferation of CD4 T effector cells. Another explanation could be a faster time course of this reaction to conventional proliferation assays that would give CLEC16A KD T cells the time to catch up. Time course experiments could clarify this issue.

From *in vivo* and *in vitro* experiments, as well as from information about the expression pattern and function of the Drosophila orthologue of *Clec16a* we hypothesized a role of this gene in central or peripheral antigen presenting cells. Alterations in their ability to present pMHC complexes to T cells are likely to change their ability to react to stimulation. As a consequence we first examined peripheral APCs as to their ability of being activated themselves, measured by surface marker expression and by their endocytotic capacity. Endosomal maturation was of special interest, since the Drosophila orthologue *ema* is crucial for endosomes to develop normally. However none of the assays performed revealed any difference due to knockdown of *Clec16a*. More detailed information on this is given in the doctoral thesis of Lilli Teresa Probst.

Other candidates for altered antigen presenting cells are central, thymic APCs like medullary and cortical epithelial cells (mTECs and cTECs). These cells are mainly responsible for negative and positive selection respectively and can thus influence the overall reactivity of T cells by selecting a certain range of TCR affinities. To gain more insight into the TECs of CLEC16A KD mice, we performed antibody staining of enriched thymic epithelial cells and analyzed them via flow cytometry. Subset staining revealed an increased cTEC compartment in CLEC16A KD thymi. We also found higher expression of the costimulatory molecules CD80 and CD86 on these cells that additionally exhibited a very high EGFP expression (Figure 41). This heightened EGFP intensity could point to an especially high shRNA level und thus higher knockdown efficiency in these cells. Of note, an EGFP dependent activation

effect can be dismissed, since Nishikawa et al. have previously shown that GFP expression in cTECs and or mTECs does not enhance cell subset ratios or activation status[230]. Medullary as well as cortical TECs have been shown to be able to stimulate T cell proliferation and to express costimulatory molecules, yet only a small fraction of cTECs was seen to express CD80 and CD86[231]. This specific subset is thus likely to be expanded in NOD CLEC16A KD mice. The increased cell number of cTECs and their heightened expression of costimulatory molecules points towards an alteration of positive selection in NOD CLEC16A KD mice. This could also provide an explanation for the impaired reactivity of T cells from these mice *in vitro* and *in vivo*. Nevertheless more information has to be obtained to support this notion. It had been shown that alterations in the proteolytic processing of proteins in the endocytic and lysosomal compartments can result in a diminished CD4 population[29] or also in the abrogation of positive selection of certain TCR specifities[33]. As the CD4 compartment as such was not reduced, we had a closer look at TCR Vβ chain distribution in those mice. In the ten Vβ chains that were tested no difference emerged (Figure 42), not out ruling out however that other Vβ chains could be affected.

To further investigate the outcome of CLEC16A KD on T cell selection we plan to also take advantage of the aforementioned NOD.SCID CLEC16A KD mice that are currently being bred. Bone marrow transfer of NOD WT cells into lethally irradiated NOD.SCID CLEC16A KD mice will give us the opportunity to follow CLEC16A sufficient T cells in their development through a CLEC16A deficient thymus and examine the effects of developing in this environment.

In summary, we generated NOD mice carrying a knockdown for CLEC16A to study its function especially on the background of type 1 diabetes, thereby seeking to clarify the reason for its association with autoimmune diabetes and other autoimmune diseases. These knockdown animals emerged to be highly protected from diabetes. This protection could

subsequently be pinpointed to be caused by a defect in T cell function evidenced by hyporesponsiveness to TCR stimuli *in vitro*. Due to its reported expression pattern and a study that showed a role in endosomal maturation of its Drosophila orthologue, we hypothesized the impaired T cell reactivity to be caused by APCs. Peripheral APCs did however not show any alterations due to CLEC16A KD. Though when examining thymic epithelial cells, we found an increased cTEC pool that also featured high expression of costimulatory molecules, pointing towards a role of CLEC16A in T cell development. Yet further studies have to be conducted to gain more insight into the mechanism in which CLEC16A is involved. Furthermore, all key experiments will be repeated with a second NOD CLEC16A KD line carrying a distinct shRNA against CLEC16A that is currently being generated, to exclude non-specific effects and support the specificity and efficiency of the knockdown, especially since this could not be achieved by molecular methods. In conclusion, we gained the first evidence about the function of an as yet unstudied gene in the course of this thesis, and linked this gene's function to the immune system, thereby providing a first possible causation for its association with autoimmune diseases.

9 Abbreviations

APC	antigen presenting cell
B6	C57BL/6J
CD	cluster of differentiation/designation
CLEC16A	C-type lectin domain family 16 member a
cTEC	cortical thymic epithelial cell
CBA	cytometric bead array
CTLA-4	cytotoxic t-lymphocyte antigen 4
CY	cyclophosphamide
DC	dendritic cell
DMEM	Dulbecco's modified Eagle medium
DN	double negative
DNA	deoxyribonucleic acid
DP	double positve
EGFP	enhanced green fluorescent protein
ELISA	enzyme-linked immunosorbent assay
ema	endosomal maturation defective
FACS	fluorescent activated cell sorting
flCTLA-4	full length cytotoxic t-lymphocyte antigen 4
Foxp3	forkhead box P3
GFP	green fluorescent protein
GITR	glucocorticoid-induced tumor necrosis factor receptor
Idd	insulin dependent diabetes
IFN	interferon
IL	interleukin
ITAM	immunoreceptor tyrosine-based activation motif
iTreg	induced Treg

KD	knockdown
KIAA0350	KI stands for “Kazusa DNA Research Institute”; “AA” are reference characters
KO	knockout
liCTLA-4	ligand independent cytotoxic t-lymphocyte antigen 4
LPS	lipopolysaccharide
LTR	long terminal repeat
MACS	magnetic cell separation
MHC	major histocompatibility complex
miRNA	micro RNA
mTEC	medullary thymic epithelial cell
NK cell	natural killer cell
NOD	non obese diabetic
nTreg	natural occurring Treg
PCR	polymerase chain reaction
PMA	phorbol 12-myristate 13-acetate
pMHC	peptide / MHC complex
qPCR	quantitative PCR
RNA	ribonucleic acid
RNAi	RNA interference
RPMI-1640	Roswell Park Memorial Institute cell culture medium
SCID	severe combined immunodeficiency
sCTLA-4	soluble cytotoxic t-lymphocyte antigen 4
shRNA	short hairpin RNA
siRNA	short interfering RNA
SNP	single nucleotide polymorphism
T1D	type 1 diabetes
TEC	thymic epithelial cell

TCR	T cell receptor
Teff	effector T cell
Tg	transgene
TRA	tissue restricted antigen
Treg	regulatory T cell
WT	wildtype

10 Bibliography

1. Goodnow, C.C., Sprent, J., Fazekas de St Groth, B. & Vinuesa, C.G. Cellular and genetic mechanisms of self tolerance and autoimmunity. *Nature* **435**, 590-597 (2005).
2. Murphy, K.M., Travers, P. & Walport, M. *Janeway's Immunobiology*. (Taylor & Francis: 2008).
3. Ignatowicz, L., Kappler, J. & Marrack, P. The repertoire of T cells shaped by a single MHC/peptide ligand. *Cell* **84**, 521-529 (1996).
4. Laufer, T.M., DeKoning, J., Markowitz, J.S., Lo, D. & Glimcher, L.H. Unopposed positive selection and autoreactivity in mice expressing class II MHC only on thymic cortex. *Nature* **383**, 81-85 (1996).
5. Wardemann, H. u. a. Predominant autoantibody production by early human B cell precursors. *Science* **301**, 1374-1377 (2003).
6. Zerrahn, J., Held, W. & Raulet, D.H. The MHC reactivity of the T cell repertoire prior to positive and negative selection. *Cell* **88**, 627-636 (1997).
7. Jacobson, D.L., Gange, S.J., Rose, N.R. & Graham, N.M. Epidemiology and estimated population burden of selected autoimmune diseases in the United States. *Clin. Immunol. Immunopathol* **84**, 223-243 (1997).
8. von Boehmer, H., Teh, H.S. & Kisielow, P. The thymus selects the useful, neglects the useless and destroys the harmful. *Immunology Today* **10**, 57-61 (1989).
9. Pui, J.C. u. a. Notch1 Expression in Early Lymphopoiesis Influences B versus T Lineage Determination. *Immunity* **11**, 299-308 (1999).
10. Zúñiga-Pflücker, J.C. T-cell development made simple. *Nat. Rev. Immunol* **4**, 67-72 (2004).
11. Lind, E.F., Prockop, S.E., Porritt, H.E. & Petrie, H.T. Mapping precursor movement through the postnatal thymus reveals specific microenvironments supporting defined stages of early lymphoid development. *J. Exp. Med* **194**, 127-134 (2001).
12. Porritt, H.E., Gordon, K. & Petrie, H.T. Kinetics of steady-state differentiation and mapping of intrathymic-signaling environments by stem cell transplantation in nonirradiated mice. *J. Exp. Med* **198**, 957-962 (2003).
13. Penit, C. Localization and phenotype of cycling and post-cycling murine thymocytes studied by simultaneous detection of bromodeoxyuridine and surface antigens. *J. Histochem. Cytochem* **36**, 473-478 (1988).
14. Wu, L. T lineage progenitors: the earliest steps en route to T lymphocytes. *Curr. Opin. Immunol* **18**, 121-126 (2006).
15. Pennington, D.J., Silva-Santos, B. & Hayday, A.C. Gammadelta T cell development--having the strength to get there. *Curr. Opin. Immunol* **17**, 108-115 (2005).
16. von Boehmer, H. u. a. Thymic selection revisited: how essential is it? *Immunol. Rev* **191**, 62-78 (2003).
17. Ciofani, M., Knowles, G.C., Wiest, D.L., von Boehmer, H. & Zúñiga-Pflücker, J.C. Stage-specific and differential notch dependency at the alphabeta and gammadelta T lineage bifurcation. *Immunity* **25**, 105-116 (2006).
18. Kyewski, B. & Klein, L. A central role for central tolerance. *Annu. Rev. Immunol* **24**, 571-606 (2006).
19. Alam, S.M. u. a. T-cell-receptor affinity and thymocyte positive selection. *Nature* **381**, 616-620 (1996).
20. Daniels, M.A. u. a. Thymic selection threshold defined by compartmentalization of Ras/MAPK signalling. *Nature* **444**, 724-729 (2006).
21. Petrie, H.T. u. a. Multiple rearrangements in T cell receptor alpha chain genes maximize the production of useful thymocytes. *J. Exp. Med* **178**, 615-622 (1993).
22. Blackman, M. u. a. The T cell repertoire may be biased in favor of MHC recognition. *Cell* **47**, 349-357 (1986).

23. Shortman, K., Vremec, D. & Egerton, M. The kinetics of T cell antigen receptor expression by subgroups of CD4+8+ thymocytes: delineation of CD4+8+3(2+) thymocytes as post-selection intermediates leading to mature T cells. *J. Exp. Med* **173**, 323-332 (1991).
24. Huesmann, M., Scott, B., Kisielow, P. & von Boehmer, H. Kinetics and efficacy of positive selection in the thymus of normal and T cell receptor transgenic mice. *Cell* **66**, 533-540 (1991).
25. Klein, L., Hinterberger, M., Wirnsberger, G. & Kyewski, B. Antigen presentation in the thymus for positive selection and central tolerance induction. *Nat. Rev. Immunol* **9**, 833-844 (2009).
26. Starr, T.K., Jameson, S.C. & Hogquist, K.A. Positive and negative selection of T cells. *Annu. Rev. Immunol* **21**, 139-176 (2003).
27. Goldrath, A.W. & Bevan, M.J. Selecting and maintaining a diverse T-cell repertoire. *Nature* **402**, 255-262 (1999).
28. Honey, K. & Rudensky, A.Y. Lysosomal cysteine proteases regulate antigen presentation. *Nat. Rev. Immunol* **3**, 472-482 (2003).
29. Nakagawa, T. u. a. Cathepsin L: critical role in Ii degradation and CD4 T cell selection in the thymus. *Science* **280**, 450-453 (1998).
30. Bowlus, C.L., Ahn, J., Chu, T. & Gruen, J.R. Cloning of a novel MHC-encoded serine peptidase highly expressed by cortical epithelial cells of the thymus. *Cell. Immunol* **196**, 80-86 (1999).
31. Carrier, A. u. a. Differential gene expression in CD3epsilon- and RAG1-deficient thymuses: definition of a set of genes potentially involved in thymocyte maturation. *Immunogenetics* **50**, 255-270 (1999).
32. Cheunsuk, S. u. a. Prss16 is not required for T-cell development. *Mol. Cell. Biol* **25**, 789-796 (2005).
33. Gommeaux, J. u. a. Thymus-specific serine protease regulates positive selection of a subset of CD4+ thymocytes. *Eur. J. Immunol* **39**, 956-964 (2009).
34. Viken, M.K. u. a. Reproducible association with type 1 diabetes in the extended class I region of the major histocompatibility complex. *Genes Immun* **10**, 323-333 (2009).
35. Mizuochi, T., Kasai, M., Kokuho, T., Kakiuchi, T. & Hirokawa, K. Medullary but not cortical thymic epithelial cells present soluble antigens to helper T cells. *J. Exp. Med* **175**, 1601-1605 (1992).
36. Kasai, M. u. a. Difference in antigen presentation pathways between cortical and medullary thymic epithelial cells. *Eur. J. Immunol* **26**, 2101-2107 (1996).
37. Mizushima, N., Yamamoto, A., Matsui, M., Yoshimori, T. & Ohsumi, Y. In Vivo Analysis of Autophagy in Response to Nutrient Starvation Using Transgenic Mice Expressing a Fluorescent Autophagosome Marker. *Mol. Biol. Cell* **15**, 1101-1111 (2004).
38. Nedjic, J., Aichinger, M., Emmerich, J., Mizushima, N. & Klein, L. Autophagy in thymic epithelium shapes the T-cell repertoire and is essential for tolerance. *Nature* **455**, 396-400 (2008).
39. Seglen, P.O. & Bohley, P. Autophagy and other vacuolar protein degradation mechanisms. *Experientia* **48**, 158-172 (1992).
40. Kuma, A. & Mizushima, N. Physiological role of autophagy as an intracellular recycling system: With an emphasis on nutrient metabolism. *Seminars in Cell & Developmental Biology* **21**, 683-690 (2010).
41. Rabinowitz, J.D. & White, E. Autophagy and Metabolism. *Science* **330**, 1344 -1348 (2010).
42. Murata, S. u. a. Regulation of CD8+ T cell development by thymus-specific proteasomes. *Science* **316**, 1349-1353 (2007).
43. Kloetzel, P.M. & Ossendorp, F. Proteasome and peptidase function in MHC-class-I-mediated antigen presentation. *Curr. Opin. Immunol* **16**, 76-81 (2004).
44. Murata, S., Takahama, Y. & Tanaka, K. Thymoproteasome: probable role in generating positively selecting peptides. *Curr. Opin. Immunol* **20**, 192-196 (2008).

45. Nitta, T. u. a. Thymoproteasome shapes immunocompetent repertoire of CD8+ T cells. *Immunity* **32**, 29-40 (2010).
46. Ernst, B., Lee, D.S., Chang, J.M., Sprent, J. & Surh, C.D. The peptide ligands mediating positive selection in the thymus control T cell survival and homeostatic proliferation in the periphery. *Immunity* **11**, 173-181 (1999).
47. Lo, W.-L. u. a. An endogenous peptide positively selects and augments the activation and survival of peripheral CD4+ T cells. *Nat. Immunol* **10**, 1155-1161 (2009).
48. Fukui, Y. u. a. Positive and negative CD4+ thymocyte selection by a single MHC class II/peptide ligand affected by its expression level in the thymus. *Immunity* **6**, 401-410 (1997).
49. van Meerwijk, J.P. u. a. Quantitative impact of thymic clonal deletion on the T cell repertoire. *J. Exp. Med* **185**, 377-383 (1997).
50. Ignatowicz, L., Kappler, J. & Marrack, P. The repertoire of T cells shaped by a single MHC/peptide ligand. *Cell* **84**, 521-529 (1996).
51. Sohn, S.J., Thompson, J. & Winoto, A. Apoptosis during negative selection of autoreactive thymocytes. *Curr. Opin. Immunol* **19**, 510-515 (2007).
52. Linsk, R., Gottesman, M. & Pernis, B. Are tissues a patch quilt of ectopic gene expression? *Science* **246**, 261 (1989).
53. Derbinski, J., Schulte, A., Kyewski, B. & Klein, L. Promiscuous gene expression in medullary thymic epithelial cells mirrors the peripheral self. *Nat. Immunol* **2**, 1032-1039 (2001).
54. Gotter, J., Brors, B., Hergenhahn, M. & Kyewski, B. Medullary epithelial cells of the human thymus express a highly diverse selection of tissue-specific genes colocalized in chromosomal clusters. *J. Exp. Med* **199**, 155-166 (2004).
55. Anderson, M.S. u. a. Projection of an immunological self shadow within the thymus by the aire protein. *Science* **298**, 1395-1401 (2002).
56. Gallegos, A.M. & Bevan, M.J. Central Tolerance to Tissue-specific Antigens Mediated by Direct and Indirect Antigen Presentation. *The Journal of Experimental Medicine* **200**, 1039 -1049 (2004).
57. Koble, C. & Kyewski, B. The thymic medulla: a unique microenvironment for intercellular self-antigen transfer. *The Journal of Experimental Medicine* **206**, 1505 - 1513 (2009).
58. Klein, L., Hinterberger, M., von Rohrscheidt, J. & Aichinger, M. Autonomous versus dendritic cell-dependent contributions of medullary thymic epithelial cells to central tolerance. *Trends in Immunology* **32**, 188-193 (2011).
59. Gardner, J.M. u. a. Deletional Tolerance Mediated by Extrathymic Aire-Expressing Cells. *Science* **321**, 843 -847 (2008).
60. Fletcher, A.L. u. a. Lymph node fibroblastic reticular cells directly present peripheral tissue antigen under steady-state and inflammatory conditions. *The Journal of Experimental Medicine* **207**, 689 -697 (2010).
61. Lee, J.-W. u. a. Peripheral antigen display by lymph node stroma promotes T cell tolerance to intestinal self. *Nat. Immunol* **8**, 181-190 (2007).
62. Josefowicz, S.Z. & Rudensky, A. Control of regulatory T cell lineage commitment and maintenance. *Immunity* **30**, 616-625 (2009).
63. Groux, H. u. a. A CD4+ T-cell subset inhibits antigen-specific T-cell responses and prevents colitis. *Nature* **389**, 737-742 (1997).
64. Chen, Y., Kuchroo, V.K., Inobe, J., Hafler, D.A. & Weiner, H.L. Regulatory T cell clones induced by oral tolerance: suppression of autoimmune encephalomyelitis. *Science* **265**, 1237-1240 (1994).
65. Neurath, M.F. u. a. Experimental granulomatous colitis in mice is abrogated by induction of TGF-beta-mediated oral tolerance. *J. Exp. Med* **183**, 2605-2616 (1996).
66. Weiner, H.L. Oral tolerance: immune mechanisms and treatment of autoimmune diseases. *Immunol. Today* **18**, 335-343 (1997).
67. Nishizuka, Y. & Sakakura, T. Thymus and reproduction: sex-linked dysgenesia of the gonad after neonatal thymectomy in mice. *Science* **166**, 753-755 (1969).

68. Sakaguchi, S., Takahashi, T. & Nishizuka, Y. Study on cellular events in postthymectomy autoimmune oophoritis in mice. I. Requirement of Lyt-1 effector cells for oocytes damage after adoptive transfer. *J. Exp. Med* **156**, 1565-1576 (1982).
69. Asano, M., Toda, M., Sakaguchi, N. & Sakaguchi, S. Autoimmune disease as a consequence of developmental abnormality of a T cell subpopulation. *J. Exp. Med* **184**, 387-396 (1996).
70. Chatila, T.A. u. a. JM2, encoding a fork head-related protein, is mutated in X-linked autoimmunity-allergic disregulation syndrome. *J. Clin. Invest* **106**, R75-81 (2000).
71. Wildin, R.S. u. a. X-linked neonatal diabetes mellitus, enteropathy and endocrinopathy syndrome is the human equivalent of mouse scurfy. *Nat. Genet* **27**, 18-20 (2001).
72. Brunkow, M.E. u. a. Disruption of a new forkhead/winged-helix protein, scurfin, results in the fatal lymphoproliferative disorder of the scurfy mouse. *Nat. Genet* **27**, 68-73 (2001).
73. Bennett, C.L. u. a. The immune dysregulation, polyendocrinopathy, enteropathy, X-linked syndrome (IPEX) is caused by mutations of FOXP3. *Nat. Genet* **27**, 20-21 (2001).
74. Fontenot, J.D., Gavin, M.A. & Rudensky, A.Y. Foxp3 programs the development and function of CD4+CD25+ regulatory T cells. *Nat. Immunol* **4**, 330-336 (2003).
75. Fontenot, J.D. u. a. Regulatory T cell lineage specification by the forkhead transcription factor foxp3. *Immunity* **22**, 329-341 (2005).
76. Hori, S., Nomura, T. & Sakaguchi, S. Control of regulatory T cell development by the transcription factor Foxp3. *Science* **299**, 1057-1061 (2003).
77. Khattri, R., Cox, T., Yasayko, S.-A. & Ramsdell, F. An essential role for Scurfin in CD4+CD25+ T regulatory cells. *Nat. Immunol* **4**, 337-342 (2003).
78. Lin, W. u. a. Regulatory T cell development in the absence of functional Foxp3. *Nat. Immunol* **8**, 359-368 (2007).
79. Gavin, M.A. u. a. Foxp3-dependent programme of regulatory T-cell differentiation. *Nature* **445**, 771-775 (2007).
80. Curotto de Lafaille, M.A. & Lafaille, J.J. Natural and adaptive foxp3+ regulatory T cells: more of the same or a division of labor? *Immunity* **30**, 626-635 (2009).
81. Germain, R.N. T-cell development and the CD4-CD8 lineage decision. *Nat. Rev. Immunol* **2**, 309-322 (2002).
82. Singer, A., Adoro, S. & Park, J.-H. Lineage fate and intense debate: myths, models and mechanisms of CD4- versus CD8-lineage choice. *Nat. Rev. Immunol* **8**, 788-801 (2008).
83. Pacholczyk, R. & Kern, J. The T-cell receptor repertoire of regulatory T cells. *Immunology* **125**, 450-458 (2008).
84. Pacholczyk, R., Ignatowicz, H., Kraj, P. & Ignatowicz, L. Origin and T cell receptor diversity of Foxp3+CD4+CD25+ T cells. *Immunity* **25**, 249-259 (2006).
85. Hsieh, C.-S. u. a. Recognition of the peripheral self by naturally arising CD25+ CD4+ T cell receptors. *Immunity* **21**, 267-277 (2004).
86. Olivares-Villagómez, D., Wang, Y. & Lafaille, J.J. Regulatory CD4(+) T cells expressing endogenous T cell receptor chains protect myelin basic protein-specific transgenic mice from spontaneous autoimmune encephalomyelitis. *J. Exp. Med* **188**, 1883-1894 (1998).
87. Apostolou, I., Sarukhan, A., Klein, L. & von Boehmer, H. Origin of regulatory T cells with known specificity for antigen. *Nat. Immunol* **3**, 756-763 (2002).
88. Kawahata, K. u. a. Generation of CD4(+)CD25(+) regulatory T cells from autoreactive T cells simultaneously with their negative selection in the thymus and from nonautoreactive T cells by endogenous TCR expression. *J. Immunol* **168**, 4399-4405 (2002).
89. Jordan, M.S. u. a. Thymic selection of CD4+CD25+ regulatory T cells induced by an agonist self-peptide. *Nat. Immunol* **2**, 301-306 (2001).
90. van Santen, H.-M., Benoist, C. & Mathis, D. Number of T reg cells that differentiate does not increase upon encounter of agonist ligand on thymic epithelial cells. *J. Exp. Med* **200**, 1221-1230 (2004).

91. Hsieh, C.-S., Zheng, Y., Liang, Y., Fontenot, J.D. & Rudensky, A.Y. An intersection between the self-reactive regulatory and nonregulatory T cell receptor repertoires. *Nat. Immunol* **7**, 401-410 (2006).
92. Lio, C.-W.J. & Hsieh, C.-S. A two-step process for thymic regulatory T cell development. *Immunity* **28**, 100-111 (2008).
93. Fontenot, J.D., Rasmussen, J.P., Gavin, M.A. & Rudensky, A.Y. A function for interleukin 2 in Foxp3-expressing regulatory T cells. *Nat. Immunol* **6**, 1142-1151 (2005).
94. Chen, W. u. a. Conversion of peripheral CD4+CD25- naive T cells to CD4+CD25+ regulatory T cells by TGF-beta induction of transcription factor Foxp3. *J. Exp. Med* **198**, 1875-1886 (2003).
95. Burchill, M.A., Yang, J., Vogtenhuber, C., Blazar, B.R. & Farrar, M.A. IL-2 receptor beta-dependent STAT5 activation is required for the development of Foxp3+ regulatory T cells. *J. Immunol* **178**, 280-290 (2007).
96. Zheng, S.G. u. a. TGF-beta requires CTLA-4 early after T cell activation to induce FoxP3 and generate adaptive CD4+CD25+ regulatory cells. *J. Immunol* **176**, 3321-3329 (2006).
97. Coombes, J.L. u. a. A functionally specialized population of mucosal CD103+ DCs induces Foxp3+ regulatory T cells via a TGF-beta and retinoic acid-dependent mechanism. *J. Exp. Med* **204**, 1757-1764 (2007).
98. Mucida, D. u. a. Oral tolerance in the absence of naturally occurring Tregs. *J. Clin. Invest* **115**, 1923-1933 (2005).
99. Sun, C.-M. u. a. Small intestine lamina propria dendritic cells promote de novo generation of Foxp3 T reg cells via retinoic acid. *J. Exp. Med* **204**, 1775-1785 (2007).
100. Curotto de Lafaille, M.A. u. a. Adaptive Foxp3+ regulatory T cell-dependent and -independent control of allergic inflammation. *Immunity* **29**, 114-126 (2008).
101. Liu, V.C. u. a. Tumor evasion of the immune system by converting CD4+CD25- T cells into CD4+CD25+ T regulatory cells: role of tumor-derived TGF-beta. *J. Immunol* **178**, 2883-2892 (2007).
102. Cobbold, S.P. u. a. Induction of foxP3+ regulatory T cells in the periphery of T cell receptor transgenic mice tolerized to transplants. *J. Immunol* **172**, 6003-6010 (2004).
103. Thornton, A.M. u. a. Expression of Helios, an Ikaros transcription factor family member, differentiates thymic-derived from peripherally induced Foxp3+ T regulatory cells. *J. Immunol* **184**, 3433-3441 (2010).
104. Shevach, E.M. Mechanisms of foxp3+ T regulatory cell-mediated suppression. *Immunity* **30**, 636-645 (2009).
105. Piccirillo, C.A. & Shevach, E.M. Cutting edge: control of CD8+ T cell activation by CD4+CD25+ immunoregulatory cells. *J. Immunol* **167**, 1137-1140 (2001).
106. Thornton, A.M. & Shevach, E.M. CD4+CD25+ immunoregulatory T cells suppress polyclonal T cell activation in vitro by inhibiting interleukin 2 production. *J. Exp. Med* **188**, 287-296 (1998).
107. Oberle, N., Eberhardt, N., Falk, C.S., Krammer, P.H. & Suri-Payer, E. Rapid suppression of cytokine transcription in human CD4+CD25 T cells by CD4+Foxp3+ regulatory T cells: independence of IL-2 consumption, TGF-beta, and various inhibitors of TCR signaling. *J. Immunol* **179**, 3578-3587 (2007).
108. Pandiyan, P., Zheng, L., Ishihara, S., Reed, J. & Lenardo, M.J. CD4+CD25+Foxp3+ regulatory T cells induce cytokine deprivation-mediated apoptosis of effector CD4+ T cells. *Nat. Immunol* **8**, 1353-1362 (2007).
109. Tran, D.Q. u. a. Selective expression of latency-associated peptide (LAP) and IL-1 receptor type I/II (CD121a/CD121b) on activated human FOXP3+ regulatory T cells allows for their purification from expansion cultures. *Blood* **113**, 5125-5133 (2009).
110. Takahashi, T. u. a. Immunologic self-tolerance maintained by CD25+CD4+ naturally anergic and suppressive T cells: induction of autoimmune disease by breaking their anergic/suppressive state. *Int. Immunol* **10**, 1969-1980 (1998).

111. Collison, L.W., Pillai, M.R., Chaturvedi, V. & Vignali, D.A.A. Regulatory T cell suppression is potentiated by target T cells in a cell contact, IL-35- and IL-10-dependent manner. *J. Immunol* **182**, 6121-6128 (2009).
112. Collison, L.W. u. a. The inhibitory cytokine IL-35 contributes to regulatory T-cell function. *Nature* **450**, 566-569 (2007).
113. Garín, M.I. u. a. Galectin-1: a key effector of regulation mediated by CD4+CD25+ T cells. *Blood* **109**, 2058-2065 (2007).
114. Gondek, D.C., Lu, L.-F., Quezada, S.A., Sakaguchi, S. & Noelle, R.J. Cutting edge: contact-mediated suppression by CD4+CD25+ regulatory cells involves a granzyme B-dependent, perforin-independent mechanism. *J. Immunol* **174**, 1783-1786 (2005).
115. Grossman, W.J. u. a. Human T regulatory cells can use the perforin pathway to cause autologous target cell death. *Immunity* **21**, 589-601 (2004).
116. Misra, N., Bayry, J., Lacroix-Desmazes, S., Kazatchkine, M.D. & Kaveri, S.V. Cutting edge: human CD4+CD25+ T cells restrain the maturation and antigen-presenting function of dendritic cells. *J. Immunol* **172**, 4676-4680 (2004).
117. Serra, P. u. a. CD40 ligation releases immature dendritic cells from the control of regulatory CD4+CD25+ T cells. *Immunity* **19**, 877-889 (2003).
118. Onishi, Y., Fehervari, Z., Yamaguchi, T. & Sakaguchi, S. Foxp3+ natural regulatory T cells preferentially form aggregates on dendritic cells in vitro and actively inhibit their maturation. *Proc. Natl. Acad. Sci. U.S.A* **105**, 10113-10118 (2008).
119. Wing, K. u. a. CTLA-4 control over Foxp3+ regulatory T cell function. *Science* **322**, 271-275 (2008).
120. Qureshi, O.S. u. a. Trans-Endocytosis of CD80 and CD86: A Molecular Basis for the Cell Extrinsic Function of CTLA-4. *Science* (2011).doi:10.1126/science.1202947
121. Joly, E. & Hudrisier, D. What is trogocytosis and what is its purpose? *Nat. Immunol* **4**, 815 (2003).
122. Grohmann, U. u. a. CTLA-4-Ig regulates tryptophan catabolism in vivo. *Nat. Immunol* **3**, 1097-1101 (2002).
123. Liang, B. u. a. Regulatory T cells inhibit dendritic cells by lymphocyte activation gene-3 engagement of MHC class II. *J. Immunol* **180**, 5916-5926 (2008).
124. Borsellino, G. u. a. Expression of ectonucleotidase CD39 by Foxp3+ Treg cells: hydrolysis of extracellular ATP and immune suppression. *Blood* **110**, 1225-1232 (2007).
125. Shalev, I. u. a. Targeted deletion of fgl2 leads to impaired regulatory T cell activity and development of autoimmune glomerulonephritis. *J. Immunol* **180**, 249-260 (2008).
126. Tisch, R. & McDevitt, H. Insulin-dependent diabetes mellitus. *Cell* **85**, 291-297 (1996).
127. Mathis, D., Vence, L. & Benoist, C. beta-Cell death during progression to diabetes. *Nature* **414**, 792-798 (2001).
128. van Belle, T.L., Coppieters, K.T. & von Herrath, M.G. Type 1 diabetes: etiology, immunology, and therapeutic strategies. *Physiol. Rev* **91**, 79-118 (2011).
129. Filippi, C.M. & von Herrath, M.G. Viral trigger for type 1 diabetes: pros and cons. *Diabetes* **57**, 2863-2871 (2008).
130. Todd, J.A. Etiology of type 1 diabetes. *Immunity* **32**, 457-467 (2010).
131. Drescher, K.M., Kono, K., Bopegamage, S., Carson, S.D. & Tracy, S. Coxsackievirus B3 infection and type 1 diabetes development in NOD mice: insulitis determines susceptibility of pancreatic islets to virus infection. *Virology* **329**, 381-394 (2004).
132. Horwitz, M.S., Fine, C., Ilic, A. & Sarvetnick, N. Requirements for viral-mediated autoimmune diabetes: beta-cell damage and immune infiltration. *J. Autoimmun* **16**, 211-217 (2001).
133. Serreze, D.V., Ottendorfer, E.W., Ellis, T.M., Gauntt, C.J. & Atkinson, M.A. Acceleration of type 1 diabetes by a coxsackievirus infection requires a preexisting critical mass of autoreactive T-cells in pancreatic islets. *Diabetes* **49**, 708-711 (2000).
134. Pescovitz, M.D. u. a. Rituximab, B-lymphocyte depletion, and preservation of beta-cell function. *N. Engl. J. Med* **361**, 2143-2152 (2009).

135. Bingley, P.J. Clinical applications of diabetes antibody testing. *J. Clin. Endocrinol. Metab* **95**, 25-33 (2010).
136. Ounissi-Benkalha, H. & Polychronakos, C. The molecular genetics of type 1 diabetes: new genes and emerging mechanisms. *Trends Mol Med* **14**, 268-275 (2008).
137. Patterson, C.C., Dahlquist, G.G., Gyürüs, E., Green, A. & Soltész, G. Incidence trends for childhood type 1 diabetes in Europe during 1989-2003 and predicted new cases 2005-20: a multicentre prospective registration study. *Lancet* **373**, 2027-2033 (2009).
138. Variation and trends in incidence of childhood diabetes in Europe. EURODIAB ACE Study Group. *Lancet* **355**, 873-876 (2000).
139. Onkamo, P., Väänänen, S., Karvonen, M. & Tuomilehto, J. Worldwide increase in incidence of Type I diabetes--the analysis of the data on published incidence trends. *Diabetologia* **42**, 1395-1403 (1999).
140. Barrett, J.C. u. a. Genome-wide association study and meta-analysis find that over 40 loci affect risk of type 1 diabetes. *Nat. Genet* **41**, 703-707 (2009).
141. Nejentsev, S. u. a. Localization of type 1 diabetes susceptibility to the MHC class I genes HLA-B and HLA-A. *Nature* **450**, 887-892 (2007).
142. Cooper, J.D. u. a. Meta-analysis of genome-wide association study data identifies additional type 1 diabetes risk loci. *Nat. Genet* **40**, 1399-1401 (2008).
143. Todd, J.A. u. a. Robust associations of four new chromosome regions from genome-wide analyses of type 1 diabetes. *Nat. Genet* **39**, 857-864 (2007).
144. Concannon, P. u. a. A human type 1 diabetes susceptibility locus maps to chromosome 21q22.3. *Diabetes* **57**, 2858-2861 (2008).
145. Smyth, D.J. u. a. A genome-wide association study of nonsynonymous SNPs identifies a type 1 diabetes locus in the interferon-induced helicase (IFIH1) region. *Nat. Genet* **38**, 617-619 (2006).
146. Mehers, K.L. & Gillespie, K.M. The genetic basis for type 1 diabetes. *Br. Med. Bull* **88**, 115-129 (2008).
147. Kristiansen, O.P., Larsen, Z.M. & Pociot, F. CTLA-4 in autoimmune diseases--a general susceptibility gene to autoimmunity? *Genes Immun* **1**, 170-184 (2000).
148. Ueda, H. u. a. Association of the T-cell regulatory gene CTLA4 with susceptibility to autoimmune disease. *Nature* **423**, 506-511 (2003).
149. Genome-wide association study of 14,000 cases of seven common diseases and 3,000 shared controls. *Nature* **447**, 661-678 (2007).
150. Concannon, P. u. a. A human type 1 diabetes susceptibility locus maps to chromosome 21q22.3. *Diabetes* **57**, 2858-2861 (2008).
151. Hakonarson, H. u. a. A genome-wide association study identifies KIAA0350 as a type 1 diabetes gene. *Nature* **448**, 591-594 (2007).
152. Hyttinen, V., Kaprio, J., Kinnunen, L., Koskenvuo, M. & Tuomilehto, J. Genetic liability of type 1 diabetes and the onset age among 22,650 young Finnish twin pairs: a nationwide follow-up study. *Diabetes* **52**, 1052-1055 (2003).
153. Awata, T. u. a. Association of type 1 diabetes with two Loci on 12q13 and 16p13 and the influence coexisting thyroid autoimmunity in Japanese. *J. Clin. Endocrinol. Metab* **94**, 231-235 (2009).
154. Zoledziewska, M. u. a. Variation within the CLEC16A gene shows consistent disease association with both multiple sclerosis and type 1 diabetes in Sardinia. *Genes Immun* **10**, 15-17 (2009).
155. Skinningsrud, B. u. a. Polymorphisms in CLEC16A and CIITA at 16p13 are associated with primary adrenal insufficiency. *J. Clin. Endocrinol. Metab* **93**, 3310-3317 (2008).
156. The expanding genetic overlap between multiple sclerosis and type I diabetes. *Genes Immun* **10**, 11-14 (2009).
157. Genome-wide association study identifies new multiple sclerosis susceptibility loci on chromosomes 12 and 20. *Nat. Genet* **41**, 824-828 (2009).
158. Márquez, A. u. a. Specific association of a CLEC16A/KIAA0350 polymorphism with NOD2/CARD15(-) Crohn's disease patients. *Eur. J. Hum. Genet* (2009).doi:10.1038/ejhg.2009.50

159. Mero, I.-L. u. a. Exploring the CLEC16A gene reveals a MS-associated variant with correlation to the relative expression of CLEC16A isoforms in thymus. *Genes Immun* **12**, 191-198 (2011).
160. Kim, S., Wairkar, Y.P., Daniels, R.W. & DiAntonio, A. The novel endosomal membrane protein Ema interacts with the class C Vps-HOPS complex to promote endosomal maturation. *J. Cell Biol* **188**, 717-734 (2010).
161. Makino, S. u. a. Breeding of a non-obese, diabetic strain of mice. *Jikken Dobutsu* **29**, 1-13 (1980).
162. Kikutani, H. & Makino, S. The murine autoimmune diabetes model: NOD and related strains. *Adv. Immunol* **51**, 285-322 (1992).
163. Anderson, M.S. & Bluestone, J.A. The NOD mouse: a model of immune dysregulation. *Annu. Rev. Immunol* **23**, 447-485 (2005).
164. Bach, J.F. Insulin-dependent diabetes mellitus as an autoimmune disease. *Endocr. Rev* **15**, 516-542 (1994).
165. Bao, M., Yang, Y., Jun, H.-S. & Yoon, J.-W. Molecular mechanisms for gender differences in susceptibility to T cell-mediated autoimmune diabetes in nonobese diabetic mice. *J. Immunol* **168**, 5369-5375 (2002).
166. Jansen, A. u. a. Immunohistochemical characterization of monocytes-macrophages and dendritic cells involved in the initiation of the insulitis and beta-cell destruction in NOD mice. *Diabetes* **43**, 667-675 (1994).
167. Ludewig, B., Odermatt, B., Landmann, S., Hengartner, H. & Zinkernagel, R.M. Dendritic cells induce autoimmune diabetes and maintain disease via de novo formation of local lymphoid tissue. *J. Exp. Med* **188**, 1493-1501 (1998).
168. Wicker, L.S. u. a. Type 1 diabetes genes and pathways shared by humans and NOD mice. *J. Autoimmun* **25 Suppl**, 29-33 (2005).
169. Hindorff, L.A. u. a. Potential etiologic and functional implications of genome-wide association loci for human diseases and traits. *Proc. Natl. Acad. Sci. U.S.A* **106**, 9362-9367 (2009).
170. MacArthur, D.G. & Tyler-Smith, C. Loss-of-function variants in the genomes of healthy humans. *Hum. Mol. Genet* **19**, R125-130 (2010).
171. Nichols, J. u. a. Validated germline-competent embryonic stem cell lines from nonobese diabetic mice. *Nat. Med* **15**, 814-818 (2009).
172. Ridgway, W.M., Healy, B., Smink, L.J., Rainbow, D. & Wicker, L.S. New tools for defining the „genetic background“ of inbred mouse strains. *Nat. Immunol* **8**, 669-673 (2007).
173. Fire, A., Albertson, D., Harrison, S.W. & Moerman, D.G. Production of antisense RNA leads to effective and specific inhibition of gene expression in C. elegans muscle. *Development* **113**, 503-514 (1991).
174. Fire, A. u. a. Potent and specific genetic interference by double-stranded RNA in Caenorhabditis elegans. *Nature* **391**, 806-811 (1998).
175. Denli, A.M., Tops, B.B.J., Plasterk, R.H.A., Ketting, R.F. & Hannon, G.J. Processing of primary microRNAs by the Microprocessor complex. *Nature* **432**, 231-235 (2004).
176. Gregory, R.I. u. a. The Microprocessor complex mediates the genesis of microRNAs. *Nature* **432**, 235-240 (2004).
177. Hutvágner, G. u. a. A cellular function for the RNA-interference enzyme Dicer in the maturation of the let-7 small temporal RNA. *Science* **293**, 834-838 (2001).
178. Hammond, S.M., Bernstein, E., Beach, D. & Hannon, G.J. An RNA-directed nuclease mediates post-transcriptional gene silencing in Drosophila cells. *Nature* **404**, 293-296 (2000).
179. Hammond, S.M., Boettcher, S., Caudy, A.A., Kobayashi, R. & Hannon, G.J. Argonaute2, a Link Between Genetic and Biochemical Analyses of RNAi. *Science* **293**, 1146 -1150 (2001).
180. Martinez, J., Patkaniowska, A., Urlaub, H., Lührmann, R. & Tuschl, T. Single-stranded antisense siRNAs guide target RNA cleavage in RNAi. *Cell* **110**, 563-574 (2002).

181. Khvorova, A., Reynolds, A. & Jayasena, S.D. Functional siRNAs and miRNAs exhibit strand bias. *Cell* **115**, 209-216 (2003).
182. Schwarz, D.S. u. a. Asymmetry in the assembly of the RNAi enzyme complex. *Cell* **115**, 199-208 (2003).
183. Hutvágner, G. & Zamore, P.D. A microRNA in a multiple-turnover RNAi enzyme complex. *Science* **297**, 2056-2060 (2002).
184. Brummelkamp, T.R., Bernards, R. & Agami, R. A system for stable expression of short interfering RNAs in mammalian cells. *Science* **296**, 550-553 (2002).
185. Brummelkamp, T.R., Bernards, R. & Agami, R. Stable suppression of tumorigenicity by virus-mediated RNA interference. *Cancer Cell* **2**, 243-247 (2002).
186. Abbas-Terki, T., Blanco-Bose, W., Déglon, N., Pralong, W. & Aebischer, P. Lentiviral-mediated RNA interference. *Hum. Gene Ther* **13**, 2197-2201 (2002).
187. Jackson, A.L. u. a. Expression profiling reveals off-target gene regulation by RNAi. *Nat Biotech* **21**, 635-637 (2003).
188. Rao, D.D., Vorhies, J.S., Senzer, N. & Nemunaitis, J. siRNA vs. shRNA: similarities and differences. *Adv. Drug Deliv. Rev* **61**, 746-759 (2009).
189. Baup, D. u. a. Variegation and silencing in a lentiviral-based murine transgenic model. *Transgenic Res* **19**, 399-414 (2009).
190. Sanger, F., Nicklen, S. & Coulson, A.R. DNA sequencing with chain-terminating inhibitors. *Proc. Natl. Acad. Sci. U.S.A* **74**, 5463-5467 (1977).
191. Laemmli, U.K. Cleavage of structural proteins during the assembly of the head of bacteriophage T4. *Nature* **227**, 680-685 (1970).
192. Pramfalk, C. u. a. Insulin receptor activation and down-regulation by cationic lipid transfection reagents. *BMC Cell Biol.* **5**, 7 (2004).
193. Read, S. u. a. Blockade of CTLA-4 on CD4+CD25+ Regulatory T Cells Abrogates Their Function In Vivo. *The Journal of Immunology* **177**, 4376 -4383 (2006).
194. Gerold, K.D. u. a. The Soluble CTLA-4 Splice Variant Protects From Type 1 Diabetes and Potentiates Regulatory T-Cell Function. *Diabetes* (2011).doi:10.2337/db11-0130
195. Lutsiak, M.E.C. u. a. Inhibition of CD4(+)25+ T regulatory cell function implicated in enhanced immune response by low-dose cyclophosphamide. *Blood* **105**, 2862-2868 (2005).
196. Harada, M. & Makino, S. Promotion of spontaneous diabetes in non-obese diabetes-prone mice by cyclophosphamide. *Diabetologia* **27**, 604-606 (1984).
197. Brode, S., Raine, T., Zaccone, P. & Cooke, A. Cyclophosphamide-induced type-1 diabetes in the NOD mouse is associated with a reduction of CD4+CD25+Foxp3+ regulatory T cells. *J. Immunol* **177**, 6603-6612 (2006).
198. Brode, S. & Cooke, A. Immune-potentiating effects of the chemotherapeutic drug cyclophosphamide. *Crit. Rev. Immunol* **28**, 109-126 (2008).
199. Alyanakian, M.-A. u. a. Diversity of regulatory CD4+T cells controlling distinct organ-specific autoimmune diseases. *Proc. Natl. Acad. Sci. U.S.A* **100**, 15806-15811 (2003).
200. Chambers, C.A., Sullivan, T.J. & Allison, J.P. Lymphoproliferation in CTLA-4-deficient mice is mediated by costimulation-dependent activation of CD4+ T cells. *Immunity* **7**, 885-895 (1997).
201. Houtman, J.C.D., Houghtling, R.A., Barda-Saad, M., Toda, Y. & Samelson, L.E. Early phosphorylation kinetics of proteins involved in proximal TCR-mediated signaling pathways. *J. Immunol* **175**, 2449-2458 (2005).
202. Tivol, E.A. u. a. Loss of CTLA-4 leads to massive lymphoproliferation and fatal multiorgan tissue destruction, revealing a critical negative regulatory role of CTLA-4. *Immunity* **3**, 541-547 (1995).
203. Leung, H.T., Bradshaw, J., Cleaveland, J.S. & Linsley, P.S. Cytotoxic T lymphocyte-associated molecule-4, a high-avidity receptor for CD80 and CD86, contains an intracellular localization motif in its cytoplasmic tail. *J. Biol. Chem* **270**, 25107-25114 (1995).
204. Valk, E. u. a. T cell receptor-interacting molecule acts as a chaperone to modulate surface expression of the CTLA-4 coreceptor. *Immunity* **25**, 807-821 (2006).

205. Iida, T. u. a. Regulation of cell surface expression of CTLA-4 by secretion of CTLA-4-containing lysosomes upon activation of CD4+ T cells. *J. Immunol* **165**, 5062-5068 (2000).
206. Linsley, P.S. u. a. Intracellular trafficking of CTLA-4 and focal localization towards sites of TCR engagement. *Immunity* **4**, 535-543 (1996).
207. Read, S. u. a. Blockade of CTLA-4 on CD4+CD25+ regulatory T cells abrogates their function in vivo. *J. Immunol* **177**, 4376-4383 (2006).
208. Read, S., Malmström, V. & Powrie, F. Cytotoxic T lymphocyte-associated antigen 4 plays an essential role in the function of CD25(+)CD4(+) regulatory cells that control intestinal inflammation. *J. Exp. Med* **192**, 295-302 (2000).
209. Alyanakian, M.-A. u. a. Diversity of regulatory CD4+T cells controlling distinct organ-specific autoimmune diseases. *Proc. Natl. Acad. Sci. U.S.A* **100**, 15806-15811 (2003).
210. Benoist, C. & Mathis, D. Positive selection of the T cell repertoire: where and when does it occur? *Cell* **58**, 1027-1033 (1989).
211. Park, F. Lentiviral vectors: are they the future of animal transgenesis? *Physiol. Genomics* **31**, 159-173 (2007).
212. Kissler, S. u. a. In vivo RNA interference demonstrates a role for Nramp1 in modifying susceptibility to type 1 diabetes. *Nat. Genet* **38**, 479-483 (2006).
213. Masteller, E.L., Chuang, E., Mullen, A.C., Reiner, S.L. & Thompson, C.B. Structural analysis of CTLA-4 function in vivo. *J. Immunol* **164**, 5319-5327 (2000).
214. Pentcheva-Hoang, T., Egen, J.G., Wojnoonski, K. & Allison, J.P. B7-1 and B7-2 selectively recruit CTLA-4 and CD28 to the immunological synapse. *Immunity* **21**, 401-413 (2004).
215. Chikuma, S., Imboden, J.B. & Bluestone, J.A. Negative regulation of T cell receptor-lipid raft interaction by cytotoxic T lymphocyte-associated antigen 4. *J. Exp. Med* **197**, 129-135 (2003).
216. Fraser, J.H., Rincón, M., McCoy, K.D. & Le Gros, G. CTLA4 ligation attenuates AP-1, NFAT and NF-kappaB activity in activated T cells. *Eur. J. Immunol* **29**, 838-844 (1999).
217. Chuang, E. u. a. The CD28 and CTLA-4 receptors associate with the serine/threonine phosphatase PP2A. *Immunity* **13**, 313-322 (2000).
218. Takahashi, T. u. a. Immunologic self-tolerance maintained by CD25(+)CD4(+) regulatory T cells constitutively expressing cytotoxic T lymphocyte-associated antigen 4. *J. Exp. Med* **192**, 303-310 (2000).
219. Friedline, R.H. u. a. CD4+ regulatory T cells require CTLA-4 for the maintenance of systemic tolerance. *J. Exp. Med* **206**, 421-434 (2009).
220. Schmidt, E.M. u. a. Ctla-4 controls regulatory T cell peripheral homeostasis and is required for suppression of pancreatic islet autoimmunity. *J. Immunol* **182**, 274-282 (2009).
221. You, S. u. a. Immunoregulatory pathways controlling progression of autoimmunity in NOD mice. *Ann. N. Y. Acad. Sci* **1150**, 300-310 (2008).
222. Bhatia, S., Edidin, M., Almo, S.C. & Nathenson, S.G. B7-1 and B7-2: similar costimulatory ligands with different biochemical, oligomeric and signaling properties. *Immunol. Lett* **104**, 70-75 (2006).
223. Araki, M. u. a. Genetic evidence that the differential expression of the ligand-independent isoform of CTLA-4 is the molecular basis of the Idd5.1 type 1 diabetes region in nonobese diabetic mice. *J. Immunol* **183**, 5146-5157 (2009).
224. Vijayakrishnan, L. u. a. An autoimmune disease-associated CTLA-4 splice variant lacking the B7 binding domain signals negatively in T cells. *Immunity* **20**, 563-575 (2004).
225. Reddy, M.V.P.L. u. a. Association between type 1 diabetes and GWAS SNPs in the southeast US Caucasian population. *Genes Immun* **12**, 208-212 (2011).
226. Wu, X. u. a. Intron polymorphism in the KIAA0350 gene is reproducibly associated with susceptibility to type 1 diabetes (T1D) in the Han Chinese population. *Clin. Endocrinol. (Oxf)* **71**, 46-49 (2009).

227. Hafler, D.A. u. a. Risk alleles for multiple sclerosis identified by a genomewide study. *N. Engl. J. Med* **357**, 851-862 (2007).
228. Rubio, J.P. u. a. Replication of KIAA0350, IL2RA, RPL5 and CD58 as multiple sclerosis susceptibility genes in Australians. *Genes Immun* **9**, 624-630 (2008).
229. Steinbrink, K., Graulich, E., Kubsch, S., Knop, J. & Enk, A.H. CD4+ and CD8+ anergic T cells induced by interleukin-10–treated human dendritic cells display antigen-specific suppressor activity. *Blood* **99**, 2468 -2476 (2002).
230. Nishikawa, Y. u. a. Biphasic Aire expression in early embryos and in medullary thymic epithelial cells before end-stage terminal differentiation. *The Journal of Experimental Medicine* **207**, 963 -971 (2010).
231. Gray, D.H.D. u. a. Developmental kinetics, turnover, and stimulatory capacity of thymic epithelial cells. *Blood* **108**, 3777 -3785 (2006).

11 Publication

Gerold KD, Zheng P, Rainbow DB, Zernecke A, Wicker LS, Kissler S.

The soluble CTLA-4 splice variant protects from type 1 diabetes and potentiates regulatory T-cell function.

Diabetes **60**, 1955-1963 (2011)